Det Kongelige Danske Videnskabernes Selskab
Matematisk-fysiske Meddelelser, bind **29**, nr. 13

Dan. Mat. Fys. Medd. **29**, no. 13 (1955)

A THEORY OF INTERFERENCE FILTERS

BY

ALFRED HERMANSEN

København 1955
i kommission hos Ejnar Munksgaard

CONTENTS

Printed in Denmark
Bianco Lunos Bogtrykkeri A-S

Introduction.

This paper describes the theory of interference filters of various types (especially interference filters with three and four silver layers, § 4 and § 5).

It will be shown how all the optical properties (such as reflectivity, transmission, phase changes at reflection, transmission, etc.) of an interference filter can be exactly calculated when the indices of refraction $\nu - i\varkappa$, n and the thicknesses t, d of the different thin layers are known as a function of the wavelength λ ($\nu - i\varkappa$ is the index of refraction and t the thickness of a metal layer). Furthermore relations are deduced between the optical constants of the reflective layers which give optimum conditions for the different types of filters.

In a following paper, it will be discussed how it is possible to measure the thicknesses of the dielectric layers on the filter base itself with an accuracy of about 20 Å and how such a filter can be made by means of the high-vacuum evaporation process for a filter area of 22 × 22 cm.

§ 1. Fresnel's Equations.

Reflection of light from and transmission through a boundary (fig. 1) between two materials 0 and 1 with indices of refraction n_0 and n_1 are determined by Fresnel's equations derived from the Maxwell equations of electrodynamics [1] & [2].

The following notations will be used:

φ angle of incidence, χ angle of refraction, and n index of refraction. s used as index means the component of the electric vector perpendicular to the plane of incidence and p used as index the component parallel to the plane of incidence.

χ is determined by SNELL's law:

$$n_0 \cdot \sin \varphi = n_1 \sin \chi . \tag{1, 1}$$

If (E_s, E_p) are the components of the electric vector of the incident plane light wave, the components of the electric vector

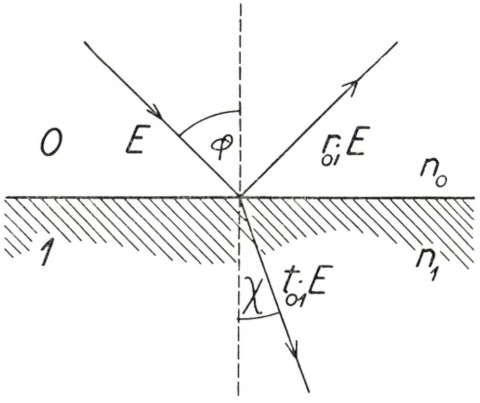

Fig. 1.

φ: Angle of incidence.
χ: Angle of refraction.
E: s or p component of electric vector of incident light wave.

of the reflected light wave $(E_s^{(R)}, E_p^{(R)})$ and of the transmitted wave $(E_s^{(T)}, E_p^{(T)})$ are determined by

$$E_s^{(R)} = E_s \cdot r_s ; \quad r_s = \frac{n_0 \cos \varphi - n_1 \cos \chi}{n_0 \cos \varphi + n_1 \cos \chi} \tag{1, 2}$$

$$E_p^{(R)} = E_p \cdot r_p ; \quad r_p = \frac{n_1 \cos \varphi - n_0 \cos \chi}{n_1 \cos \varphi + n_0 \cos \chi} \tag{1, 3}$$

$$E_s^{(T)} = E_s \cdot t_s ; \quad t_s = 1 + r_s . \tag{1, 4}$$

$$E_p^{(T)} = E_p \cdot t_p ; \quad t_p = (1 + r_p) \cdot \frac{n_0}{n_1} . \tag{1, 5}$$

The direction of the light is $0 \rightarrow 1$.

If the direction of the light is the opposite $1 \rightarrow 0$, n_0 must be interchanged with n_1 and φ with χ.

The following relations are satisfied:

$$r_{01} = -r_{10} \tag{1, 6}$$

$$t_{01} \cdot t_{10} - r_{01} \cdot r_{10} = 1 \tag{1, 7}$$

(valid either for the s or the p component).

At a normal angle of incidence ($\varphi = \chi = 0$) only one component of the electric vector is present, and the FRESNEL equations in this special case are the following:

$$r_{01} = \frac{n_0 - n_1}{n_0 + n_1}. \tag{1, 8}$$

$$t_{01} = 1 + r_{01}. \tag{1, 9}$$

Direction of the light: $0 \rightarrow 1$.

(The reason why $r_s = -r_p$ when $\varphi = 0$ is that $E_s = -E_p$ for the incident wave by definition [1]).

All these equations are also valid when the material 1 is absorbent (especially a metal). In this case the index of refraction n_1 is represented by a complex number $n_1 = \nu - i\varkappa$ and χ is a complex angle determined by (1, 1).

In accordance with [3] we define $a - ib = n_1 \cos\chi$; from (1, 1) we get $a - ib = \sqrt{(\nu - i\varkappa)^2 - n_0^2 \sin^2\varphi} = i\sqrt{g + i \cdot 2\nu\varkappa}$ (with $g = \varkappa^2 + n_0^2 \sin^2\varphi - \nu^2$), and from this equation we then obtain

$$b = \sqrt{\frac{1}{2}\left(g + \sqrt{g^2 + (2\nu\varkappa)^2}\right)}, \tag{1, 10}$$

and

$$a = \frac{\nu\varkappa}{b}. \tag{1, 11}$$

By introducing $n_1 \cos\chi = a - ib$ into (1, 2) and (1, 3) the FRESNEL equations can be written as follows:

$$r_s = \varrho_s \cdot e^{i\delta_s} = \frac{1 - \dfrac{1}{n_0 \cos\varphi}(a - ib)}{1 + \dfrac{1}{n_0 \cos\varphi}(a - ib)} \tag{1, 12}$$

TABLE 1. Angle of incidence $\varphi = 45°$.

a			b		
$\varkappa$ \ ν	0.1	0.2	$\varkappa$ \ ν	0.0	0.1	0.2
1.0	0.08174	0.16402	1.0	1.2247	1.2234	1.2194
1.5	.09048	18114	1.5	1.6583	1.6578	1.6561
2.0	.09429	.18865	2.0	2.1213	2.1211	2.1203
2.5	.09623	.19249	2.5	2.5981	2.5979	2.5975
3.0	.09734	.19468	3.0	3.0822	3.0821	3.0819
3.5	.09803	.19605	3.5	3.5707	3.5707	3.5705
4.0	.09847	.19695	4.0	4,0620	4,0620	4,0619
4.5	.09879	.19759	4.5	4,5552	4,5552	4,5551
5.0	.09902	.19803	5.0	5.0498	5.0497	5.0497
5.5	.09918	.19837	5.5	5.5453	5.5453	5.5453
6.0	.09931	.19863	6.0	6.0415	6.0415	6.0415
c			h			
$\varkappa$ \ ν	0.1	0.2	$\varkappa$ \ ν	0.0	0.1	0.2
1.0	0.10893	0.21819	1.0	0.8165	0.8165	0.8166
1.5	.10690	.21378	1.5	1.3568	1.3570	1.3578
2.0	.10476	.20945	2.0	1.8856	1.8858	1.8863
2.5	.10335	.20668	2.5	2.4056	2.4057	2.4061
3.0	.10245	.20490	3.0	2.9200	2.9201	2.9203
3.5	.10185	.20372	3.5	3.4307	3.4307	3.4309
4.0	.10146	.20291	4.0	3.9389	3.9390	3.9391
4.5	.10117	.20232	4.5	4.4455	4.4455	4.4456
5.0	.10096	.20191	5.0	4.9507	4.9508	4.9508
5.5	.10080	.20159	5.5	5.4551	5.4551	5.4551
6.0	.10068	.20134	6.0	5.9588	5.9588	5.9588

$$r_p = \varrho_p \cdot e^{i\delta_p} = -\frac{\left(1 - \frac{\cos\varphi}{n_0}(c - ih)\right)}{\left(1 + \frac{\cos\varphi}{n_0}(c - ih)\right)} \qquad (1, 13)$$

with

$$c - ih = \left(\frac{2\,b^2 - (\varkappa^2 - \nu^2)}{a^2 + b^2}\right) \cdot a - i\left(\frac{2\,a^2 + \varkappa^2 - \nu^2}{a^2 + b^2}\right) \cdot b. \qquad (1, 14)$$

If the light wave with the angle of incidence φ coming from air ($n_0 = 1$) is first to pass under the angle of refraction ψ through

TABLE 2. Angle of incidence $\varphi = 60°$.

	a		*b*		
$\varkappa$ \ ν	0.1	0.2	$\varkappa$ \ ν	0.0	0.1	0.2
1.0	0.07569	0.15192	1.0	1.3229	1.3213	1.3165
1.5	.08664	.17349	1.5	1.7321	1.7313	1.7292
2.0	.09178	.18365	2.0	2.1794	2.1791	2.1780
2.5	.09450	.18904	2.5	2.6458	2.6456	2.6449
3.0	.09608	.19218	3.0	3.1225	3.1224	3.1220
3.5	.09708	.19416	3.5	3.6056	3.6055	3.6052
4.0	.09774	.19548	4.0	4.0927	4.0926	4.0925
4.5	.09820	.19640	4.5	4.5826	4.5825	4.5824
5.0	.09853	.19707	5.0	5.0744	5.0744	5.0743
5.5	.09878	.19756	5.5	5.5678	5.5678	5.5677
6.0	.09898	.19795	6.0	6.0622	6.0622	6.0621

	c		*h*		
$\varkappa$ \ ν	0.1	0.2	$\varkappa$ \ ν	0.0	0.1	0.2
1.0	0.10809	0.21680	1.0	0.7559	0.7555	0.7542
1.5	.10826	.21658	1.5	1.2990	1.2992	1.2998
2.0	.10625	.21249	2.0	1.8352	1.8355	1.8361
2.5	.10461	.20920	2.5	2.3623	2.3624	2.3628
3.0	.10346	.20692	3.0	2.8823	2.8823	2.8827
3.5	.10268	.20534	3.5	3.3975	3.3976	3.3978
4.0	.10211	.20422	4.0	3.9094	3.9095	3.9096
4.5	.10170	.20341	4.5	4.4189	4.4190	4.4191
5.0	.10141	.20280	5.0	4.9266	4.9267	4.9268
5.5	.10117	.20235	5.5	5.4331	5.4331	5.4332
6.0	.10099	.20199	6.0	5.9385	5.9385	5.9385

a dielectric layer with the index of refraction n (before reaching the boundary) (a, b) *and* (c, h) *will be unchanged* as g is unchanged. $(n_0 \cdot \sin\varphi = n \cdot \sin\psi)$ and in (1, 12) and (1, 13) we have only to change n_0 to n and $\cos\varphi$ to $\cos\psi$.

In Tables 1—3 (a, b) and (c, h) are given as functions of $(\nu, \varkappa)$ with angles of incidence $\varphi = 45°$, $60°$, and $75°$, respectively, and with $n_0 = 1{,}0$ (only to be used for silver). From these tables it is apparent that for $\nu < 0.2$ it will be sufficient in most cases to use the approximation:

TABLE 3. Angle of incidence $\varphi = 75°$.

	a		*b*		
$\varkappa$ \ ν	0.1	0.2	$\varkappa$ \ ν	0.0	0.1	0.2
1.0	0.07202	0.14457	1.0	1.3903	1.3886	1.3834
1.5	.08412	.16846	1.5	1.7841	1.7833	1.7808
2.0	.09006	.18023	2.0	2.2210	2.2206	2.2193
2.5	.09329	.18663	2.5	2.6801	2.6798	2.6791
3.0	.09519	.19041	3.0	3.1517	3.1515	3.1510
3.5	.09640	.19282	3.5	3.6308	3.6307	3.6304
4.0	.09721	.19442	4.0	4.1150	4.1149	4.1147
4.5	.09777	.19555	4.5	4.6025	4.6024	4.6023
5.0	.09819	.19637	5.0	5.0924	5.0923	5.0923
5.5	.09849	.19699	5.5	5.5842	5.5842	5.5841
6.0	.09873	.19746	6.0	6.0773	6.0772	6.0772

	c		*h*		
$\varkappa$ \ ν	0.1	0.2	$\varkappa$ \ ν	0.0	0.1	0.2
1.0	10677	.21428	1.0	0.7193	0.7185	0.7163
1.5	.10874	.21758	1.5	1.2611	1.2612	1.2616
2.0	.10708	.21415	2.0	1.8010	1.8011	1.8017
2.5	.10538	.21076	2.5	2.3320	2.3321	2.3326
3.0	.10413	.20823	3.0	2.8556	2.8557	2.8560
3.5	.10321	.20641	3.5	3.3739	3.3739	3.3742
4.0	.10256	.20512	4.0	3.8882	3.8883	3.8885
4.5	.10208	.20416	4.5	4.3998	4.3998	4.4000
5.0	.10171	.20344	5.0	4.9092	4.9092	4.9093
5.5	.10144	.20288	5.5	5.4171	5.4171	5.4172
6.0	.10122	.20244	6.0	5.9237	5.9238	5.9238

$$b = \sqrt{g}; \quad a = \frac{\nu\varkappa}{\sqrt{g}}; \quad h = \frac{\varkappa^2}{\sqrt{g}} \quad \text{and} \quad c = \left(2 - \frac{\varkappa^2}{g}\right) a \qquad (g = \varkappa^2 + n_0^2 \sin^2\varphi). \tag{1, 15}$$

In the case of normal incidence ($\varphi = 0$) we obtain

$$r_{01} = \varrho_0 \cdot e^{i\delta_0} = \frac{1 - \left(\frac{\nu}{n_0} - i\frac{\varkappa}{n_0}\right)}{1 + \left(\frac{\nu}{n_0} - i\frac{\varkappa}{n_0}\right)}. \tag{1, 16}$$

TABLE 4. $180 - \delta_0$ (in degrees).

$\varkappa$ \ ν	0.0	0.1	0.2	0.3
1.0	90.000	89.713	88.850	87.423
1.1	84.547	84.289	83.517	82.235
1.2	79.611	79.380	78.690	77.547
1.3	75.137	74.931	74.317	73.300
1.4	71.075	70.892	70.346	69.444
1.5	67.381	67.218	66.732	65.931
1.6	64.011	63.866	63.435	62.723
1.7	60.931	60.803	60.419	59.785
1.8	58.109	57.995	57.652	57.088
1.9	55.517	55.415	55.109	54.605
2.0	53.130	53.039	52.765	52.314
2.1	50.927	50.845	50.599	50.194
2.2	48.888	48.814	48.594	48.229
2.3	46.997	46.930	46.732	46.403
2.4	45.240	45.180	45.000	44.703
2.5	43.603	43.548	43.386	43.117
2.6	42.075	42.026	41.878	41.634
2.7	40.647	40.601	40.467	40.244
2.8	39.308	39.267	39.144	38.941
2.9	38.051	38.014	37.902	37.716
3.0	36.870	36.836	36.732	36.563
3.1	35.757	35.726	35.632	35.475
3.2	34.708	34.679	34.592	34.449
3.3	33.717	33.690	33.610	33.478
3.4	32.779	32.754	32.680	32.558
3.5	31.891	31.868	31.800	31.686
3.6	31.048	31.027	30.964	30.859
3.7	30.248	30.228	29.170	29.072
3.8	29.487	29.469	29.414	29.324
3.9	28.763	28.746	28.695	28.611
4.0	28.072	28.057	28.009	27.930
4.1	27.414	27.399	27.355	27.281
4.2	26.785	26.771	26.730	26.661
4.3	26.184	26.171	26.132	26.068
4.4	25.609	25.596	25.560	25.500
4.5	25.058	25.046	25.012	24.955
4.6	24.529	24.519	24.487	24.433
4.7	24.023	24.013	23.983	24.932
4.8	23.537	23.527	23.499	23.451
4.9	23.069	23.060	23.033	22.988
5.0	22.620	22.611	22.586	22.544

TABLE 4 (continued).

$\varkappa$ \ ν	0.0	0.1	0.2	0.3
5.0	22.620	22.611	22.586	22.544
5.1	22.187	22.179	22.155	22.116
5.2	21.771	21.763	21.741	21.703
5.3	21.370	21.363	21.341	21.305
5.4	20.983	20.976	20.956	20.922
5.5	20.610	20.603	20.584	20.552
5.6	20.249	20.243	20.225	20.194
5.7	19.901	19.895	19.878	19.849
5.8	19.565	19.559	19.543	19.515
5.9	19.239	19.234	19.218	19.192
6.0	18.925	18.920	18.905	18.879

The FRESNEL equations in reflection (1, 12—13—16) are all written in the following manner: $\varrho \cdot e^{i\delta} = \dfrac{1-(x-iy)}{1+(x-ix)}$ (x and y are positive numbers).

The reflectivity is

$$R = \varrho^2 = \frac{1+x^2+y^2-2x}{1+x^2+y^2+2x} \qquad (1, 17)$$

and the phase change δ at reflection is determined by

$$tg\,\delta = -\frac{2y}{x^2+y^2-1}. \qquad (1, 18)$$

To calculate (ϱ_0, δ_0) at normal incidence and (ϱ_s, δ_s); (ϱ_p, δ_p) at oblique incidence, mathematical tables of ϱ (1, 17) and δ (1, 18) as a function of (x, y) would have been of great value.

$$(0 < y < 20 \quad \text{and} \quad 0 < x < 2{,}0).$$

By calculation of ϱ intervals in x: 0.01 and in y: 0.1 and by calculation of δ intervals in x: 0.1 and in y: 0.01. However, such mathematical tables are not available.

In this paper only a small table of δ as a function of $(\nu, \varkappa)$ is given (Table 4).

When once r is calculated, $t = \xi \cdot e^{i\beta}$ can most easily be calculated from (1, 4—5—9) by means of *A Table for Use in the Addition of Complex Numbers* calculated by JØRGEN RYBNER and K. STEENBERG SØRENSEN [4].

§ 2. "Fresnel's Factors" for a System of Thin Layers.

We consider a plane infinite incident wave of light; just before it reaches System I fig. 2 the s or p component of the electric vector at the point A we shall denote E_A (complex number).

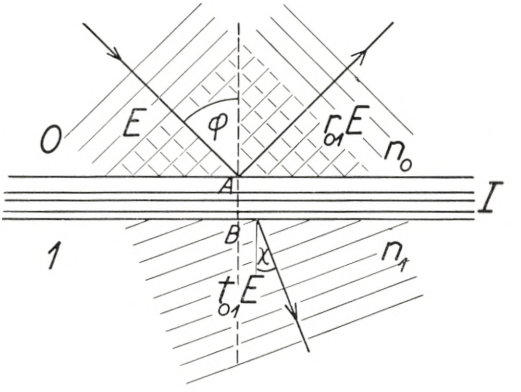

Fig. 2.
A system of thin layers I sandwiched between material 0 and material 1. System I may consist of one or more thin layers, the thickness of each being less than a few wavelengths of light.
E: s or p component of the electric vector.

After reflection from System I the component considered has now at the point A the value $E_A^{(R)}$ and after transmission through System I the value $E_B^{(T)}$ at the point B. We now define the Fresnel factors (r, t) for the system of thin layers I by the following:

$$r_{01} = \frac{E_A^{(R)}}{E_A} \qquad \text{and} \qquad t_{01} = \frac{E_B^{(T)}}{E_A}.$$

Direction of light: $0 \rightarrow 1$ and s and p components still considered separately (indices not written).

When the direction of the light is the opposite: $1 \rightarrow 0$ the Fresnel factors belonging to I are defined by

$$r_{10} = \frac{E_B^{(R)}}{E_B} \qquad \text{and} \qquad t_{10} = \frac{E_A^{(T)}}{E_B}.$$

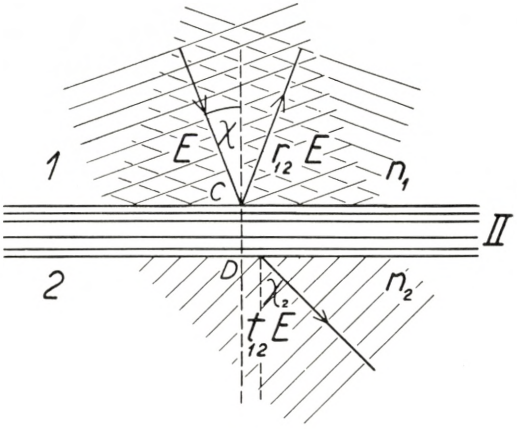

Fig. 3.
Another system of thin layers sandwiched between material 1 and material 2.

Next we consider a second system of thin layers II (fig. 3). The FRESNEL factors of this System II are defined in the same way as for System I by:

$$r_{12} = \frac{E_C^{(R)}}{E_C}; \quad t_{12} = \frac{E_D^{(T)}}{E_C} \quad \text{(direction of light: } 1 \rightarrow 2\text{)}$$

and

$$r_{21} = \frac{E_D^{(R)}}{E_D}; \quad t_{21} = \frac{E_C^{(T)}}{E_D} \quad \text{(direction of light: } 2 \rightarrow 1\text{)}$$

Now Systems I and II are combined to form a new system of thin layers I + II as shown on fig. 4.

It is now easy to express the FRESNEL factors $r_{02} = \frac{E_A^{(R)}}{E_A}$ and $t_{02} = \frac{E_D^{(T)}}{E_A}$ belonging to I + II by the FRESNEL factors r_{01}, t_{01}; r_{10}, t_{10} and r_{12}, t_{12}; r_{21}, t_{21}, belonging to Systems I and II, respectively.

If we consider the oscillations of the plane (infinite) wave which takes place in the layer between Systems I and II, we find by superposition of the wave systems in reflected light at point A directly from fig. 4 (by considering the plane wave front):

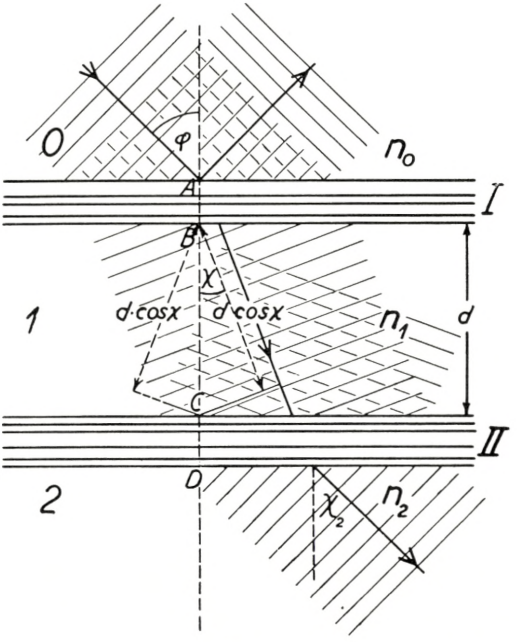

Fig. 4.
System I (fig. 2) and System II (fig. 3) combined to make a new System I + II. Material 1 forms a thin layer with thickness d between I and II.

$$E_A^{(R)} = E_A \cdot r_{02} = E_A \cdot r_{01} + E_A \cdot t_{01} \cdot e^{-i\frac{x}{2}} \cdot r_{12} \cdot e^{-i\frac{x}{2}} \cdot t_{10} +$$

$$E_A \cdot t_{01} \cdot e^{-i\frac{x}{2}} \cdot r_{12} \cdot e^{-i\frac{x}{2}} \cdot r_{10} \cdot e^{-i\frac{x}{2}} \cdot r_{12} \cdot e^{-i\frac{x}{2}} \cdot t_{10}$$

$$+ E_A \cdot t_{01} \cdot e^{-i\frac{x}{2}} \cdot r_{12} \cdot e^{-i\frac{x}{2}} \cdot r_{10} \cdot e^{-i\frac{x}{2}} \cdot r_{12} \cdot e^{-i\frac{x}{2}} \cdot r_{10} \cdot e^{-i\frac{x}{2}} \cdot r_{12} \cdot e^{-i\frac{x}{2}} \cdot t_{10}$$

$$+ \text{etc.} = E_A \cdot r_{01} + E_A \cdot t_{01} \cdot t_{10} \cdot r_{12} \cdot e^{-ix} \cdot \sum_{m=0}^{\infty} (r_{12} \cdot r_{10})^m \cdot e^{-imx}$$

$$= E_A \left(r_{01} + \frac{t_{01} \cdot t_{10} \cdot r_{12} \cdot e^{-ix}}{1 - r_{12} \cdot r_{10} \cdot e^{-ix}} \right).$$

From which follows:

$$r_{02} = \frac{r_{01} - r_{12}(r_{01} \cdot r_{10} - t_{01} \cdot t_{10}) \cdot e^{-ix}}{1 - r_{12} \cdot r_{10} \cdot e^{-ix}} \qquad (2, 1)$$

with

$$x = \frac{2\pi n_1}{\lambda} \cdot 2d\cos\chi = \frac{4\pi dn_1 \cos\chi}{\lambda} \qquad (2, 2)$$

(derived directly from fig. 4).

In transmission we find in the same way by superposition of all the plane waves oscillating between I and II:

$$t_{02} = t_{01} \cdot t_{12} \cdot e^{-i\frac{x}{2}} \sum_{m=0}^{\infty} (r_{12} \cdot r_{10})^m \cdot e^{-imx},$$

from which follows:

$$t_{02} = \frac{t_{01} \cdot t_{12} \cdot e^{-i\frac{x}{2}}}{1 - r_{12} \cdot r_{10} \cdot e^{-ix}}. \qquad (2, 3)$$

The reflectivity of System I + II (with direction of the incoming light $0 \rightarrow 2$) is

$$R_{02} = r_{02} \cdot \bar{r}_{02} \qquad (2, 4)$$

($\bar{r}_{02}$ means the complex conjugate number of r_{02}).

The transmitted energy through I + II can be derived from POYNTING's theorem of electrodynamics [1] to be

$$T'_{02} = t_{02} \cdot \bar{t}_{02} \cdot \frac{n_2 \cos\chi_2}{n_0 \cos\varphi}, \qquad (2, 5)$$

where χ_2 is the angle of refraction in material 2.

To derive r_{20} and t_{20} we only have to interchange the indices 0 and 2 in (2, 1) and (2, 3).

The following relation is valid:

$$\frac{t_{02}}{t_{20}} = \frac{t_{01} \cdot t_{12}}{t_{10} \cdot t_{21}}. \qquad (2, 6)$$

The fundamental formulae (2, 1—3) have been developed by ABELÈS [5] in much the same way as here by summing an infinite system of interfering wave systems. Recently, however, ISHIGURO and KATO [6] have developed (2, 1—3) directly from the boundary conditions of electrodynamics by using a matrix representation. This rigorously proves that (2, 1—3) are valid also when material 1 is absorbent, with an index of refraction

$\nu - i\varkappa$. In this case we have to put

$$x = \frac{4\pi}{\lambda} \cdot d\,(a - ib),$$

where (a, b) are determined by (1, 10—11), and we obtain

$$e^{-ix} = e^{-\frac{4\pi d \cdot b}{\lambda}} \cdot e^{-i\frac{4\pi d \cdot a}{\lambda}}.$$

First we consider a special case of the fundamental equations (2, 1—3), where System I is only a boundary (all layers in

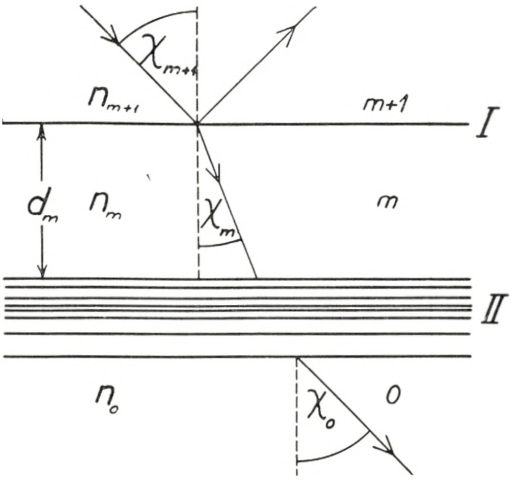

Fig. 5.
The direction of the light is the opposite of that used in fig. 4.

System I have zero thickness) and System II consists of $m - 1$ thin layers (fig. 5). In this special case we obtain from (1, 6—7)

$$r_{m+1,\,m} = -\,r_{m,\,m+1} \quad \text{and} \quad t_{m+1,\,m} \cdot t_{m,\,m+1} - r_{m+1,\,m} \cdot r_{m,\,m+1} = 1$$

and when this is introduced into (2, 1) and (2, 3) and when the notations $r_{12} = r_{m,0}$ and $t_{12} = t_{m,0}$ are used, we get the following fundamental recurrence formulae: (s or p component)

$$r_{m+1,\,0} = \frac{r_{m+1,\,m} + r_{m,\,0} \cdot e^{-ix_m}}{1 + r_{m+1,\,m} \cdot r_{m,\,0} \cdot e^{-ix_m}} \qquad (2, 7)$$

$$t_{m+1,0} = \frac{t_{m+1,m} \cdot t_{m,0} \cdot e^{-i\frac{x_m}{2}}}{1 + r_{m+1,m} \cdot r_{m,0} \cdot e^{-ix_m}} \tag{2, 8}$$

$$x_m = \frac{4\pi d_m \cdot n_m \cdot \cos \chi_m}{\lambda}. \tag{2, 9}$$

$r_{m+1,m}$, $t_{m+1,m}$ are determined by (1, 2—3) (when $n_0 = n_{m+1}$ $n_1 = n_m$ $\chi_{m+1} = \varphi$ and $\chi_m = \chi$ are introduced), i. e.

$$r^{(s)}_{m+1,m} = \frac{n_{m+1} \cdot \cos \chi_{m+1} - n_m \cdot \cos \chi_m}{n_{m+1} \cdot \cos \chi_{m+1} + n_m \cdot \cos \chi_m} \tag{2, 10}$$

$$r^{(p)}_{m+1,m} = \frac{n_m \cdot \cos \chi_{m+1} - n_{m+1} \cdot \cos \chi_m}{n_m \cdot \cos \chi_{m+1} + n_{m+1} \cdot \cos \chi_m} \tag{2, 11}$$

$$t^{(s)}_{m+1,m} = 1 + r^{(s)}_{m+1,m} \tag{2, 12}$$

$$t^{(p)}_{m+1,m} = (1 + r^{(p)}_{m+1,m}) \cdot \frac{n_{m+1}}{n_m}. \tag{2, 13}$$

The reflectivity of the system is determined by:

$$R_{m+1,0} = r_{m+1,0} \cdot \bar{r}_{m+1,0}; \tag{2, 14}$$

the energy transmitted through the system is:

$$T'_{m+1,0} = t_{m+1,0} \cdot \bar{t}_{m+1,0} \cdot \frac{n_0 \cos \chi_0}{n_{m+1} \cdot \cos \chi_{m+1}}, \tag{2, 15}$$

and all other optical properties (such as phase change by reflection, transmission, etc.) of a system of m thin layers (absorbent or not) can be calculated when d_m and n_m are known.

From the fundamental formulae (2, 7—15) it is now easy to show that the following relations are valid:

$$\frac{1 + r^{(s)}_{m+1,0}}{t^{(s)}_{m+1,0}} = \frac{1 + r^{(s)}_{m,0} \cdot e^{-ix_m}}{t^{(s)}_{m,0} \cdot e^{-i\frac{x_m}{2}}} \quad (s \text{ and } 0 \text{ components}) \tag{2, 16 a}$$

$$\frac{1+r^{(p)}_{m+1,0}}{t^{(p)}_{m+1,0}} = \frac{1+r^{(p)}_{m,0}\cdot e^{-ix_m}}{t^{(p)}_{m,0}\cdot e^{-i\frac{x_m}{2}}}\cdot\frac{n_{m+1}}{n_m} \quad (p \text{ components}) \quad (2,\ 16\ b)$$

and

$$\frac{1-r^{(s)}_{m+1,0}}{1+r^{(s)}_{m+1,0}} = \frac{n_m\cdot\cos\chi_m}{n_{m+1}\cdot\cos\chi_{m+1}}\cdot\left(\frac{1-r^{(s)}_{m,0}\cdot e^{-ix_m}}{1+r^{(s)}_{m,0}\cdot e^{-ix_m}}\right) \quad (2,\ 17\ a)$$

$$\frac{1-r^{(p)}_{m+1,0}}{1+r^{(p)}_{m+1,0}} = \frac{n_{m+1}\cdot\cos\chi_m}{n_m\cdot\cos\chi_{m+1}}\cdot\left(\frac{1-r^{(p)}_{m,0}\cdot e^{-ix_m}}{1+r^{(p)}_{m,0}\cdot e^{-ix_m}}\right). \quad (2,\ 17\ b)$$

Further, if the upper layer m (with thickness d_m) is transparent (dielectric layer), we get

$$\left.\begin{aligned} n_{m+1}\cdot\cos\chi_{m+1}\cdot\frac{(1-\bar{r}_{m+1,0}\cdot r_{m+1,0})}{\bar{t}_{m+1,0}\cdot t_{m+1,0}} = \\ n_m\cdot\cos\chi_m\cdot\frac{(1-\bar{r}_{m,0}\cdot r_{m,0})}{t_{m,0}\cdot\bar{t}_{m,0}} \end{aligned}\right\} \quad (2,\ 18\ a)$$

(valid both for s and p components).

By means of (2, 14—15) this can be expressed by

$$\frac{1-R_{m+1,0}}{T'_{m+1,0}} = \frac{1-R_{m,0}}{T'_{m,0}}, \quad (2,\ 18\ b)$$

i. e. *if to a system of thin layers (absorbent or not) is added one or more transparent layers,* $\frac{1-R}{T'}$ *remains constant.* This theorem has first been proved to be generally valid by F. Abelès [7].

For only one layer we deduce from (2, 6) and (2, 10—13)

$$t_{20} = t_{02}\cdot\frac{n_2\cos\chi_2}{n_0\cos\chi_0},$$

and by induction we get generally for a system of $m-1$ layers

$$t_{m,0} = t_{0,m}\cdot\frac{n_m\cdot\cos\chi_m}{n_0\cdot\cos\chi_0}. \quad (2,\ 19)$$

The transmission through the system is (2, 15)

$$T'_{m,0} = t_{m,0} \cdot \bar{t}_{m,0} \cdot \frac{n_0 \cos \chi_0}{n_m \cdot \cos \chi_m} = t_{0,m} \cdot \bar{t}_{0,m} \cdot \frac{n_m \cdot \cos \chi_m}{n_0 \cdot \cos \chi_0} = T'_{0,m} \quad (2, 20)$$

i. e. *at a system of thin layers the transmission remains the same if the direction of the light is reversed.* (The layers can be absorbent or not, the material above and below the system of thin layers must not be absorbent). Other general proofs of this theorem have been given by MAYER [2] and ABELÈS [7].

§ 3. Interference Filters with *Two* Systems of Reflective Layers I and II. (Spec. two silver layers).

An interference filter can very generally be defined as a thin dielectric layer enclosed between two strong reflective systems of thin layers I and II (fig. 6).

We now make the assumption that the reflectivity and the transmission (and phase change by reflection or transmission) of each

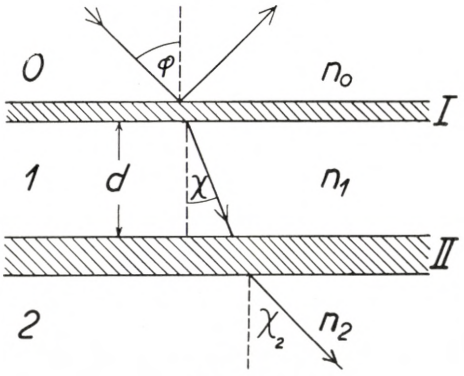

Fig. 6.

of the systems I and II considered separately, only show a small variation with the wavelength $\left(\text{within each spectral region of } \frac{\lambda}{10}\right)$ or expressed more simply: I or II must not be interference filters themselves.

For this simple type of interference filters many general properties can be derived directly from (2, 1—3).

If in (2, 1—3) the following substitutions are made:

$$r_{01} = \sqrt{R_{01}} \cdot e^{i\delta_{01}} \quad r_{10} = \sqrt{R_{10}} \cdot e^{i\delta_{10}} \quad r_{12} = \sqrt{R_{12}} \cdot e^{i\delta_{12}} \quad \text{and}$$

$$t_{01} = \sqrt{T_{01}} \cdot e^{i\beta_{01}} \quad t_{10} = \sqrt{T_{10}} \cdot e^{i\beta_{10}} \quad t_{12} = \sqrt{T_{12}} \cdot e^{i\beta_{12}}$$

(δ is the phase change at reflection and β the phase change at transmission) and if we further introduce

$$\sigma \cdot e^{i\alpha} = 1 - \frac{t_{01} \cdot t_{10}}{r_{01} \cdot r_{10}} = 1 - \sqrt{\frac{T_{01} \cdot T_{10}}{R_{01} \cdot R_{10}}} \cdot e^{i(\beta_{01} + \beta_{10} - \delta_{01} - \delta_{10})}. \qquad (3, 1\,a)$$

$$\boldsymbol{R} = \sqrt{R_{10} \cdot R_{12}} \qquad (3, 1\,b)$$

and

$$y = x - \delta_{10} - \delta_{12}, \qquad (3, 1\,c)$$

we get the following general formulae:

$$r_{02} = \sqrt{R_{02}(\lambda)} \cdot e^{i\delta_{02}(\lambda)} = \frac{\sqrt{R_{01}}\,(1 - \sigma \boldsymbol{R} \cdot e^{-i(y-\alpha)})\, e^{i\delta_{01}}}{(1 - \boldsymbol{R} \cdot e^{-iy})} \qquad (3, 2)$$

$$t_{02} = \sqrt{T_{02}(\lambda)} \cdot e^{i\beta_{02}(\delta)} = \frac{\sqrt{T_{01} \cdot T_{12}} \cdot e^{-i\left(\frac{x}{2} - \beta_{01} - \beta_{12}\right)}}{(1 - \boldsymbol{R} \cdot e^{-iy})}. \qquad (3, 3)$$

The intensity of the reflected light $R_{02}(\lambda)$ and of the transmitted light $I(\lambda)$ (in proportion to the intensity of the incident light $I_s^{(0)} = 1$ or $I_p^{(0)} = 1$; s and p components are treated separately) are from (3, 2—3) and (2, 4—5) determined to be:

$$R_{02}(\lambda) = \frac{R_{01}(1 - 2\,\sigma \boldsymbol{R} \cdot \cos(y - \alpha) + (\sigma \boldsymbol{R})^2)}{(1 - 2\,\boldsymbol{R} \cos y + \boldsymbol{R}^2)} \qquad (3, 4)$$

(direction of light: $0 \rightarrow 2$),
and if we define

$$\boldsymbol{T}_1 = \frac{n_1 \cdot \cos\chi}{n_0 \cos\varphi} \cdot T_{01} \quad \text{and} \quad \boldsymbol{T}_2 = \frac{n_2 \cdot \cos\chi_2}{n_1 \cos\chi} \cdot T_{12}$$

we get the intensity distribution for the transmitted light

$$I(\lambda) = \frac{\boldsymbol{T}_1 \cdot \boldsymbol{T}_2}{1 - 2\boldsymbol{R}\cos y + \boldsymbol{R}^2} \qquad (3, 5\text{ a})$$

or written in a more convenient manner

$$I(\lambda) = \frac{\boldsymbol{T}_1 \cdot \boldsymbol{T}_2}{(1-\boldsymbol{R})^2} \frac{1}{\left(1 + \frac{4\boldsymbol{R}}{(1-\boldsymbol{R})^2} \cdot \sin^2 \frac{y}{2}\right)} \qquad (3, 5\text{ b})$$

($I(\lambda)$ will according to (2, 20) be the same if the direction of the light is reversed).

The wavelengths λ_m at which $I(\lambda)$ reach a maximum are determined by

$$y = 360^0 (m - 1) \qquad m = 1, 2, 3 \ldots\ldots$$

and the wavelengths $\lambda_{m+\frac{1}{2}}$ at which $I(\lambda)$ becomes a minimum by

$$y = 180^0 (2m - 1) \qquad m = 1, 2, 3 \ldots\ldots$$

The Determination of $y(\lambda)$ or of $\lambda(y)$.

This determination is important in calculating λ_m and $I(\lambda)$ in the neighbourhood of λ_m.

$$y = \frac{360}{\lambda} \cdot 2\, dn_1 \cdot \cos\chi - (\delta_{10} + \delta_{12}) \quad \left\{ \begin{array}{l} \text{(when } y \text{ is mea-} \\ \text{sured in degrees)} \end{array} \right\} \qquad (3, 6\text{ a})$$

or

$$\frac{360 + y}{360} = \frac{1}{\lambda} \cdot \left(2\, dn_1 \cos\chi + \frac{(360 - (\delta_{10} + \delta_{12}))}{360} \cdot \lambda\right) \qquad (3, 6\text{ b})$$

δ_{01} and δ_{12} are dependent on the wavelength λ.
We now define

$$Z(\lambda) = \left(\frac{360 - \delta_{10}(\lambda) - \delta_{12}(\lambda)}{360}\right) \cdot \lambda. \qquad (3, 7)$$

By introducing $Z(\lambda)$ and λ_m (corresponding to $y = 360 \cdot (m - 1)$) into (3, 6 b) we get the following fundamental equations:

$$m\lambda_m = 2\, dn_1 \cdot \cos\chi + Z(\lambda_m) \qquad (3, 8)$$

and

$$\frac{360 + y}{360} = \frac{1}{\lambda}(m \cdot \lambda_m + Z(\lambda) - Z(\lambda_m)). \qquad (3, 9)$$

If I and II (fig. 6) each consist of only one silver layer, $Z(\lambda)$ will only show a small dependence upon λ (fig. 8 below). If, however, I and II consist of a combination of one silver layer and several quarter wavelength layers of dielectrics with low and high index of refraction or of $\frac{\lambda}{4}$-dielectric layers alone, the dependence of $\delta_{10} + \delta_{12}$ upon λ in the neighbourhood of λ_m must in each case be calculated by means of (2, 7) and next $y(\lambda)$ by (3, 6 a). (The results of such calculations of $y(\lambda)$ are shown in fig. 49 p. 86 and in fig. 51 p. 90).

From (3, 5—9) we are now able to calculate $I(\lambda)$ in detail. However, it will often be sufficient to describe $I(\lambda)$ by means of the following quantities:

1. The values of λ_m (from (3, 8) or direct from (3, 6 a));

2. The values of

$$I_{\max} = I(\lambda_m) = \frac{\boldsymbol{T}_1(\lambda_m) \cdot \boldsymbol{T}_2(\lambda_m)}{(1 - \boldsymbol{R}(\lambda_m))^2}; \qquad (3, 10)$$

3. The contrast factor

$$F = \frac{I_{\max}}{I_{\min}} = \frac{I(\lambda_m)}{I\left(\lambda_{m+\frac{1}{2}}\right)} = \frac{\boldsymbol{T}_1(\lambda_m) \cdot \boldsymbol{T}_2(\lambda_m)}{\boldsymbol{T}_1\left(\lambda_{m+\frac{1}{2}}\right) \cdot \boldsymbol{T}_2\left(\lambda_{m+\frac{1}{2}}\right)} \cdot \left(\frac{1 + \boldsymbol{R}\left(\lambda_{m+\frac{1}{2}}\right)}{1 - \boldsymbol{R}(\lambda_m)}\right)^2. \qquad (3, 11\text{ a})$$

If R and T with sufficient accuracy are independent of λ $\left(\text{within the wavelength region } \lambda_{m+\frac{1}{2}} < \lambda < \lambda_{m-\frac{1}{2}}\right)$ the contrast factor is simply expressed by

$$F = \frac{I_{\max}}{I_{\min}} = \left(\frac{1 + \boldsymbol{R}}{1 - \boldsymbol{R}}\right)^2; \quad (\boldsymbol{R} = \sqrt{R_{10} \cdot R_{12}}). \qquad (3, 11\text{ b})$$

4. The half intensity band width W_2 defined by

$$I\left(\lambda_m \pm \frac{W_2}{2}\right) = \frac{1}{2} \cdot I(\lambda_m)$$

and the tenth intensity band width W_{10} defined by

$$I\left(\lambda_m \pm \frac{W_{10}}{2}\right) = \frac{1}{10} \cdot I(\lambda_m).$$

If we introduce $y = 360^0 (m - 1) + \gamma_k$ (where γ_k is a small angle corresponding to the k'th intensity band width W_k), we find (from (3, 5 b))

$$I\left(\lambda_m \pm \frac{W_k}{2}\right) = \frac{\boldsymbol{T}_1 \cdot \boldsymbol{T}_2}{(1 - \boldsymbol{R})^2} \cdot \frac{1}{\left(1 + \frac{4\boldsymbol{R}}{(1-\boldsymbol{R})^2} \sin^2\left(\frac{\gamma_k}{2}\right)\right)}$$

and this is by definition equal to

$$\frac{1}{k} \cdot I(\lambda_m) = \frac{1}{k} \cdot \frac{\boldsymbol{T}_1 \boldsymbol{T}_2}{(1 - \boldsymbol{R})^2}.$$

So we obtain

$$\frac{4\boldsymbol{R}}{(1-\boldsymbol{R})^2} \sin^2\left(\frac{\gamma_k}{2}\right) = k - 1 \quad \text{and} \quad \sin\frac{\gamma_k}{2} = \frac{(1-\boldsymbol{R})\sqrt{1-k}}{2\sqrt{\boldsymbol{R}}} \quad (3, 12\,\text{a})$$

or approximately

$$\gamma_k = \frac{180}{\pi} \cdot \frac{(1-\boldsymbol{R})\sqrt{k-1}}{\sqrt{\boldsymbol{R}}} \quad (3, 12\,\text{b})$$

degree.

In the neighbourhood of $\lambda = \lambda_m$ we have approximately

$$y(\lambda) = 360^0 \cdot \left(m - 1 - f \cdot \frac{(\lambda - \lambda_m)}{\lambda_m}\right), \text{ where } f = -\left(\frac{dy}{d\lambda}\right)_{\lambda=\lambda_m} \cdot \frac{\lambda_m}{360}, \quad (3,13\text{a})$$

and as $y = 360 \cdot (m - 1) + \gamma_k$ corresponds to $\lambda_m - \lambda = \frac{W_k}{2}$ we obtain $\frac{\gamma_k}{180} = \frac{f \cdot W_k}{\lambda_m}$, and from (3, 12 b) we finally get

$$W_k = \frac{\lambda_m}{f} \cdot \frac{(1 - \boldsymbol{R})}{\pi \cdot \sqrt{\boldsymbol{R}}} \cdot \sqrt{1 - k},$$

and in particular we get

$$W_2 = \frac{\lambda_m}{f} \cdot \frac{(1 - \boldsymbol{R})}{\pi \cdot \sqrt{\boldsymbol{R}}} \qquad (3, 14)$$

and

$$W_{10} = 3 \cdot W_2. \qquad (3, 15)$$

When I and II (fig. 6) are silver layers we have approximately $y(\lambda) = 360 \cdot \left(\frac{m \cdot \lambda_m}{\lambda} - 1\right)$ according to p. 21 and in this case we simply get

$$f = m \qquad (m = 1, 2, 3 \ldots\ldots).$$

In case of filters where I and II (fig. 6) consist of several layers f will be different from an integer.

If the mean reflectivity $\boldsymbol{R} = \sqrt{R_{10} \cdot R_{12}}$ is increased W_2 (3, 14) will decrease and $F = \frac{I_{\max}}{I_{\min}}$ (3, 11) will increase. However, because of absorption in I and II (fig. 6) $I_{\max}$ (3, 10) will rapidly decrease. If we assume that the absorption in both I and II is $A = (A_{10} = A_{12})$, $I_{\max}$ is expressed by:

$$I_{\max} = \frac{(1 - R_{10} - A)(1 - R_{12} - A)}{(1 - \sqrt{R_{10} \cdot R_{12}})^2}. \qquad (3, 16)$$

It is now easy to show that for a definite (constant) value of $\boldsymbol{R} = \sqrt{R_{10} \cdot R_{12}}$ (i. e. for a definite value of the contrast factor) $I_{\max}$ will reach its highest value when $R_{12} = R_{10} = (\boldsymbol{R})$ (i. e. when I and II have the same reflectivity; for a definite (constant) value of R_{12}, however, $I_{\max}$ will reach its highest value when $R_{10} = R_{12} \cdot (1 - A)^2$).

From the above considerations it is obvious that one of the greatest problems in producing interference filters is that of finding a material (consisting of one or more thin layers) with a sufficiently high reflectivity R throughout a spectral region of reasonable length (as great as possible).

In most applications an interference filter is used at normal incidence ($\varphi = 0$). A small deviation $\Delta\varphi$ from parallelism of the incident light gives rise to a shift, say $\Delta\lambda_m$, towards violet according to (3, 8). If $\frac{Z(\lambda_m) - Z(\lambda_m + \Delta\lambda_m)}{m}$ is sufficiently small we get

5.
$$\Delta\lambda_m = \frac{1}{2}\frac{(\Delta\varphi)^2}{n_1^2} \cdot \left(\lambda_m - \frac{Z(\lambda_m)}{m}\right). \qquad (3, 17)$$

However, the dependence of Z upon wavelength often makes this calculation of $\Delta\lambda_m$ more difficult.

At an oblique angle of incidence all the formulae (3, 1—16) must be written separately for s and p components. (3, 8) especially will split up into

$$m \cdot \lambda_m^{(s)} = 2\, d n_1 \cos\chi + Z_s(\lambda_m^{(s)}) \qquad (3, 18\,a)$$

and

$$m\lambda_m^{(p)} = 2\, d n_1 \cos\chi + Z_p(\lambda_m^{(p)}). \qquad (3, 18\,b)$$

Because of the difference in δ_s and δ_p (evident from (1, 12—14)) Z_s and Z_p will usually be unequal and result in a splitting up into two transmission peaks at $\lambda_m^{(s)}$ and $\lambda_m^{(p)}$, respectively, the one polarized perpendicular upon and the other parallel to the plane of incidence.

At an oblique angle of incidence φ a small deviation $\Delta\varphi$ in the angle of incidence will give rise to a shift in wavelength of $\Delta\lambda_m$ determined by means of the derivate of (3, 8):

$$\Delta\lambda_m = -\frac{\left(\lambda_m - \frac{Z(\lambda_m)}{m}\right)\sin 2\varphi}{2\left(\left(\frac{n}{n_0}\right)^2 - \sin^2\varphi\right)} \cdot \Delta\varphi \qquad (3, 19)$$

(Z regarded as constant and angle of incidence φ in material with index of refraction n_0).

It should be noticed that this is a first order deviation in $\Delta\varphi$ as opposed to (3, 17) at $\varphi = 0$.

The Properties of the Filter (fig. 6) in Reflection.

If no absorption takes place in I and II we have

$$I(\lambda) + R_{02}(\lambda) = 1 \quad \text{(conservation of energy)}$$

(in this special case we have $R_{02} = R_{20}$ according to (2, 20)).

From (3, 4—5 a) we get

$$I(\lambda) + R_{02}(\lambda) = \frac{(1-R_{10})(1-R_{12})}{1-2\boldsymbol{R}\cos y+\boldsymbol{R}^2} + \frac{R_{01}(1-2\sigma\boldsymbol{R}\cdot\cos(y-\alpha)+(\sigma\boldsymbol{R})^2)}{1-2\boldsymbol{R}\cos y+\boldsymbol{R}^2}$$

with $\boldsymbol{R} = \sqrt{R_{10}\cdot R_{12}}$.

This will only be equal to 1 if

$$\alpha = 0 \quad \text{and} \quad \sigma = \frac{1}{R_{10}}\left(= \frac{1}{R_{01}}\right) \tag{3, 20}$$

as $\sigma\cdot e^{i\alpha}$ at the same time must satisfy (3, 1 a).

With a thin metal layer (such as *Al* or *Ag*) absorption takes place in I and then α will no longer be zero, but with layers which are almost opaque α will only have a small negative value (less than one degree). In this case we get as a first approximation

$$\sigma = \frac{1-A}{R_{01}} \quad (A \text{ absorption in I}). \tag{3, 21}$$

The condition for obtaining $R_{02}(\lambda) = 0$ at a definite wavelength is (from (3, 4))

$$1 - 2\sigma\boldsymbol{R}\cos(y-\alpha) + (\sigma\boldsymbol{R})^2 = 0$$

or

$$\cos(y-\alpha) = \frac{1+(\sigma\boldsymbol{R})^2}{2\sigma\boldsymbol{R}}.$$

This quantity is always $\geqslant 1$, i. e. $R_{02}(\lambda) = 0$ only if

$$\underline{\sigma\boldsymbol{R} = 1} \qquad (\boldsymbol{R} = \sqrt{R_{10}\cdot R_{12}}), \tag{3, 22}$$

and this takes place at

$$y = \alpha^\circ + 360^\circ(m-1).$$

If I is not absorbent

$$\sigma \boldsymbol{R} = \frac{1}{R_{10}} \cdot \sqrt{R_{10} \cdot R_{12}} = \sqrt{\frac{R_{12}}{R_{10}}};$$

in this case the condition for zero intensity of $R_{02}(\lambda)$ is $R_{12} = R_{10}$ (it is immaterial whether II is absorbent or not).

If I is absorbent and $R_{10} = R_{12}$ no value of λ exist at which $R_{02}(\lambda) = 0$; however, it is possible to find a value of R_{10} at which the equation (3, 22) is satisfied (as a first approximation we get $R_{01} = (1 - A)^2 \cdot R_{12}$). In this case $R_{02}(\lambda) = 0$ is satisfied at wavelengths determined by $y = \alpha + 360 \cdot (m - 1)$ in combination with (3, 9). The wavelength at which the maximum of transmission occurs is determined by $y = 360 \cdot (m - 1)$. Hence it follows that a small difference results between $\lambda_{\max}$ in transmission and $\lambda_{\min}$ in reflection. The same will be the case if $R_{10} = R_{12}$ and I is absorbent.

The Fabry-Perot *Filter* $ML_{2m}M$.

The simplest of the types of interference filters treated above is the Fabry-Perot filter which simply consists of two silver layers M with a dielectric layer L_{2m} in between. (L_{2m} means a $2\,m \cdot \frac{\lambda}{4}$ layer). The name of this filter originates from the fact that the filter is a Fabry-Perot interferometer with a very small spacing between the reflecting surfaces. The first production and description of filters of this type are due to Geffcken [8].

It is important to note that the filter blank need not be more accurately polished than an ordinary optical surface as the different thin layers all follow the irregularities of the blank. (It is unnecessary to use an interferometer plate as filter blank).

In order to calculate the properties of this filter the first step is to make numerical calculations of R, T, δ, β, σ, α ....., etc., for silver layers of different thicknesses t and at different wavelengths λ.

The reflectivity R_∞ and the phase change δ_0 at the boundary between an opaque silver layer and a dielectric with an index of refraction n_0 are determined (at normal incidence) by (1, 17—18) when we put $x - iy = \frac{\nu}{n_0} - i\frac{\varkappa}{n_0}$. When n_0 increases R_∞ decreases, which means that only dielectrics with a low index

of refraction can be used for interference filters of the type $ML_{2m}M$. (L means a $\frac{\lambda}{4}$-layer with *low* index of refraction).

In the numerical calculations (the results of which are given in Tables 6—13) it is assumed that $n = 1.36$ on both sides of the silver layer (fig. 7). In practice one side of the silver layer is bounded by glass (or cement) with $n = 1.5$; the influence upon R_{10} and T will, however, be small as compared with the experimental uncertainty in determining $\nu - i\varkappa$. $n_0 = 1.36$ has been chosen because this corresponds to the index of refraction obtained by slow evaporation of cryolite. The index of refraction of MgF_2 too is only slightly higher than 1.36.

The different values of $\nu - i\varkappa$ published [2] vary greatly, depending partly upon the conditions by producing the silver layers and partly upon the different optical methods by which $\nu - i\varkappa$ is measured. The most reliable values of $\varkappa$ seem to be those published by SCHULZ [9], which were determined by measurements of δ_0 at the boundary between the air and a nearly opaque silver layer. Furthermore from accurate measurements of R and T at nearly opaque silver layers published by KUHN [10] ν can be calculated from $R_\infty = R + T$. We get

$$\nu = \frac{1.02 + \varkappa^2}{2} \cdot \left(\frac{1 - R_\infty}{1 + R_\infty}\right)$$

when as a first approximation $\nu^2 = 0.02$ is adopted.

The values of $\nu - i\varkappa$ employed in the following numerical calculations are given in Table 5.

TABLE 5.

λ	ν	$\varkappa$	R_∞
3800	0.20	1.77	0.82
4000	0.18	1.95	0.86
4500	0.14	2.42	0.92
5000	0.14	2.89	0.94
5500	0.15	3.36	0.95
6000	0.15	3.82	0.96
6560	0.13	4.27	0.97
7100	0.14	4.68	0.97
7680	0.15	5.11	0.98

TABLE 6. $\lambda = 4000$ Å $\quad \nu - i\varkappa = 0.18 - i\ 1.95$.

t in Å	R	T	A	$\left(\frac{T}{1-R}\right)^2$	$\left(\frac{1+R}{1-R}\right)^2$	$180-\delta^\circ$	β°	σ	$-\alpha^\circ$
150	.1852	.7179	.0969	.7762	2.12	75°13	7°38	4.8495	11°92
200	.2881	.5956	.1163	.6999	3.27	73.44	8.79	3.0427	10.48
250	.3889	.4809	.1302	.6194	5.17	72.16	9.72	2.2145	8.98
300	.4802	.3801	.1397	.5347	8.11	71.23	10.24	1.7719	7.53
350	.5585	.2954	.1461	.4477	12.5	70.56	10.43	1.5118	6.21
400	.6231	.2266	.1503	.3615	18.6	70.11	10.36	1.3489	5.05
500	.7155	.1297	.1548	.2080	36.4	69.61	9.66	1.1706	3.25
550	.7469	.0972	.1559	.1475	47.6	69.49	9.13	1.1211	2.57
600	.7709	.0725	.1566	.1001	59.8	69.42	8.52	1.0865	2.03
∞	.8414	.00	.1586	.00		69.48			

TABLE 7. $\lambda = 4500$ Å $\quad \nu - i\varkappa = 0.14 - i\ 2.42$.

t in Å	R	T	A	$\left(\frac{T}{1-R}\right)^2$	$\left(\frac{1+R}{1-R}\right)^2$	$180-\delta$	β	σ	$-\alpha$
150	.2560	.6662	.0778	.8017	2.85	70.29	14.39	3.5903	7.69
200	.3838	.5266	.0896	.7304	5.04	67.08	17.40	2.3613	4.66
250	.4997	.4042	.0961	.6527	9.00	64.64	19.57	1.7997	5.18
300	.5970	.3038	.0992	.5683	15.7	62.84	21.06	1.5012	4.11
350	.6748	.2250	.1002	.4785	26.5	61.54	22.00	1.3271	3.22
400	.7351	.1649	.1000	.3876	42.9	60.62	22.53	1.2191	2.50
500	.8150	.0869	.0981	.2204	96.2	59.57	22.74	1.1031	1.47
∞	.9060	.00	.0940	.00		58.55			

TABLE 8. $\lambda = 5000$ Å $\quad \nu - i\varkappa = 0.14 - i\ 2.89$.

t in Å	R	T	A	$\left(\frac{T}{1-R}\right)^2$	$\left(\frac{1+R}{1-R}\right)^2$	$180-\delta$	β	σ	$-\alpha$
150	.3290	.5955	.0755	.7878	3.92	64.56	20.62	2.8009	6.21
200	.4717	.4456	.0827	.7114	7.76	60.35	24.63	1.9374	4.88
250	.5902	.3247	.0851	.6279	15.1	57.29	27.34	1.5439	3.81
300	.6825	.2328	.0847	.5375	28.1	55.12	29.12	1.3363	2.825
350	.7516	.1652	.0832	.4422	49.7	53.61	30.49	1.2160	2.119
400	.8022	.1165	.0813	.3470	83.0	52.56	31.17	1.1422	1.582
500	.8649	.0573	.0778	.1799	190.6	51.35	31.57	1.0644	0.873
∞	.9282	.00	.0718	.00		50.32			

TABLE 9. $\lambda = 5500$ Å $\quad \nu - i\varkappa = 0.15 - i\ 3.36$.

t in Å	R	T	A	$\left(\frac{T}{1-R}\right)^2$	$\left(\frac{1+R}{1-R}\right)^2$	$180-\delta$	β	σ	$-\alpha$
150	.4009	.5234	.0757	.7633	5.44	59.11	26.22	2.2978	5.291
200	.5495	.3713	.0792	.6792	11.8	54.29	30.83	1.6697	3.932
250	.6634	.2582	.0784	.5884	24.4	50.95	33.92	1.3847	2.872
300	.7462	.1779	.0759	.4913	47.3	48.67	35.89	1.2349	2.087
350	.8051	.1220	.0729	.3914	85.8	47.13	37.09	1.1488	1.513
400	.8463	.0834	.0703	.2976	144.3	46.10	37.76	1.0965	1.097
500	.8951	.0389	.0660	.1377	326.4	44.94	38.10	1.0422	0.575
∞	9399	.00	.0601	.00		44.00			

TABLE 10. $\lambda = 6000$ Å $\quad \nu - i\varkappa = 0.15 - i\ 3.82$.

t in Å	R	T	A	$\left(\frac{T}{1-R}\right)^2$	$\left(\frac{1+R}{1-R}\right)^2$	$180-\delta$	β	σ	$-\alpha$
150	.4690	.4609	.0701	.7535	7.65	54.47	31.27	1.9771	4.222
200	.6179	.3119	.0702	.6661	17.93	49.28	36.27	1.5007	2.986
250	.7239	.2087	.0674	.5712	38.98	45.82	39.48	1.2853	2.100
300	.7965	.1392	.0643	.4681	77.93	43.54	41.48	1.1726	1.479
350	.8466	.0930	.0604	.3676	144.9	42.03	42.66	1.1082	1.045
400	.8803	.0622	.0575	.2698	246.7	41.04	43.31	1.0693	0.741
500	.9188	.0278	.0534	.1175	558.4	39.96	43.63	1.0296	0.374
∞	.9516	.00	.0484	.00		39.12			

TABLE 11. $\lambda = 6560$ Å $\quad \nu - i\varkappa = 0.13 - i\ 4.27$.

t in Å	R	T	A	$\left(\frac{T}{1-R}\right)^2$	$\left(\frac{1+R}{1-R}\right)^2$	$180-\delta$	β	σ	$-\alpha$
150	.5291	.4149	.0560	.7764	10.5	50.86	35.76	1.7811	2.971
200	.6748	.2709	.0543	.6937	26.5	45.40	40.96	1.3991	2.084
250	.7728	.1763	.0509	.6022	60.9	41.87	44.39	1.2265	1.386
300	.8375	.1152	.0473	.5023	127.9	39.59	46.45	1.1364	0.956
350	.8802	.0756	.0442	.3975	246.3	38.10	47.66	1.0850	0.668
400	.9084	.0498	.0418	.2956	434.1	37.14	48.36	1.0542	0.466
500	.9398	.0218	.0384	.1305	1038.3	36.09	48.80	1.0228	0.230
∞	.9654	.00	.0346	.00		35.31			

TABLE 12. $\lambda = 7100$ Å $\quad \nu - i\varkappa = 0.14 - i\ 4.68$.

t in Å	R	T	A	$\left(\frac{T}{1-R}\right)^2$	$\left(\frac{1+R}{1-R}\right)^2$	$180-\delta$	β	σ	$-\alpha$
150	.5711	.3739	0550	.7600	13.4	47.63	39.00	1.6518	2.669
200	.7104	.2375	0521	6726	34.9	42.13	44.34	1.3324	1.770
250	.8004	.1517	0479	5776	81.4	38.65	47.62	1.1881	1.187
300	.8582	.0977	0441	4747	171.7	36.43	49.60	1.1128	.808
350	.8957	.0634	0409	3695	330.3	35.00	50.77	1.0701	.558
400	.9202	.0414	0384	2691	579.0	34.09	51.41	1.0445	.386
450	.9363	.0271	0366	1810	924.0	33.50	51.70	1.0286	.269
500	.9470	.0173	.0357	.1066	1349.5	33.11	51.78	1.0180	.182
∞	.9685	.00	.0315	.00		32.38			

TABLE 13. $\lambda = 7680$ Å $\quad \nu - i\varkappa = 0.15 - i\ 5.11$.

t in Å	R	T	A	$\left(\frac{T}{1-R}\right)^2$	$\left(\frac{1+R}{1-R}\right)^2$	$180-\delta$	β	σ	$-\alpha$
150	.6100	.3363	.0537	.7436	17.0	44.63	42.01	1.5489	2.384
200	.7419	.2085	.0496	.6527	45.5	39.14	47.34	1.2794	1.543
250	.8241	.1310	.0449	.5544	107.5	35.75	50.54	1.1578	1.017
300	.8756	.0834	.0410	.4498	227.3	33.62	52.44	1.0944	.684
350	.9086	.0537	.0377	.3447	436.1	32.26	53.54	1.0585	.468
400	.9299	.0348	.0353	.2464	757.9	31.39	54.14	1.0370	.321
450	.9438	.0227	.0335	.1632	1196.3	30.82	54.40	1.0237	.223
500	.9530	.0148	.0322	·0997	1726.7	30.46	54.45	1.0153	.155
∞	.9713	.00	0.287	.00		29.78			

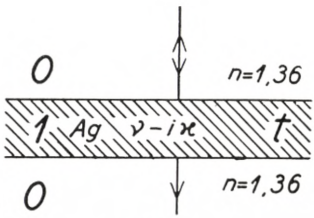

Fig. 7.

Tables 6—13 are calculated by means of (2, 7—9) and (1, 16—18), which in the special case indicated in fig. 7 become:

$$\sqrt{R}\cdot e^{i\delta} = r_{01}\frac{1-e^{-ix}}{1-r_{01}^2\cdot e^{-ix}} \qquad (3,\ 23)$$

$$\sqrt{T}\cdot e^{i\beta} = \frac{(1-r_{01}^2)\,e^{-i\frac{x}{2}}}{1-r_{01}^2\cdot e^{-ix}} \qquad (3,\ 24)$$

$$r_{01} = \frac{1-\left(\frac{\nu}{n_0}-i\frac{\varkappa}{n_0}\right)}{1+\frac{\nu}{n_0}-i\frac{\varkappa}{n_0}} \qquad (3,\ 25)$$

and

$$e^{-ix} = e^{-\frac{4\pi\varkappa t}{\lambda}}\cdot e^{-i\frac{4\pi\nu t}{\lambda}}. \qquad (3,\ 26)$$

To calculate $R(\lambda)$ of a FABRY-PEROT filter we must further calculate $\sigma e^{i\alpha} = 1-\frac{T}{R}e^{i(2\beta-2\delta)}$ from the calculated values of (R, δ) and (T, β).

All these calculations have been carried out directly from (3, 23—26) by means of RYBNER's tables [4].

In the calculations it is assumed that $\nu - i\varkappa$ at a definite wavelength λ is independent of the thickness t of the silver layer.

The formulae (3, 23—26) depend only upon the variable quantities in the combinations $\frac{\nu(\lambda)-i\varkappa(\lambda)}{n_0}$ and $\frac{\nu(\lambda)-i\varkappa(\lambda)}{\lambda}t$.

If the index of refraction n_0 is changed to n' the tables can still be used if the λ scale is changed to λ' and the t scale to t'; the transformation is determined by

$$\frac{\nu(\lambda')-i\varkappa(\lambda')}{n_0} = \frac{\nu(\lambda)-i\varkappa(\lambda)}{n'} \text{ and } \frac{\nu(\lambda')-i\varkappa(\lambda')}{\lambda'}t' = \frac{\nu(\lambda)-i\varkappa(\lambda)}{\lambda}t,$$

i. e. $t' = \frac{n'}{n_0}\cdot\frac{\lambda'}{\lambda}\cdot t$, and if approximately $\nu(\lambda)-i\varkappa(\lambda) = (k_1-ik_2)\cdot\lambda$, then $\lambda' = \frac{n_0}{n'}\cdot\lambda$ and $t' = t$. (This will be a good approximation for δ because it only slightly depends upon ν).

From Tables 6—13 graphs of $Z(\lambda, t) = \left(\frac{180-\delta_0(\lambda,\ t)}{180}\right)\cdot\lambda$ can be made for different thicknesses t of the silver layers (fig. 8).

If the filter consists of two silver layers of different thicknesses t' and t''

$$Z_{\text{res}} = \frac{360 - \delta_0(t') - \delta_0(t'')}{360} = \frac{1}{2}(Z(\lambda_1, t') + Z(\lambda_1, t'')).$$

These graphs (fig. 8) are important because it is possible when $Z(\lambda)$ is known to determine the optical thickness nd which

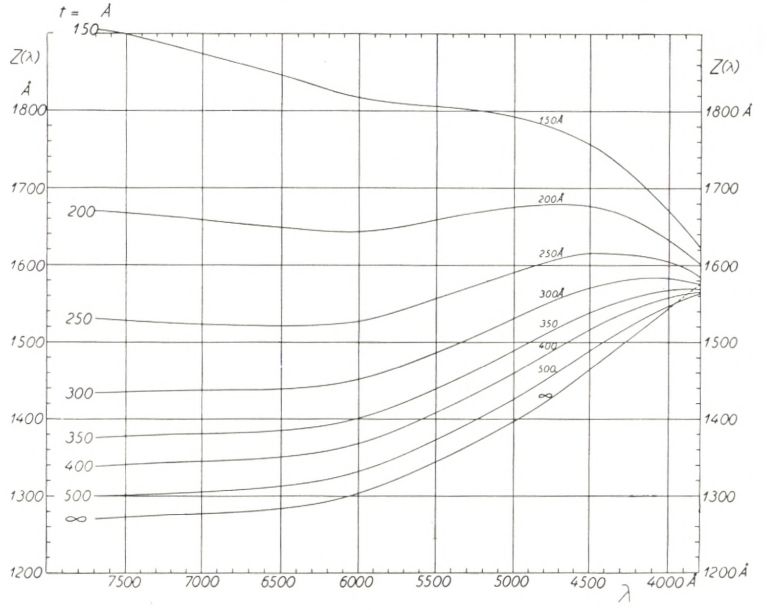

Fig. 8.

corresponds to a definite λ_m. (From (3, 8)). Inversely, if λ_m are measured spectroscopically and d is measured for one definite wavelength, $Z(\lambda)$ can be determined directly by experiment. (This has been done by SCHULZ [9]; with $n = 1$ this gives a determination of $\varkappa(\lambda)$).

The half intensity band width W_2 has not been calculated in the tables for each t, λ value. For this reason a table of

$$W_2(R) = \frac{(1-R)\,5500}{\pi\sqrt{R}\cdot 2}$$

is added (Table 14) corresponding to a filter with $\lambda_m = 5500$ Å and $m = 2$. From this table W_2' corresponding to another λ_m

can easily be calculated by means of

$$W_2'(R) = W_2(R) \cdot \frac{\lambda_m}{m \cdot 2750}.$$

TABLE 14.

R	W_2 in Å	R	W_2 in Å	R	W_2 in Å
0.75	252.7	0.84	152.8	0.93	63.5
.76	241.0	.85	142.4	.94	54.2
.77	229.4	.86	132.2	.95	44.9
.78	218.0	.87	122.0	.96	35.7
.79	206.8	.88	112.0	.97	26.7
.80	195.7	.89	102.1	.98	17.7
.81	184.8	.90	92.3	.99	8.8
.82	174.0	.91	82.6		
.83	163.3	.92	73.0		

When R, T, $y(\lambda)$ are calculated it is possible to calculate line shapes at different wavelengths and thicknesses of the silver layers. In all the following graphs it has simply been chosen to calculate the wavelength scale by means of (3, 9) with the approx. $Z(\lambda) = Z(\lambda_m)$. If $y = 360 \cdot (m - 1) + \gamma$ (γ a small angle), we get:

$$\lambda = \frac{360\, m \cdot \lambda_m}{360\, m + \gamma}, \qquad (3, 27\ a)$$

and this combined with (3, 5 b)

$$I(\lambda) = \frac{\boldsymbol{T}^2}{(1-\boldsymbol{R})^2} \frac{1}{\left(1 + \frac{4\boldsymbol{R}}{(1-\boldsymbol{R})^2} \sin^2 \frac{\gamma}{2}\right)} \qquad (3, 27\ b)$$

determines the intensity distribution in the neighbourhood of a peak.

Furthermore R and T of the silver layers are regarded as constant in all the following graphs throughout the spectral region considered in the graphs. If the variation of R, T, etc., upon wavelength within the line were taken into account, the calculations would be rather tedious and only result in deviations in

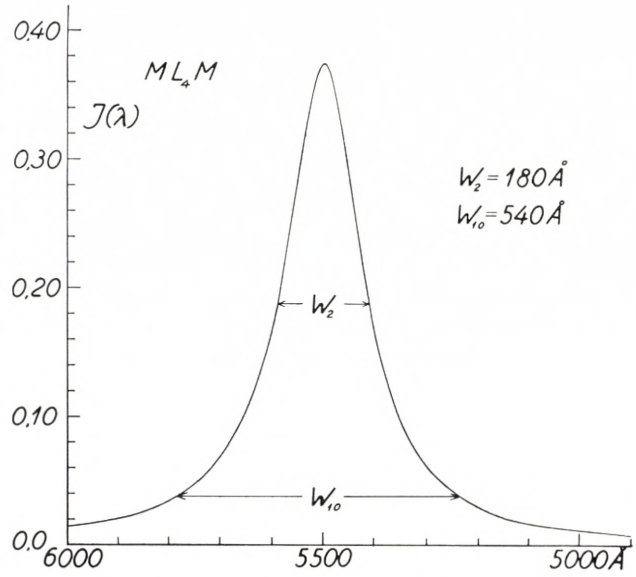

Fig. 9.
2nd order filter. W_2 calculated from (3,14) is 181 Å and $W_{10} = 3 \cdot W_2 = 543$ Å
$\nu - i\varkappa = 0.15 - i\ 3.36$.

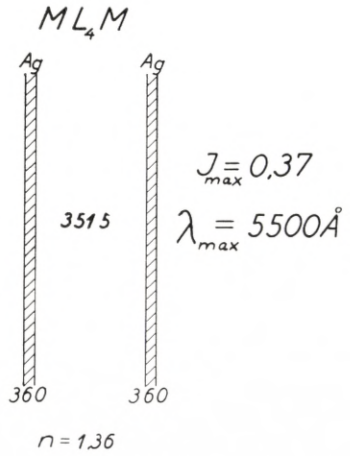

Fig. 10.
(All measures in Å).
FABRY-PEROT filter 2nd order. The peak of the 1st order is at about 10800 Å and the peak of the 3rd order at about 3750 Å. The line shape (2nd order) is shown in fig. 9.

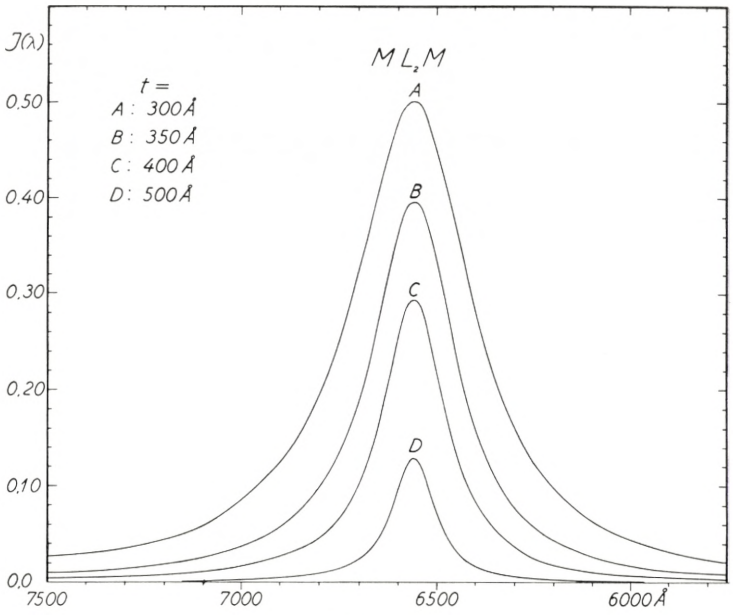

Fig. 11.

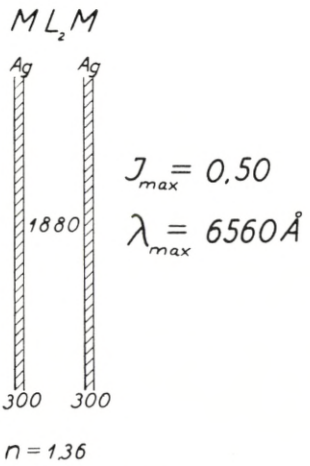

Fig. 12.
1st order filter ($m = 1$) (the peak of the 2nd order is at 3400 Å). (Curve A in fig. 11).

the "wings" of the line and even here the effect is small as compared with the experimental uncertainty in $v - i\varkappa$. The deviations will be the greatest for a filter of the first order.

In fig. 9 is shown the line shape of a FABRY-PEROT filter of the 2nd order, and fig. 10 shows the relative thicknesses of the thin layers. In fig. 11 line shapes have been calculated with different thicknesses t of the silver layers and with peak transmission at 6560 Å. The rapid decrease in $I_{\max}$ with increasing t is apparent.

Furthermore is it possible to calculate $R(\lambda)$ for a filter of the type $ML_{2m}M$ by means of (3, 2) or (3, 4). (3, 2) becomes

$$R(\lambda) = \frac{R \cdot \left| 1 - \sigma \boldsymbol{R} \cdot e^{-i(y-\alpha)} \right|^2}{\left| 1 - \boldsymbol{R} \cdot e^{-iy} \right|^2}; \quad (R = \boldsymbol{R}). \qquad (3, 28)$$

The wavelength scale is calculated by means of (3, 27 a). Fig. 13 and in fig. 14 show the results of such calculations of the intensity distribution $R(\lambda)$ in reflected light (at normal incidence).

In fig. 13 the same filter is considered as in fig. 11 Curve C in transmission. (Each silver layer has a thickness of 400 Å;

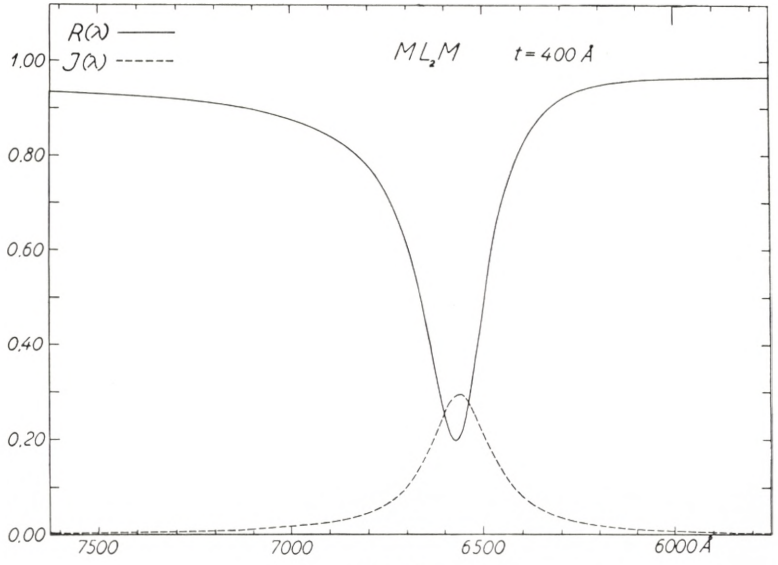

Fig. 13.
$R(\lambda)$ and $I(\lambda)$ for a FABRY-PEROT filter with the silver layers of equal thickness (t = 400 Å).

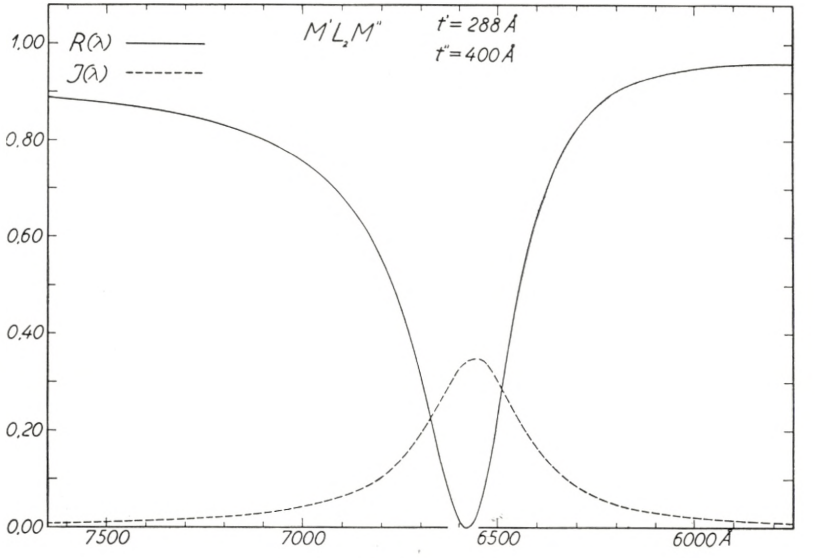

Fig. 14.
$R(\lambda)$ and $I(\lambda)$ for a FABRY-PEROT filter. The silver layers are of unequal thickness ($t'' = 400$ Å and $t' = 288$ Å) t' is determined in such a way that $\sigma \boldsymbol{R} = 1$; ($\boldsymbol{R} = \sqrt{R' \cdot R''}$).

$R = 0.908$). The small negative value of $\alpha = -0^0.466$ (Table 11) gives rise to an asymmetric line shape of $R(\lambda)$. Furthermore it should be noted that the minimum value of $R(\lambda)$ turns out to be as high as 0.20 and the minimum is found at a wavelength a little higher than the wavelength at which $I(\lambda)$ has a maximum in transmission.

In fig. 14 a filter $M'L_2M''$ is considered with the two silver layers of unequal thickness. $t'' = 400$ Å and $t' = 288$ Å is determined in such a way (from Table 11) that $\sigma \boldsymbol{R} = 1$; $\boldsymbol{R} = \sqrt{R' \cdot R''} = 0.864$ (the reflection takes place from the t' side of the filter), $R(\lambda) = 0$ at $y = \alpha = -1^0.060$ (see page 25). This calculation shows that it is possible to extinguish a spectral line by means of a reflection interference filter. $I_{max} = 0.34$ ($I_{max} = 0.45$ of a filter with the two silver layers of equal thickness and with a reflectivity equal to the mean reflectivity of the filter in fig. 14. $R = \sqrt{R' \cdot R''} = 0.86$).

Reflection interference filters with an opaque metal layer at the bottom (e. g. aluminium) have first been treated in theory

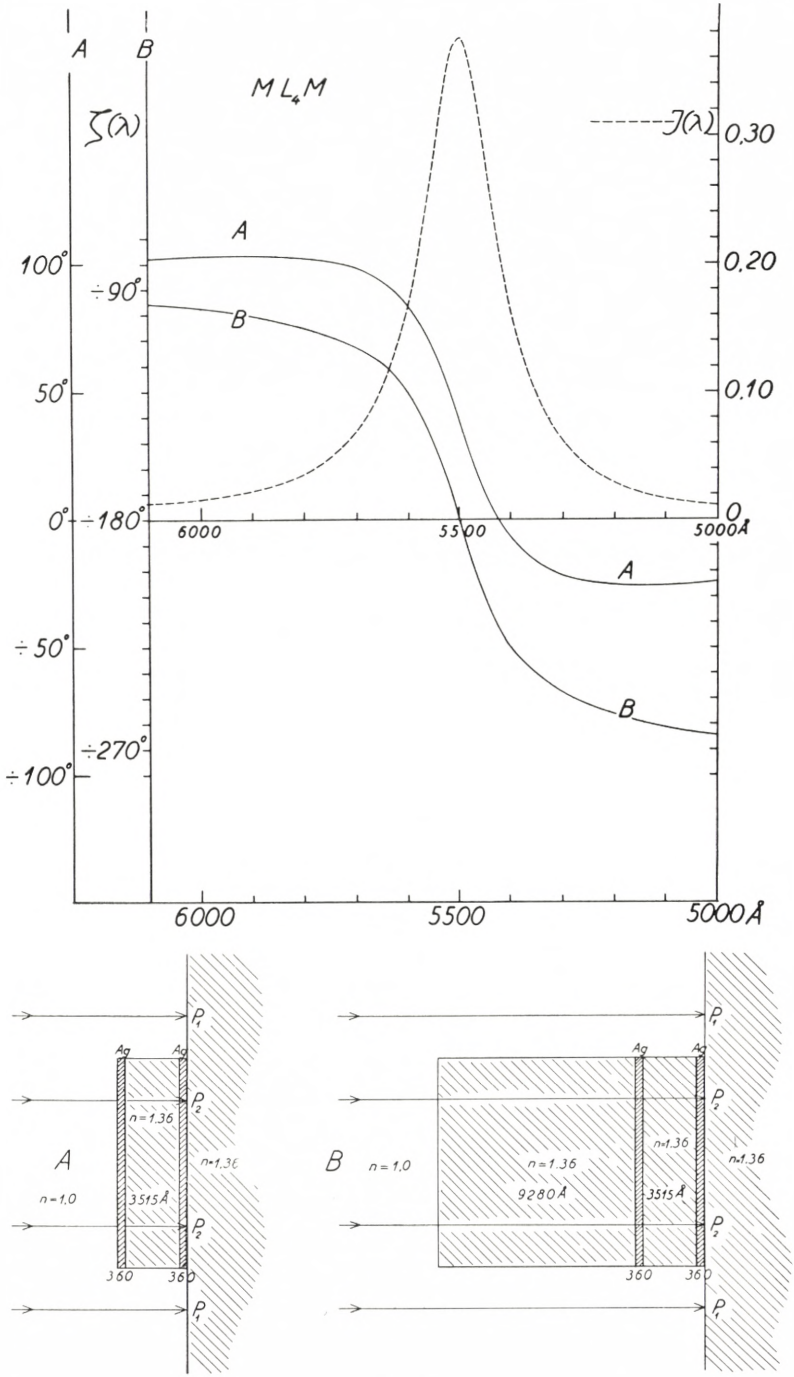

Fig. 15.

A FABRY-PEROT interference filter used as phase plate. Unbroken lines: A. The filter is on one side bounded by air. B. To the filter is added a thin dielectric layer in such a way that the phase difference at the peak is —180°. Broken line: $I(\lambda)$ for the filter (the same as the filter in fig. 10).

and practice by HADLEY and DENNISON [11]. These reflection filters have the great advantage of also being applicable to the infrared and ultraviolet spectral region, but have the disadvantage that rather broad spectral regions are reflected.

By means of (3, 2—3) and RYBNER's tables [4] it is furthermore easy to calculate the phase change at reflection and transmission, as a function of the wavelength, in the neighbourhood of a peak. As the phase change at transmission by interference filters is of special interest in the phase contrast microscope as shown by LOCQUIN [12], a calculation has been made in the case of the filter in fig. 10. The results are given in fig. 15. In the case of A the phase difference between P_2 (light passing through the phase plate) and P_1 (light passing outside the phase plate) is (from (3, 3))

$$\zeta(\lambda) = \left((\beta_{01} + \beta_{12}) - \frac{360}{\lambda} \cdot nd - \varepsilon(\lambda)\right) + \frac{360}{\lambda}(2t + d); \qquad (3,29)$$

t is the thickness of the silver layers and $\varepsilon(\lambda)$ is determined from $\varrho \cdot e^{i\varepsilon(\lambda)} = 1 - \boldsymbol{R} \cdot e^{-iy}$. — The phase changes at transmission through the silver layers are determined from Table 9. The approximations $\beta_{01} = \beta_{12} = \beta$ and $\beta = \beta_0 - k \cdot \lambda$ have been made. If, as in the case of B (fig. 15), a thin dielectric layer (with index of refraction n and thickness d_1) is added to the phase plate, the phase difference $-\frac{360}{\lambda} \cdot (n-1) \cdot d_1$ has to be added to $\zeta(\lambda)$ in (3, 29). In fig. 15 curve B, d_1 is determined in such a way that the phase difference is $-180°$ at $\lambda_m = 5500$ Å. The graphs correspond very closely to those previously published by DUFOUR [13]. By the use of a combination of the type B (fig. 15) it is possible to change from a negative to a positive contrast of the image by a variation of wavelength.

Calculation of $I(\lambda)_s$ and $I(\lambda)_p$ at an Oblique Angle of Incidence.

When the angle of incidence φ is increased from $\varphi = 0$, a shift of λ_m towards violet, and a splitting up in two components $\lambda_m^{(s)}$ and $\lambda_m^{(p)}$ result. The first problem now is to calculate $\lambda_m^{(s)}$, $\lambda_m^{(p)}$ when $\lambda_m^{(0)}$, $n(\lambda)$ and $\nu(\lambda) - i\varkappa(\lambda)$ are known. The calculation

is carried out by means of (3, 18):

$$m \cdot \lambda_m^{(s)} = 2\, dn \cos\chi + Z_s(\lambda_m^{(s)}),$$

where

$$Z_s(\lambda_m^{(s)}) = \left(\frac{360 - \delta_{10}^{(s)}(\lambda_m^{(s)}) - \delta_{12}^{(s)}(\lambda_m^{(s)})}{360}\right) \cdot \lambda_m^{(s)}$$

(and analogous equations for the p component).

A first approximation of $\lambda_{\frac{p+s}{2}}^{(1)} = \frac{\lambda_m^{(s)} + \lambda_m^{(p)}}{2}$ can be calculated by means of (3, 8) $m \cdot \lambda_{\frac{p+s}{2}}^{(1)} = 2\, dn \cos\chi + Z_0(\lambda_m^{(0)})$ with $2\, dn = m\lambda_m^{(0)} - Z_0(\lambda_m^{(0)})$, ($\lambda_m^{(0)}$ corresponds to λ_m at $\varphi = 0$ and $Z_0(\lambda_m^{(0)})$ is determined from fig. 8) and a second approximation $\lambda_{\frac{p+s}{2}}^{(2)}$ by $m \cdot \lambda_{\frac{p+s}{2}}^{(2)} = 2\, dn \cos\chi + Z_0\left(\lambda_{\frac{p+s}{2}}^{(1)}\right)$ and perhaps a third approximation has to be determined (by means of (3, 8) and fig. 8).

Now it is evident from Table 4 that δ $\left(\text{and } Z = \frac{180 - \delta}{180} \cdot \lambda\right)$ only show a small dependence upon ν when as at silver $\nu < 0.2$. For this reason $\frac{Z_0(\lambda)}{\lambda}$ (fig. 8) can be regarded as a function of $\frac{\varkappa(\lambda)}{n}$ and $\frac{\varkappa(\lambda) \cdot t}{\lambda}$ only: $\frac{Z_0(\lambda, t)}{\lambda} = F\left(\frac{\varkappa(\lambda)}{n}, \frac{\varkappa(\lambda) \cdot t}{\lambda}\right)$.

At oblique incidence we have (1, 12—13)

$$\frac{Z_s(\lambda, t)}{\lambda} = F\left(\frac{b}{n\cos\chi}, \frac{b \cdot t}{\lambda}\right) \quad \text{and} \quad \frac{Z_p(\lambda, t)}{\lambda} = F\left(\frac{h\cos\chi}{n}, \frac{b \cdot t}{\lambda}\right).$$

A first approximation of Z_s and Z_p can now be determined by means of fig. 8 if (λ, t) are transformed to (λ', t') by means of the equations

$$\frac{\varkappa(\lambda_s')}{n} = \frac{b\left(\lambda_{\frac{p+s}{2}}\right)}{n \cdot \cos\chi}; \quad \frac{\varkappa(\lambda_s')}{\lambda_s'} \cdot t_s' = \frac{b\left(\lambda_{\frac{p+s}{2}}\right) \cdot t}{\lambda_{\frac{p+s}{2}}}$$

and

$$\frac{\varkappa(\lambda'_p)}{n} = \frac{h\left(\lambda_{\frac{p+s}{2}}\right)}{n} \cdot \cos\chi; \quad \frac{\varkappa(\lambda'_p)}{\lambda'_p} \cdot t'_p = \frac{b\left(\lambda_{\frac{p+s}{2}}\right) \cdot t}{\lambda_{\frac{p+s}{2}}};$$

(λ'_s, t'_s) are then determined by

$$\varkappa(\lambda'_s) = \frac{b(\lambda)}{\cos\chi}; \quad t'_s = \frac{\lambda'_s}{\lambda} \cdot t \cdot \cos\chi \tag{3, 30}$$

and

$$(\lambda'_p, t'_p) \quad \text{by} \quad \varkappa(\lambda'_p) = h(\lambda) \cdot \cos\chi; \quad t'_p = \frac{\lambda'_p}{\lambda} \cdot \frac{b(\lambda) \cdot t}{\varkappa(\lambda'_p)} \tag{3, 31}$$

$\left(\text{where } \lambda = \lambda_{\frac{p+s}{2}}\right)$.

From (λ'_s, t'_s) we now determine $Z_0(\lambda'_s, t'_s)$ from fig. 8 and we then get $Z_s\left(\lambda_{\frac{p+s}{2}}\right) = \frac{\lambda_{\frac{p+s}{2}}}{\lambda'_s} \cdot Z_0(\lambda'_s, t'_s)$. Finally λ_s is determined by $m\lambda_s = 2\,dn\cos\chi + Z_s\left(\lambda_{\frac{p+s}{2}}\right)$ and λ_p is determined in quite an analogous way. $b(\lambda)$, $h(\lambda)$ are determined from Tables 1—3 corresponding to $\varkappa = \varkappa\left(\lambda_{\frac{p+s}{2}}\right)$. ($\lambda_0 = \lambda_m^{(0)}$; $\lambda_s = \lambda_m^{(s)}$ and $\lambda_p = \lambda_m^{(p)}$).

Now the same calculation must be repeated with λ_s instead of λ in (3, 30) and λ_p instead of λ in (3, 31) and a further repetition may be necessary if (λ_s, λ_p) deviate more than 20 Å from the previous approximation (for a filter of the first order).

Above, the index of refraction n of the dielectric has been regarded as independent of the wavelength and equal for both the s and p component. However, dispersion as well as birefringence can easily be taken into account in the formulae (3, 30—31) if necessary.

When λ_s and λ_p have been calculated in the way mentioned above, line shapes can be calculated by (3, 27) when first the s and p components of R and T have been calculated by means of (1, 12—13) and (3, 23—24) $\left(\text{with } x = \frac{4\pi t}{\lambda}(a - ib)\right)$.

To show the applicability of the above procedure calculations (for different φ) have been made in the case of a FABRY-PEROT filter (1st order) with $\lambda_0 = 6560$ Å, $t = 350$ Å and $n = 1.36$.

(At $\varphi = 0$ the line shape of this filter is seen in fig. 11 Curve B). The different approximations before reaching the correct values of λ_s and λ_p are shown in Table 15 and the line shapes in figs. 16—18.

TABLE 15. ($\lambda_0 = 6560$ Å)

φ		15°	30°	45°	60°	75°
From fig. 8	$\lambda^{(1)}_{\frac{s+p}{2}}$	6466	6198	5836	5375	5028 Å
	$\lambda^{(2)}_{\frac{s+p}{2}}$	6466	6206	5833	5440	5139
	$\lambda^{(3)}_{\frac{s+p}{2}}$	..	..	5833	5435	5120
From fig. 8 and (3,30—31)	$\lambda^{(1)}_s$	..	..	5632	5106	4695
	$\lambda^{(1)}_p$	..	..	6047	5760	5624
	$\lambda^{(2)}_s$	..	..	5647	5135	4730
	$\lambda^{(2)}_p$	..	..	6038	5770	5565
Directly from (3,23—24)	$\lambda^{(3)}_s$	..	..	5642	5130	4720
	$\lambda^{(3)}_p$	..	..	6039	5770	5580
Calculated from (3,32)	"n" ...	1.534	1.542	1.553	1.556	1.559

HADLEY and DENNISON [11 a] have used an approximate formula to enable a direct calculation of n from measurements of $\lambda_{\frac{p+s}{2}} = \dfrac{\lambda_p + \lambda_s}{2}$ at oblique incidence.

From (3, 6 a)

$$\frac{360}{\lambda_0} \cdot 2\, dn - 2\, \delta_0(\lambda_0) = 360\, (m - 1)$$

and

$$180 \cdot \left(\frac{1}{\lambda_s} + \frac{1}{\lambda_p}\right) \cdot 2\, dn \cdot \cos\chi - (\delta_s(\lambda_s) + \delta_p(\lambda_p)) = 360\, (m - 1)$$

they get

$$\frac{360}{\lambda_0} \cdot 2\, dn = \frac{360}{2}\left(\frac{1}{\lambda_s} + \frac{1}{\lambda_p}\right) \cdot 2\, dn \cos\chi + 2\,\delta_0 - (\delta_s + \delta_p).$$

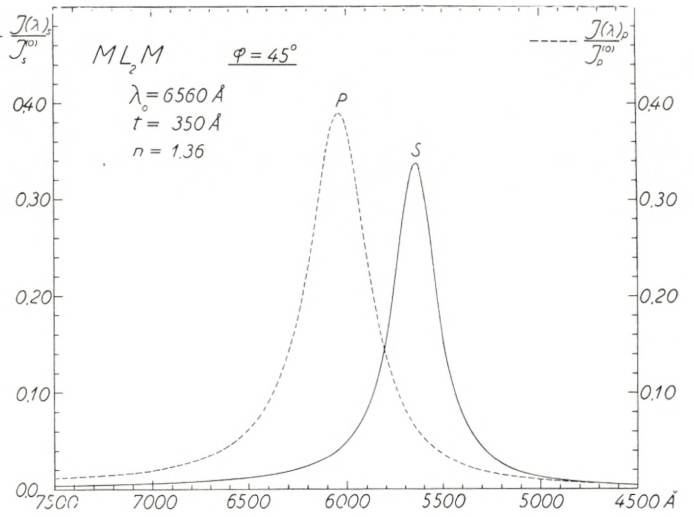

Fig. 16.

Then the approximation $2\delta_0(\lambda_0) = \delta_s(\lambda_s) + \delta_p(\lambda_p)$ is introduced and the following formula results:

$$\cos\chi = \frac{\lambda_{\frac{s+p}{2}}}{\lambda_0}$$

or

$$n = \frac{\sin\varphi}{\sqrt{1 - \left(\frac{\lambda_{\frac{p+s}{2}}}{\lambda_0}\right)^2}} \left(\text{with } \frac{1}{\lambda_{\frac{p+s}{2}}} = \frac{1}{\lambda_p} + \frac{1}{\lambda_s} \simeq \frac{1}{\frac{\lambda_p + \lambda_s}{2}} \right). \quad (3, 32)$$

If this approximation should be useful then n calculated from (3, 32) by substituting the (λ_s, λ_p) values from Table 15 should turn out to be about 1.36. However, as shown below in Table 15 "n" calculated from (3, 32) is as high as 1.55. This shows that the approximation (3, 32) cannot be used (by filters of lower order) and this explains why HADLEY and DENNISON [11a] find values of n much too high. λ_s and λ_p are not only dependent upon λ_0 (at $\varphi = 0$), n and φ but also upon $\varkappa(\lambda)$, and this will particularly be the case for a filter of the first order ($m = 1$) as shown in figs. 16—18. At higher orders ($m \simeq 8$—10) the splitting up $\lambda_p - \lambda_s$ is m times smaller, and the error in $\lambda_{\frac{p+s}{2}}$ in using

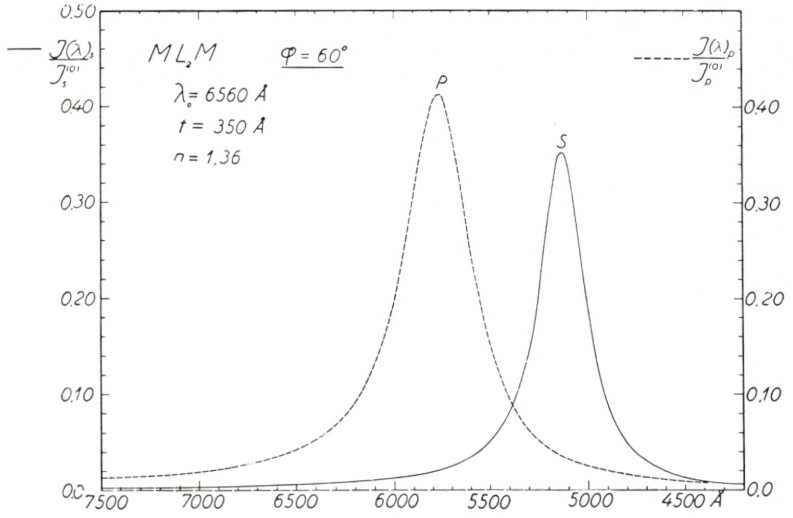

Fig. 17.

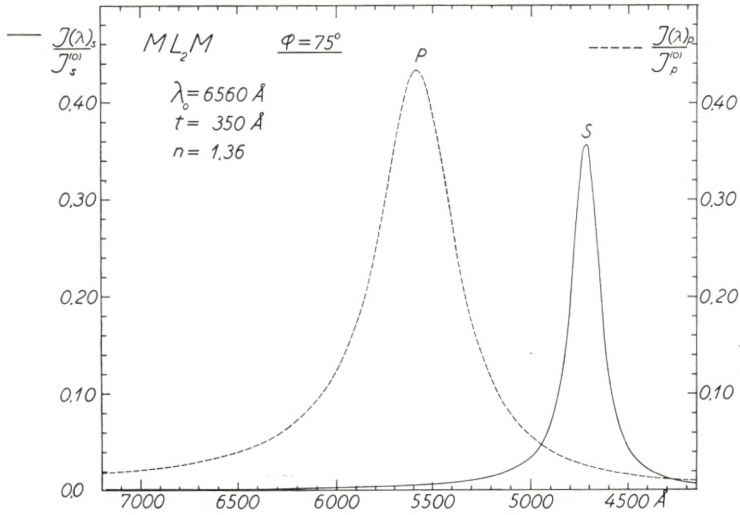

Fig. 18.

the approximation $\delta_0(\lambda_0) = \dfrac{\delta_s(\lambda_s) + \delta_p(\lambda_p)}{2}$ is m times smaller; in this case λ_s and λ_p will be nearly independent of $\varkappa(\lambda)$ and (3, 32) can be employed with a tolerable approximation.

(λ_s, λ_p) can easily be measured by a spectroscope at various

angles of incidence and we hereby obtain information on $n(\lambda)$ and $\varkappa(\lambda)$ (especially for a filter of the first order). Moreover, determinations of W_2 and I_{max} by means of a spectrophotometer fix R and T of the silver layers.

If the incident light is unpolarized and has the intensity $I_0 = 2 \cdot I_s^{(0)} = 2 \cdot I_p^{(0)}$, $I(\lambda)$ of the transmitted light is

$$I(\lambda) = \frac{I_0}{2}\left(\frac{I(\lambda)_s}{I_s^{(0)}} + \frac{I(\lambda)_p}{I_p^{(0)}}\right)$$

(the ordinates of the s and p curves of figs. 16—18 have to be added together and divided by 2).

The degree of polarization (the s direction compared with the p direction) will at the wavelength λ_s be $\frac{I(\lambda_s)_s}{I(\lambda_s)_p}$ and the degree of polarization at the wavelength λ_p (the p direction compared with the s direction) $\frac{I(\lambda_p)_p}{I(\lambda_p)_s}$, this can easily be read off figs. 16—18. If the FABRY-PEROT filter should be used at oblique incidence to isolate a spectral line and simultaneously act as polarizer it would be best to use the p component.

TABLE 16.

$$\cos\chi = \sqrt{1 - \frac{\sin^2\varphi}{n^2}}$$

n \ φ	5°	10°	15°	30°	45°	60°	75°	80°
1.30	0.99775	0.99104	0.97998	0.92308	0.83913	0.74580	0.66927	0.65278
1.31	.99778	.99118	.98029	.92429	.84181	.75031	.67551	.65943
1.32	.99782	.99131	.98059	.92548	.84442	.75469	.68155	.66587
1.33	.99785	.99144	.98088	.92664	.84696	.75895	.68742	.67210
1.34	.99788	.99157	.99117	.92778	.84944	.76309	.69310	.67816
1.35	.99791	.99169	.98145	.92889	.85185	.76712	.69861	.68399
1.36	.99794	.99182	.98172	.92997	.85421	.77104	.70396	.68967
1.37	.99797	.99193	.98199	.93102	.85651	.77486	.70915	.69518
1.38	.99800	.99205	.98226	.93205	.85875	.77857	.71420	.70052
1.39	.99803	.99217	.98251	.93306	.86094	.78219	.71910	.70572
1.40	.99806	.99228	.98276	.93405	.86307	.78571	.72386	.71076
1.52	.99835	.99343	.98535	.94417	.88483	.82122	.77132	.76089
2.36	.99932	.99729	.99397	.97730	.95406	.93024	.91240	.90877

Before leaving the theory of interference filters of the FABRY-PEROT type, the TURNER frustrated total reflection filter should be briefly mentioned. This ingeniously constructed filter (indicated by A. F. TURNER [14] and [15]) is based on frustrated total reflection instead of reflection from silver layers and is constructed by evaporation on the hypotenuse surface of a flint glass prism, first a low index layer, then the high index spacer layer and again another low index layer, and finally another flint glass prism is cemented to the first. As no absorption occurs, R can reach a value so close to 1 that W_2 can be as low as 10 Å, the limit is set by the crystalline structure of the fluoride layers [16]. Because of the oblique angle of incidence (high value of χ) two components (s and p) result, each with an intensity about 0.50. The filter has the disadvantage that it is of a limited area and that a very small deviation $\left(\frac{1}{3}^{\circ}\right)$ from parallelism of the incident light will result in a shift greater than $\frac{1}{2} W_2$ (follows from (3, 19)). Furthermore, in most applications one of the components (s or p) must be extinguished by a polarizer. However, BILLINGS [17] has tried to construct a filter of this type with a birefringent material as spacer layer to avoid a splitting up in two components at a definite angle of incidence. The theory of a TURNER filter is the same as for a FABRY-PEROT filter, but the reflectivity must be calculated by special equations deduced directly from the MAXWELL equations of electrodynamics [17] and [17 a].

Before more complicated filters are treated a short summary of the most characteristic properties of the FABRY-PEROT filter will be given. The contrast factor $F = \frac{I_{\max}}{I_{\min}}$ is determined by the reflectivity R alone, $R < 1 - A$, where A is the absorption coefficient in the silver layer, i. e. $F < \left(\frac{1 + R_{\infty}}{1 - R_{\infty}}\right)^2 = \left(\frac{2 - A}{A}\right)^2$.

The half intensity band width W_2 can be made as small as 40—50 Å, when the order m is sufficiently high. However, to extinguish the neighbouring peaks it is necessary to combine the filter with another interference filter of lower order or with absorption filters, but then $I_{\max}$ drops considerably. The most serious drawback of the FABRY-PEROT filter is that the contrast factor F (for a reasonable $I_{\max}$) is only about 200 (Tables 6—13),

which means that this filter cannot be used for an efficient isolation of spectral lines. Moreover the colour will be impure (with an I_{max} as high as 0.40) on account of the spectral region far from the peak. For this reason it would be of some value to examine the possibility of making filters with higher contrast factors F consisting of three or four silver layers and two or three dielectric layers, respectively (with the same or multiple thickness).

§ 4. Interference Filters with *Three* Systems of Reflective Layers I, II, and III (e. g. three silver layers).

Three systems of thin layers are considered (fig. 19). As previously when considering two systems we make the assumption that R, T, δ, β, etc., belonging to each of the systems I, II, and III, considered separately, vary only slightly with the wavelength $\left(\text{within each wavelength span of about } \frac{\lambda}{10}\right)$ or in other words I, II, and III must not be interference filters themselves (e. g. each of the systems may consist of a silver layer combined with quarter wavelength layers of dielectrics).

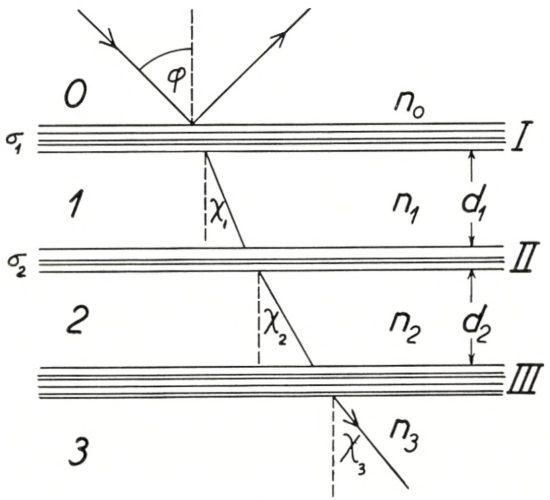

Fig. 19.
The notations used are analogous to those used in fig. 6

$$\sigma_1 \cdot e^{i\alpha_1} = 1 - \frac{t_{01} \cdot t_{10}}{r_{01} \cdot r_{10}} \qquad \sigma_2 \cdot e^{i\alpha_2} = 1 - \frac{t_{12} \cdot t_{21}}{r_{12} \cdot r_{21}}$$

If now II + III is regarded as a single system (II in fig. 4) we deduce directly from the fundamental equations (2, 1—3) when Index 2 is interchanged with Index 3:

$$r_{03} = \frac{r_{01}\,(1 - r_{10}\cdot r_{13}\cdot\sigma_1\cdot e^{-ix_1 + i\alpha_1})}{1 - r_{10}\cdot r_{13}\cdot e^{-ix_1}}; \quad t_{03} = \frac{t_{01}\cdot t_{13}\cdot e^{-i\frac{x_1}{2}}}{1 - r_{10}\cdot r_{13}\cdot e^{-ix_1}}$$

and once again from (2, 1—3) (now II and III in fig. 19 are equal to I and II in fig. 4) (r_{13}, t_{13}) can be expressed by

$$r_{13} = \frac{r_{12}\,(1 - r_{21}\cdot r_{23}\cdot\sigma_2\cdot e^{-ix_2 + i\alpha_2})}{1 - r_{21}\cdot r_{23}\cdot e^{-ix_2}}; \quad t_{13} = \frac{t_{12}\cdot t_{23}\cdot e^{-i\frac{x_2}{2}}}{1 - r_{21}\cdot r_{23}\cdot e^{-ix_2}}$$

and when (r_{13}, t_{13}) are substituted in (r_{03}, t_{03}) we obtain:

$$r_{03} = \frac{r_{01}\,((1 - r_{21}\cdot r_{23}\cdot e^{-ix_2}) - e^{-ix_1 + i\alpha_1}\cdot r_{10}\cdot r_{12}\cdot\sigma_1\,(1 - r_{21}\cdot r_{23}\cdot\sigma_2\cdot e^{-ix_2 + i\alpha_2}))}{(1 - r_{21}\cdot r_{23}\cdot e^{-ix_2}) - e^{-ix_1}\cdot r_{10}\cdot r_{12}\,(1 - r_{21}\cdot r_{23}\cdot\sigma_2\cdot e^{-ix_2 + i\alpha_2})}$$

and

$$t_{03} = \frac{t_{01}\cdot t_{12}\cdot t_{23}\cdot e^{-i\frac{x_1}{2} - i\frac{x_2}{2}}}{(1 - r_{21}\cdot r_{23}\cdot e^{-ix_2}) - e^{-ix_1}\cdot r_{10}\cdot r_{12}\,(1 - r_{21}\cdot r_{23}\cdot\sigma_2\cdot e^{-ix_2 + i\alpha_2})}$$

or by introducing the notations

$$r_{01} = \sqrt{R_{01}}\cdot e^{i\delta_{01}} \quad r_{12} = \sqrt{R_{12}}\cdot e^{i\delta_{12}} \ldots \text{ etc.} \quad t_{01} = \sqrt{T_{01}}\cdot e^{i\beta_{01}} \ldots \text{ etc.},$$

and

$$\boldsymbol{R}_1 = \sqrt{R_{10}\cdot R_{12}}; \quad y_1 = x_1 - \delta_{10} - \delta_{12}; \quad x_1 = \frac{360}{\lambda}\cdot 2\,d_1 n_1 \cos\chi_1 \quad (4, 1$$

related to the dielectric layer 1 and

$$\boldsymbol{R}_2 = \sqrt{R_{21}\cdot R_{23}}; \quad y_2 = x_2 - \delta_{21} - \delta_{23}; \quad x_2 = \frac{360}{\lambda}\cdot 2\,d_2\cdot n_2\cdot\cos\chi_2 \,(4, 1$$

related to the dielectric layer 2.

We obtain the fundamental formulae:

$$\sqrt{R_{03}(\lambda)}\cdot e^{i\delta_{03}} = \frac{\sqrt{R_{01}}\cdot e^{i\delta_{01}}\cdot((1 - \boldsymbol{R}_2\cdot e^{-iy_2}) - e^{-i(y_1 - \alpha_1)}\cdot\boldsymbol{R}_1\sigma_1(1 - \boldsymbol{R}_2\cdot\sigma_2\cdot e^{i(y_2 - \alpha_2)}))}{(1 - \boldsymbol{R}_1\cdot e^{-iy_1} - \boldsymbol{R}_2\cdot e^{-iy_2} + \boldsymbol{R}_1\cdot\boldsymbol{R}_2\cdot\sigma_2\cdot e^{-i(y_1 + y_2) + i\alpha_2})} (4,$$

$$\sqrt{T_{03}(\lambda)}\cdot e^{i\beta_{03}} = \frac{\sqrt{T_{01}\cdot T_{12}\cdot T_{23}}\cdot e^{i\left(\beta_{01}+\beta_{12}+\beta_{23}\right)-i\left(\frac{x_1}{2}+\frac{x_2}{2}\right)}}{\left(1-\boldsymbol{R}_1\cdot e^{-iy_1}-\boldsymbol{R}_2\cdot e^{iy_2}+\boldsymbol{R}_1\cdot\boldsymbol{R}_2\cdot\sigma_2\cdot e^{-i(y_1+y_2)+i\alpha_2}\right)}. \qquad (4,\,3)$$

The intensity distribution in transmission is given by

$$I(\lambda) = \frac{\boldsymbol{T}_1\cdot\boldsymbol{T}_2\cdot\boldsymbol{T}_3}{\left|1-\boldsymbol{R}_1\cdot e^{-iy_1}-\boldsymbol{R}_2\cdot e^{-iy_2}+\boldsymbol{R}_1\cdot\boldsymbol{R}_2\cdot\sigma_2\cdot e^{-i(y_1+y_2)+i\alpha_2}\right|^2}. \qquad (4,\,4)$$

When the following notations are introduced in (4, 3):

$$\boldsymbol{T}_1 = T_{01}\cdot\frac{n_1\cos\chi_1}{n_0\cos\varphi};\quad \boldsymbol{T}_2 = T_{12}\cdot\frac{n_2\cdot\cos\chi_2}{n_1\cdot\cos\chi_1}\quad\text{and}\quad \boldsymbol{T}_3 = T_{23}\cdot\frac{n_3\cos\chi_3}{n_2\cos\chi_2}$$

($\boldsymbol{T}_1$, $\boldsymbol{T}_2$, and $\boldsymbol{T}_3$ denote the energy transmitted through each of the systems I, II, or III considered separately).

$I(\lambda)$ is maximum or minimum when the denominator vice versa is minimum or maximum (as it is assumed that the numerator is almost independent of the wavelength).

The denominator is

$$\left.\begin{aligned}
&(1-\boldsymbol{R}_1 e^{-iy_1}-\boldsymbol{R}_2\cdot e^{-iy_2}+\boldsymbol{R}_1\boldsymbol{R}_2\sigma_2\cdot e^{-i(y_1+y_2-\alpha_2)})\\
&\times(1-\boldsymbol{R}_1 e^{iy_1}-\boldsymbol{R}_2 e^{iy_2}+\boldsymbol{R}_1\boldsymbol{R}_2\sigma_2\cdot e^{i(y_1+y_2-\alpha_2)}) =\\
&1+\boldsymbol{R}_1^2+\boldsymbol{R}_2^2+(\sigma_2\boldsymbol{R}_1\boldsymbol{R}_2)^2-2\,\boldsymbol{R}_2\cos y_2-2\,\boldsymbol{R}_1\cos y_1\\
&+2\sigma_2\boldsymbol{R}_1\boldsymbol{R}_2\cos(y_1+y_2-\alpha_2)+2\,\boldsymbol{R}_1\boldsymbol{R}_2\cos(y_2-y_1)\\
&-2\,\sigma_2\boldsymbol{R}_1\boldsymbol{R}_2^2\cos(y_1-\alpha_2)-2\,\sigma_2\boldsymbol{R}_2\boldsymbol{R}_1^2\cos(y_2-\alpha_2).
\end{aligned}\right\} \qquad (4,\,5)$$

We now make the assumption that $y_1 = y_2$ and obtain

$$\left.\begin{aligned}
&+\boldsymbol{R}_1^2+\boldsymbol{R}_2^2+(\sigma_2\boldsymbol{R}_1\boldsymbol{R}_2)^2-2\,(\boldsymbol{R}_1+\boldsymbol{R}_2)\cos y+2\,\sigma_2\boldsymbol{R}_1\boldsymbol{R}_2\cos(2\,y-\alpha_2)\\
&-2\,\sigma_2\boldsymbol{R}_1\boldsymbol{R}_2\,(\boldsymbol{R}_1+\boldsymbol{R}_2)\cos(y-\alpha_2).
\end{aligned}\right\} \qquad (4,\,6)$$

The minimum or maximum of the denominator is determined by the fact that the first derivative should be equal to zero, i. e.

$$+\boldsymbol{R}_2)\,(\sin y+\sigma_2\cdot\boldsymbol{R}_1\boldsymbol{R}_2\sin(y-\alpha_2))-2\,\sigma_2\boldsymbol{R}_1\boldsymbol{R}_2\sin(2\,y-\alpha_2)=0. \qquad (4,\,7)$$

So far no approximations have been made, but now we introduce the approximation $\alpha_2 = 0$ (from Tables 6—13 it is to be expected that this will be a good approximation when the absorption is low and the reflectivity high of the central System II).

In the case of $\alpha_2 = 0$ (4, 7) simply reduces to

$$\sin y \cdot ((\boldsymbol{R}_1 + \boldsymbol{R}_2)(1 + \sigma_2 \cdot \boldsymbol{R}_1 \boldsymbol{R}_2) - 4\,\sigma_2 \cdot \boldsymbol{R}_1 \boldsymbol{R}_2 \cdot \cos y) = 0 .$$

Max. or min. occur when $\sin y = 0$ *i.e.* $y = 360^\circ \cdot (m-1)$ and when

$$\cos y = \frac{(\boldsymbol{R}_1 + \boldsymbol{R}_2)(1 + \sigma_2 \cdot \boldsymbol{R}_1 \cdot \boldsymbol{R}_2)}{4\,\sigma_2 \cdot \boldsymbol{R}_1 \cdot \boldsymbol{R}_2} . \qquad (4, 8)$$

This means: If the quantity (4, 8) is greater than or equal to unity, $I(\lambda)$ will only have a single maximum (for a specific order m) at $y = 360^\circ \cdot (m-1)$; $m = 1, 2, 3 \ldots\ldots$

If, however, the quantity (4, 8) is less than unity, two neighbouring maxima of $I(\lambda)$ will occur at $y = \pm v + 360^\circ \cdot (m-1)$; $m = 1, 2, 3 \ldots\ldots$ determined by (4, 8) and now a relative minimum at $y = 360^\circ \cdot (m-1)$.

If $R_{10} = R_{23}$ and $R_{12} = R_{21}$ (especially I and III identical), we simply have $\boldsymbol{R}_1 = \boldsymbol{R}_2 = \boldsymbol{R}$, and the condition of obtaining a single peak (for a specific order) is in this symmetrical case:

$$\frac{1 + \sigma_2 \boldsymbol{R}^2}{2\,\sigma_2 \boldsymbol{R}} \geqslant 1 \qquad \text{or} \qquad \boldsymbol{R} \leqslant 1 - \sqrt{1 - \frac{1}{\sigma_2}} . \qquad (4,9)$$

If $\boldsymbol{R} = \sqrt{R_{10} \cdot R_{12}}$ and the approximation (3, 21) $\sigma_2 = \dfrac{1-A}{R_{12}}$ are introduced into (4, 8), we arrive at

$$\sqrt{R_{12}} \geqslant \frac{2\,(1-A)\sqrt{R_{10}}}{(1-A)R_{10} + 1} . \qquad (4, 10)$$

Dufour has in 1949 [18] developed an approximate theory for interference filters with three silver layers. He requires that $R_{20} = R_{23}$ at $y = 360^\circ \cdot (m-1)$ and from this condition a relation between R_{12} and R_{10} (similar to (4, 10)) is obtained. $R_{20} = R_{23}$ will give the highest value of $I_{\max}$ for a definite value of $R_{20} \cdot R_{23}$

(see page 23). However, in the case of three reflecting layers as opposed to a FABRY-PEROT filter, the contrast factor is not solely dependent on $R_{20} \cdot R_{23}$, so the introduction of the condition $R_{20} = R_{23}$ seems unnatural. But when $A = 0$, DUFOUR's equation is identical with (4, 10), and when the absorption coefficient A is small, DUFOUR's equation only deviates slightly from (4, 10).

When only one peak is present ((4, 9) is satisfied) I_{max} and $F = \frac{I_{max}}{I_{min}}$ are determined approximately ($\alpha_2 = 0$) directly by (4, 4) on introducing $y = 360° \cdot (m-1)$ and $y = 180° \cdot (2m-1)$, respectively:

$$I_{max} = \frac{\boldsymbol{T}_1 \cdot \boldsymbol{T}_2 \cdot \boldsymbol{T}_3}{(1 - \boldsymbol{R}_1 - \boldsymbol{R}_2 + \sigma_2 \cdot \boldsymbol{R}_1 \cdot \boldsymbol{R}_2)^2} \qquad (4, 11)$$

and

$$F = \frac{I_{max}}{I_{min}} = \left(\frac{1 + \boldsymbol{R}_1 + \boldsymbol{R}_2 + \sigma_2 \cdot \boldsymbol{R}_1 \cdot \boldsymbol{R}_2}{1 - \boldsymbol{R}_1 - \boldsymbol{R}_2 + \sigma_2 \cdot \boldsymbol{R}_1 \cdot \boldsymbol{R}_2}\right)^2. \qquad (4, 12)$$

However, when using silver layers this contrast factor will only be correct for higher order filters. For $m = 1$ or 2, R and T will vary considerably from λ_{max} to λ_{min}, the true contrast factor on the red side of the peak will be greater than F calculated from (4, 12), and the true contrast factor on the violet side of the peak will be smaller than (4, 12).

Calculation of W_2 and W_{10}.

In the case of $\alpha_2 = 0$ and $y_1 = y_2 = y$ (4, 4) can conveniently be written as follows:

$$I(\lambda) = \frac{\boldsymbol{T}_1 \cdot \boldsymbol{T}_2 \cdot \boldsymbol{T}_3}{\boldsymbol{A} + \boldsymbol{B} \sin^2 \frac{y}{2} + \boldsymbol{C} \cdot \sin^4 \frac{y}{2}} \qquad (4, 13)$$

with

$$\boldsymbol{A} = (1 - \boldsymbol{R}_1 - \boldsymbol{R}_2 + \sigma_2 \boldsymbol{R}_1 \cdot \boldsymbol{R}_2)^2 \qquad (4, 13\,a)$$

$$\boldsymbol{B} = 4\,((\boldsymbol{R}_1 + \boldsymbol{R}_2)(1 + \sigma_2 \boldsymbol{R}_1 \cdot \boldsymbol{R}_2) - 4\,\sigma_2 \boldsymbol{R}_1 \boldsymbol{R}_2) \qquad (4, 13\,b)$$

and

$$\boldsymbol{C} = 16\,\sigma_2 \boldsymbol{R}_1 \cdot \boldsymbol{R}_2. \qquad (14, 13\,c)$$

When only one peak is present $\boldsymbol{B} \geqslant 0$ and if two peaks exist, we have $\boldsymbol{B} < 0$, and the wavelengths of the two peaks are determined by (4, 8) or by

$$\sin \frac{y}{2} = \pm \sqrt{\frac{\boldsymbol{B}}{2\,\boldsymbol{C}}}.$$

In the case of one peak the W_k defined by

$$I\left(\lambda_m \pm \frac{W_k}{2}\right) = \frac{1}{k} \cdot I\,(\lambda_m)$$

are determined by means of

$$(k-1)\,\boldsymbol{A} = \boldsymbol{B} \sin^2 \frac{\gamma_k}{2} + \boldsymbol{C} \sin^4 \frac{\gamma_k}{2}$$

and by

$$W_k = \frac{\gamma_k \cdot \lambda_m}{f \cdot 180}, \quad f = -\frac{\lambda_m}{360} \cdot \left(\frac{dy}{d\lambda}\right)_{\lambda = \lambda_m}$$

when $y = 360 \cdot (m-1) \pm \gamma_k$ corresponds to $\lambda_m \mp \frac{W_k}{2}$. In the case of $\boldsymbol{B} = 0$ (the line shape corresponds to the "limit" between one and two peaks) these equations can easily be solved; we obtain:

$$\sin \frac{\gamma_k}{2} = \sqrt[4]{\frac{(k-1) \cdot \boldsymbol{A}}{\boldsymbol{C}}}$$

and approximately

$$W_k = \frac{2\,\lambda_m}{\pi \cdot f} \sqrt[4]{\frac{(k-1) \cdot \boldsymbol{A}}{\boldsymbol{C}}}$$

and for $k = 2$

$$W_2 = \frac{\lambda_m \cdot \sqrt{1 - \boldsymbol{R}_1 - \boldsymbol{R}_2 + \sigma_2 \boldsymbol{R}_1 \boldsymbol{R}_2}}{\pi \cdot f \cdot \sqrt[4]{\sigma_2 \boldsymbol{R}_1 \cdot \boldsymbol{R}_2}}, \tag{4, 14}$$

and we further get the relation

$$W_{10} = \sqrt{3} \cdot W_2. \tag{4, 15}$$

Table 17 contains the results of calculations made in the special case of 3 silver layers placed in a dielectric with $n = 1.36$

TABLE 17.

λ $\nu - i\varkappa$ t''	$R_{12}(=R'')$ $T_{12}(=T'')$ σ_2	$R_{10}(=R')$ $T_{10}(=T')$	t' t'' in Å	I_{max}	$F = \frac{I_{max}}{I_{min}}$	W_2 (2·order) in Å	W_{10} (2·order) in Å
4000 0.18—i 1.95 600	0.7708 0.0725 1.0865	0.6684 0.1796	449 600	0.152	580	260	450
4000 0.18—i 1.95 500	0.7155 0.1297 1.1706	0.5342 0.3217	334 500	0.297	162	357	618
4500 0.14—i 2.42 500	0.8150 0.0868 1.1031	0.5914 0.3095	297 500	0.406	420	317	549
5000 0.14—i 2.89 500	0.8649 0.0573 1.0644	0.6575 0.2577	286 500	0.404	1000	282	489
5500 0.15—i 3.36 500	0.8951 0.0389 1.0422	0.7126 0.2105	280 500	0.379	2300	252	436
6000 0.15—i 3.82 500	0.9188 0.0278 1.0296	0.7508 0.1830	269 500	0.386	4800	231	400
6560 0.13—i 4.27 500	0.9398 0.0218 1.0228	0.7702 0.1789	249 500	0.463	7700	222	385
6560 0.13—i 4.27 400	0.9084 0.0498 1.0542	0.6583 0.2872	194 400	0.585	1400	339	587
7100 0.14—i 4.68 450	0.9363 0.0271 1.0286	0.7416 0.2077	217 450	0.516	5000	268	464
7680 0.15—i 5.11 450	0.9438 0.0227 1.0237	0.7615 0.1900	212 450	0.507	7300	265	458

$\boldsymbol{R}_1 = \boldsymbol{R}_2 = \boldsymbol{R}$ and $y_1 = y_2$ (i. e. a symmetrical filter as shown in figs. 22 and 24). The calculations are carried out by means of Tables 6—13. When the thickness of the central silver layer t'' has been chosen, $\boldsymbol{R}$ can be calculated from (4, 9)

$$\left(\boldsymbol{R} = 1 - \sqrt{1 - \frac{1}{\sigma_2}};\ \boldsymbol{R} = \sqrt{R' \cdot R''}\right)$$

so that only one peak results. Next, R', t', T' and from these quantities $I_{\max}$ and $F = \dfrac{I_{\max}}{I_{\min}}$ are calculated by means of (4, 11—12), and finally W_2 and W_{10} are calculated from (4, 14—15).

In practice, however, α_2 is not zero, but has some small value (Tables 6—13). To get an idea of the true intensity distribution $I(\lambda)$ in the neighbourhood of λ_m numerical calculations have been carried out for different values of t' and t'' for the silver layers, directly from (4, 4) written in the form

$$I(\lambda) = \frac{\boldsymbol{T}_1^2 \cdot \boldsymbol{T}_2}{\varrho_1^2 \left| 1 - \dfrac{\varrho_2}{\varrho_1} \cdot e^{i(\varepsilon_2 - \varepsilon_1) - iy} \right|^2} = \frac{\boldsymbol{T}_1^2 \cdot \boldsymbol{T}_2}{(\varrho_1 \cdot \varrho_3)^2} \qquad (4, 16)$$

with

$$\varrho_1 \cdot e^{i\varepsilon_1} = 1 - \boldsymbol{R} e^{-iy} \qquad (4, 16\text{ a})$$

$$\varrho_2 \cdot e^{i\varepsilon_2} = 1 - \sigma_2 \boldsymbol{R} \cdot e^{-i(y - \alpha_2)} \qquad (4, 16\text{ b})$$

and

$$\varrho_3 \cdot e^{i\varepsilon_3} = 1 - \frac{\varrho_2}{\varrho_1} \cdot e^{i(\varepsilon_2 - \varepsilon_1 - y)}. \qquad (4, 16\text{ c})$$

The calculations have been carried out by means of RYBNER's tables [4]. In fig. 20 a first order filter $M'L_2M''L_2M'$ of this type is considered. The thickness of the inner silver layer is $t'' = 400$ Å ($\sigma_2 = 1.0542$ and $\alpha_2 = -0.°466$) for all the curves. The thicknesses of the two outer silver layers t' are A: 150 Å, B: 200 Å (just exceeding the value of R′ at which only one peak occurs (see Table 17)) and C: 400 Å (the three silver layers have the same thickness and two peaks appear which have somewhat different but low intensities).

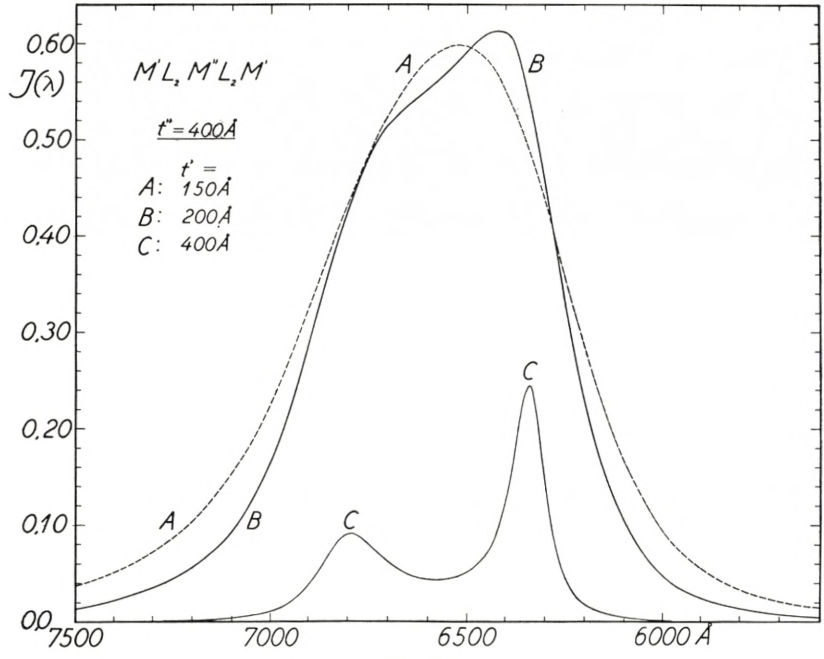

Fig. 20.
$I(\lambda)$ for filters of the type $M'L_2M''L_2M'$ the thickness of M'' is 400 Å in all cases. The thickness of M' is, A: 150 Å, B: 200 Å and C: 400 Å. The thickness of L_2 is chosen such that for $M'L_2M''$ is $\lambda_{max} = 6560$ Å.

From fig. 20 (and from further calculations not given here) it follows *that the value of R' at which I_{max} has its highest value when R'' is constant, is very near the value of R' determined by*

$$R' = \frac{1}{R''} \cdot \left(1 - \sqrt{1 - \frac{1}{\sigma_2}}\right)^2. \qquad (4, 9)$$

In fig. 21 again a filter of the type $M'L_2M''L_2M'$ is considered (solid line) but here the thickness of the central silver layer is $t'' = 500$ Å ($\sigma_2 = 1.0228$ $\alpha_2 = -0.230°$) and the outer silver layers has a thickness of $t' = 250$ Å. (This corresponds very closely to a value of R' which satisfies (4, 9)). For comparison an $I(\lambda)$ curve for a FABRY-PEROT filter ML_2M (fig. 11, A) has been added (fig. 21 broken line) the thickness $t = 300$ Å for the M-layers has been chosen in such a way that I_{max} is about the same for the two filters. The advantages of the compound filter

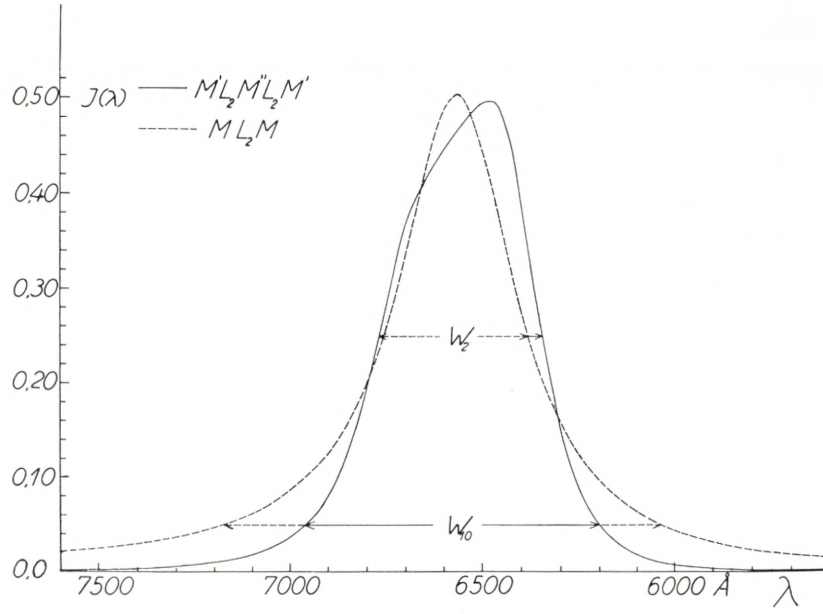

Fig. 21.
Solid line: $I(\lambda)$ for a filter $M'L_2M''L_2M'$ with $t'' = 500$ Å and $t' = 250$ Å. Broken line: $I(\lambda)$ for a filter ML_2M with $t = 300$ Å. The thickness of the L_2 layers are determined as for fig. 20.

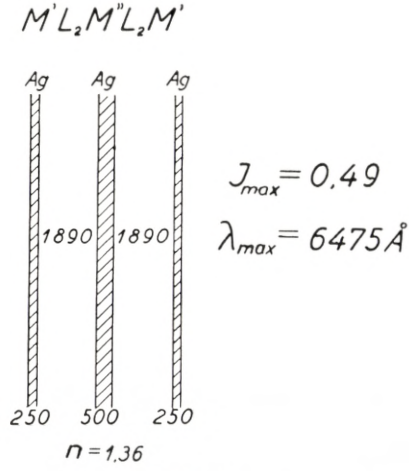

Fig. 22.
The filter the intensity curve of which is the solid line in fig. 21.

$M'L_2M''L_2M'$ is apparent from fig. 21. W_2 (for the filter $M'L_2M''L_2M'$) is (read off from fig. 21) 410 Å and $W_{10} = 760$ Å in good agreement with the values given in Table 17.

Both in fig. 20 and in fig. 21 it is assumed that $\nu - i\varkappa = 0.13 - i\ 4.27$ (in the wavelength region considered) and the thickness d of the dielectric layers has been determined in such a way that a filter $M'L_2M''$ would have had peak transmission at $\lambda = 6560$ Å. The wavelength scale has been determined according to (3, 27 a) by

$$\lambda = \frac{6560}{1 + \frac{y}{360}}.$$

A comparison between fig. 20 and fig. 21 shows that the thickness t'' of the central silver layer M'' has to be chosen rather great to obtain a W_2 value of about the same size as for a FABRY-PEROT filter with the same I_{max}.

In fig. 23 $I(\lambda)$ is shown for two filters $M'L_4M''L_4M'$ green 2nd order $t'' = 500$ Å ($\sigma_2 = 1.0422$; $\alpha_2 = -0.575°$) in the case of both the filters. For the solid line curve $t' = 280$ Å (determined such that R' satisfies (4, 9)) and for the broken curve $t' = 330$ Å ((4, 8) is less than unity, i. e. two peaks and

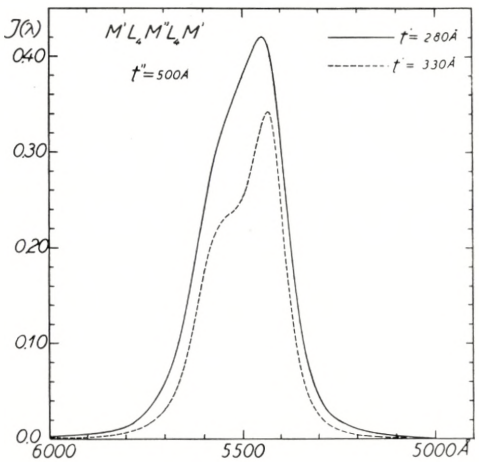

Fig. 23.
$I(\lambda)$ for two filters of the type $M'L_4M''L_4M \cdot t''$ = 500 Å for both filters. Solid line: $t' = 280$ Å. Broken line: $t' = 330$ Å. d is determined such that $\lambda_{max} = 5500$ Å for the filter $M'L_4M''$.

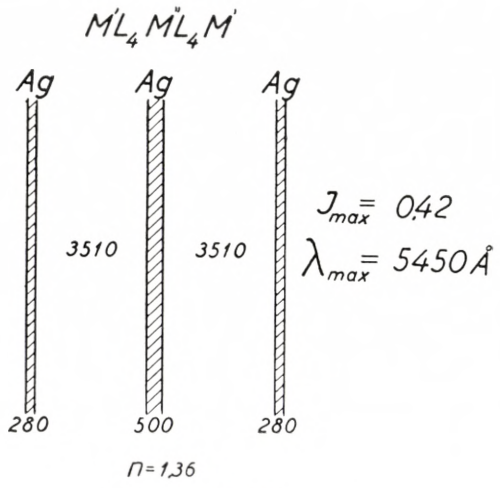

Fig. 24.
The filter $I(\lambda)$ of which is the solid line curve of fig. 23.

a lower $I_{\max}$ result). $v - i\varkappa = 0.15 - i \cdot 3.36$ and the wavelength scale has been calculated from (3, 27 a)

$$\lambda = \frac{5500}{1 + \frac{\gamma}{720}}$$

with $\gamma = y - 360$. The thickness d of the dielectric layers L_2 is determined in accordance with (3, 8) so that a filter of the construction $M'L_4M''$ would have had $\lambda_{\max}$ equal to 5500 Å.

In fig. 25 the solid line curve is the same as the solid line curve in fig. 23 (i. e. $I(\lambda)$ for the filter fig. 24). The broken line curve is the intensity

$$I(\lambda) = \frac{0.379}{1 + 2127.2 \cdot \sin^4\left(\frac{\gamma}{2}\right)}$$

calculated from (4, 13) with the approximation $\alpha_2 = 0$. The actual small value of $\alpha_2 = -0.575°$ gives rise to an asymmetric line shape and a shift in $\lambda_{\max}$ towards violet. Another difference is that the exact calculation (with $\alpha_2 = -0.575°$) predicts an $I_{\max}$ about 10 per cent. larger than obtained by the approximative theory with $\alpha_2 = 0$. (The same is apparent from fig. 20 and fig. 21 as compared with Table 17).

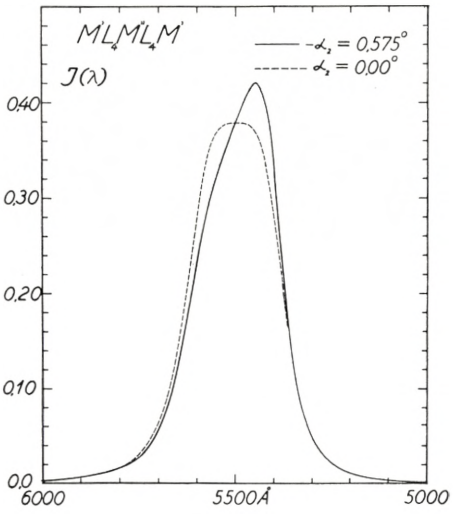

Fig. 25.
Unbroken line: $I(\lambda)$ for the filter in fig. 24. $\alpha_2 = -0.575°$.
Broken line: $I(\lambda)$ calculated from (4, 13) with $\alpha_2 = 0$.

The deviations between the two curves in fig. 25 are the greatest in the very neighbourhood of the peak, but W_2 and particularly W_{10} will be very nearly equal for the two curves.

If the three silver layers have the same thickness, two widely separated peaks result (fig. 20 curve C). If the thickness of the central silver layer is now decreased, the separation between the two peaks will increase and because of the increase in α_2 (caused by the decrease in the thickness of an absorbent layer) the asymmetry will be more and more pronounced. (Fig. 27 solid line corresponding to the filter in fig. 28 a). If, however, a thin ZnS layer ($n_1 = 2.36$) is used as the central reflecting layer, we have $\alpha_2 = 0$, and in this case $I(\lambda)$ can be calculated exactly from (4, 13), and λ_{max} is determined by (4, 8).

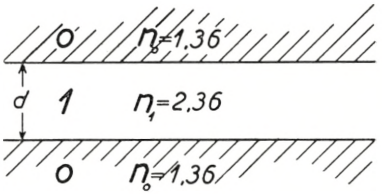

Fig. 26.

R and T for the ZnS layer (fig. 26) are determined by (3, 23—24)

$$\sqrt{R}\cdot e^{i\delta} = r_{01}\frac{(1-e^{-ix})}{1-r_{01}^2\cdot e^{-ix}} \quad \text{and} \quad \sqrt{T}\cdot e^{i\beta} = \frac{(1-r_{01}^2)\cdot e^{-i\frac{x}{2}}}{1-r_{01}^2\cdot e^{-ix}}$$

with

$$r_{01} = \frac{n_0 - n_1}{n_0 + n_1} \quad \text{and} \quad x = 360\cdot\frac{2\,dn_1}{\lambda}.$$

From these equations follows $R + T = 1$ (conservation of energy) and

$$\frac{1}{R} = 1 + \frac{(1-r_{01}^2)^2}{4\cdot r_{01}^2\sin^2\frac{x}{2}} \qquad (4, 17)$$

and

$$\sigma_2\cdot e^{i\alpha_2} = 1 - \frac{T}{R}\cdot e^{i(2\beta-2\delta)} = 1 + \frac{(1-r_{01}^2)}{4\,r_{01}^2\sin^2\frac{x}{2}} \text{ i.e. } \sigma_2 = \frac{1}{R} \text{ and } \alpha_2 = 0$$

in accordance with (3, 20).

From these formulae it is easy to calculate the intensity distribution $I(\lambda)$ for a definite value of the thickness d of the ZnS layer.

In fig. 27 solid line $I(y)$ has been calculated for $t' = 150$ Å

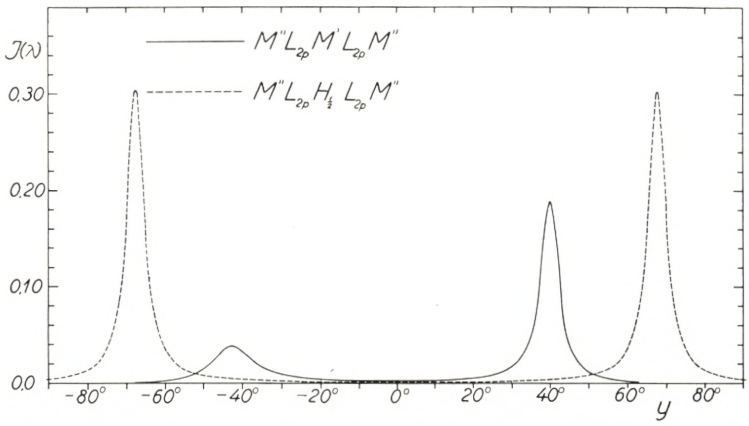

Fig. 27.
Solid line: $I(\lambda)$ for the filter $M''L_2M'L_2M''$ constructed as shown in fig. 28 a. Broken line curve: $I(\lambda)$ for the filter $M''L_2H_{\frac{1}{2}}L_2M''$ constructed as shown in fig. 28 b.

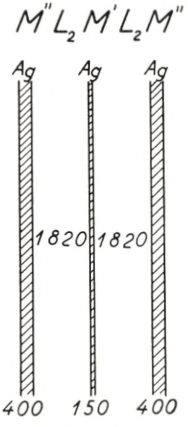

Fig. 28 a.

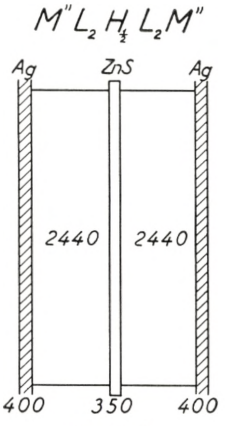

Fig. 28 b.

Fig. 28 a. The filter, $I(\lambda)$ of which is indicated in fig. 27 solid line. Fig. 28 b. The filter $I(\lambda)$ of which is indicated in fig. 27 broken line. The low index layers L_2 of the filters are determined in such a way that the filters $M''L_2M'$, and $M''L_2H_{\frac{1}{2}}$ both have peak transmission at $\lambda = 6560$ Å.

(thickness of the central silver layer) and $t'' = 400$ Å (thickness of the outer silver layers) by means of (4, 16).

In fig. 27 broken line

$$I(y) = \frac{0.002122}{1.4057 - 9.0178 \sin^2 \frac{y}{2} + 14.5352 \sin^4 \frac{y}{2}}$$

has been calculated corresponding to $x = 90°$ ($\frac{\lambda}{8}$-layer at $\lambda = 6560$ Å) for the ZnS layer. The thickness of both the silver layers is 400 Å and x and $\nu - i\varkappa = 0.13 - i.\,4.\,27$ has been regarded as independent of the wavelength. This is only a rough approximation in the case of $p = 1$ as on figs. 28 a—b, but will be a good approximation in the neighbourhood of 6560 Å for a filter of higher order ($p \simeq 8$—10). Fig. 29 shows the approximate distri-

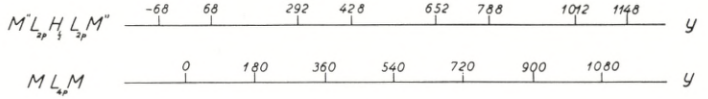

Fig. 29.

The positions of the peaks on the y scale for a higher order filter $M''L_{2p}H_{\frac{1}{2}}L_{2p}M''$ as compared with the position of the peaks for a FABRY-PEROT filter $M''L_{4p}M''$.

bution on the y-scale of the peaks for such a filter $M''L_{2p}H\frac{1}{2}L_{2p}M''$ as compared with the distribution of the peaks for a FABRY-PEROT filter $M''L_{4p}M''$ (which is very nearly equally spaced). I_{max} is the same for both filters in accordance with (2, 18 b).

The Filter $M'L_4M''L_4M'$ Used as Phase Plate.

Fig. 30 shows the phase change at transmission for a filter $M'L_4M''L_4M'$ (like that in fig. 24). The calculation is quite analogous to that on page 39 for a FABRY-PEROT filter. The phase plate is shown at the bottom of fig. 30. The phase difference between P_2 (light passing through the phase plate) and P_1 (light passing outside the phase plate) is according to (4, 3)

$$\left.\begin{aligned}\zeta(\lambda) = \left(\beta_{01} + \beta_{12} + \beta_{23} - \frac{360}{\lambda} \cdot 2\,dn - \varepsilon_3(\lambda)\right) + \\ \frac{360}{\lambda}(2t' + t'' + 2d)\end{aligned}\right\} \quad (4, 18)$$

making the approximations

$$\beta_{01} = \beta_{23} \quad \text{and} \quad \beta_{01} + \beta_{23} + \beta_{12} = \beta_0 - k \cdot \lambda.$$

$\varepsilon_3(\lambda)$ (the phase change from multiple reflections in the layers) is calculated from (4, 16 c). The phase change is zero in the neighbourhood of the peak and a change from negative ($+ 90°$) to positive ($- 90°$) contrast of the image is possible by means of a small alteration of the wavelength.

The Intensity $R(\lambda)$ in Reflection.

The intensity distribution $R(\lambda)$ in the reflected light from a filter of this type can without any approximation be calculated from (4, 2). A general analysis of the properties of the filter $M'L_{2p}M''L_{2p}M'$ in reflection has not been carried out here (as it would only be a rough approximation to place $\alpha_1 = 0$), but $R_{03}(\lambda)$ has been calculated directly from (4, 2) in three special cases of the filters the transmission curves of which are shown

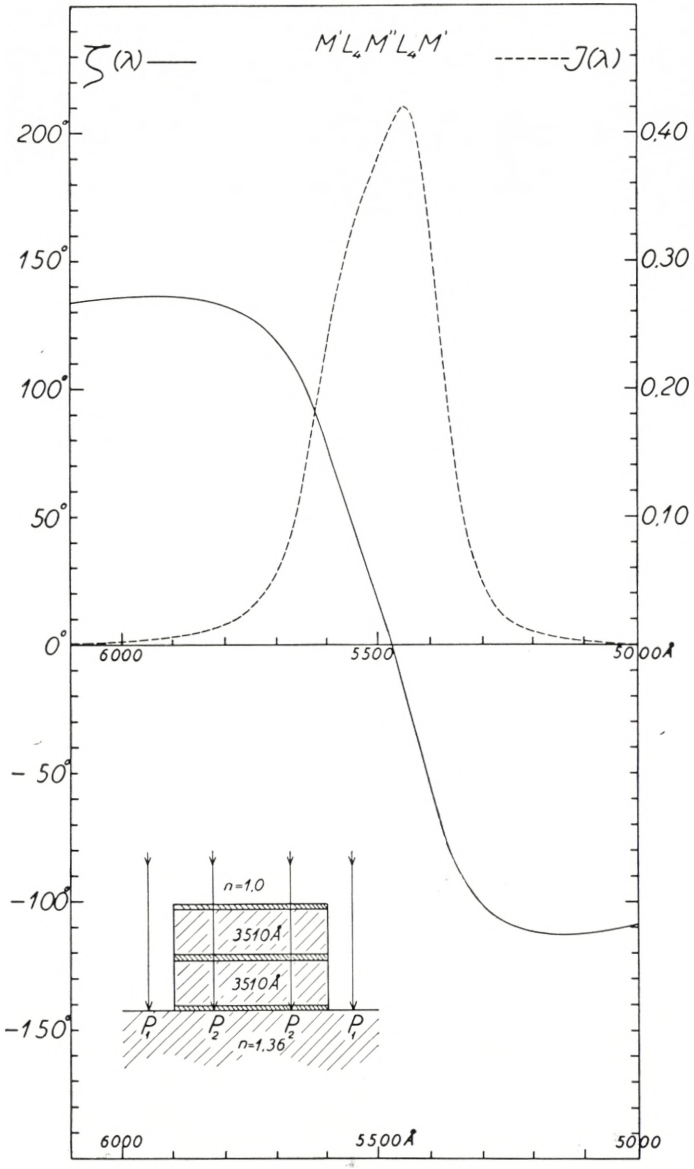

Fig. 30.

Solid line: Phase change at transmission through an interference filter of the type $M' L_4 M'' L_4 M'$. (Phase difference between P_2 and P_1).

Broken line: $I(\lambda)$ for the same filter. (The same as the solid line curve in figs. 24 and 25). The phase plate is shown below in the left corner of fig. 30).

in fig. 20 Curve B, fig. 21 (unbroken line) and fig. 23 (unbroken line). (4, 2) can be written

$$R_{03}(\lambda) = \frac{R_{01} \cdot \left| 1 - \sigma_1 \boldsymbol{R} \cdot \frac{\varrho_2}{\varrho_1} \cdot e^{i(\varepsilon_2 - \varepsilon_1) - i(y - \alpha_1)} \right|^2}{\left| 1 - \boldsymbol{R} \cdot \frac{\varrho_2}{\varrho_1} \cdot e^{i(\varepsilon_2 - \varepsilon_1) - iy} \right|^2}$$

$$\varrho_1 \cdot e^{i\varepsilon_1} = 1 - \boldsymbol{R} \cdot e^{-iy}, \quad \varrho_2 \cdot e^{i\varepsilon_2} = 1 - \sigma_2 \boldsymbol{R} \cdot e^{-i(y - \alpha_2)}$$

and

$$\varrho_3 \cdot e^{i\varepsilon_3} = 1 - \boldsymbol{R} \cdot \frac{\varrho_2}{\varrho_1} \cdot e^{i(\varepsilon_2 - \varepsilon_1) - iy}$$

have been calculated above (4, 16 a—c), and if further

$$\varrho_4 \cdot e^{i\varepsilon_4} = 1 - \sigma_1 \cdot \boldsymbol{R} \cdot \frac{\varrho_2}{\varrho_1} \cdot e^{i(\varepsilon_2 - \varepsilon_1) - i(y - \alpha_1)}$$

is calculated, we simply get

$$R_{03}(\lambda) = R_{01} \cdot \left(\frac{\varrho_4}{\varrho_3} \right)^2.$$

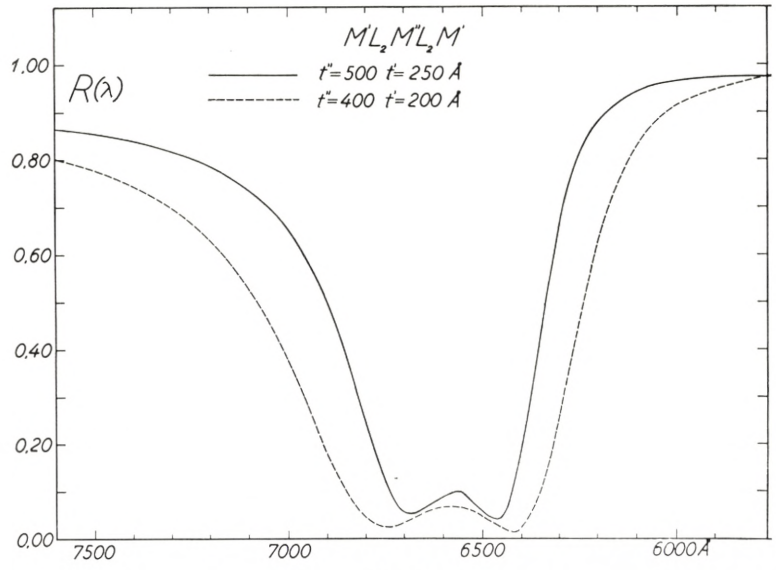

Fig. 31.
Intensity distribution in reflection from the filters of the type $M' L_2 M'' L_2 M'$. Unbroken line: Reflection from the filter in fig. 22 and with transmission curve in fig. 21 (unbroken line) $\alpha_1 = -1.386°$ and $\alpha_2 = -0.230°$. Broken line: Reflection from the filter the transmission curve of which is given in fig. 20. Curve B. $\alpha_1 = -2.084°$ and $\alpha_2 = -0.466°$.

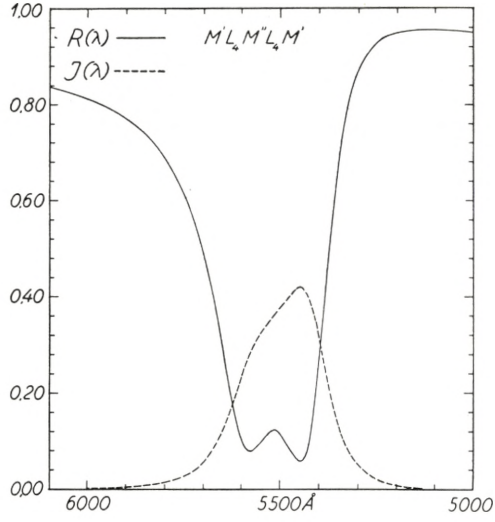

Fig. 32.
Unbroken line: Intensity distribution in reflection from the filter in fig. 24. $\alpha_1 = -2.401°$ and $\alpha_2 = -0.575°$. Broken line: Intensity distribution at transmission through the same filter.

The three curves of $R(\lambda)$ (fig. 31—32) have much the same trends and are characterized by having two minima and, as in the case of fig. 13, the minima do not reach zero.

Recently GEFFCKEN [19] has also considered filters of this type with three silver layers.

§ 5. Interference Filters with *Four* Systems of Reflective Layers. (e. g. four silver layers).

The same assumption is adopted here, as in the previous sections, viz. that each of the systems I, II, III, and IV, when considered separately, do not act as interference filters themselves.

The treatment in this section is quite analogous to that of § 4. The following notations are used here as previously:

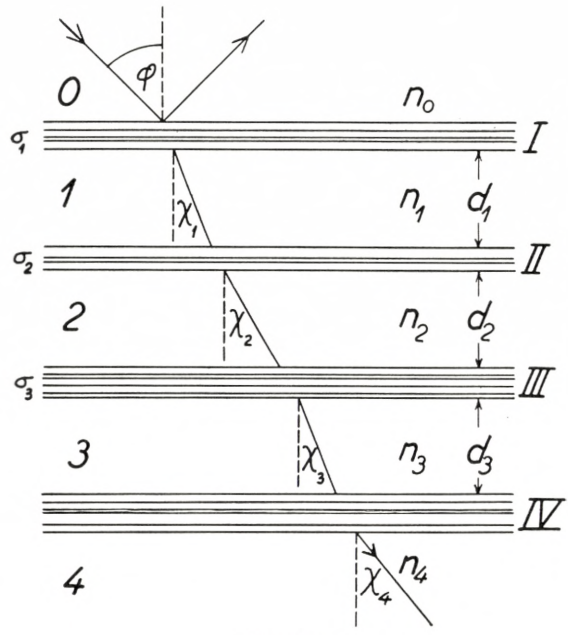

Fig. 33.

$$x_q = \frac{2\, d_q \cdot n_q \cdot \cos \chi_q}{\lambda} \qquad y_q = x_q - \delta_{q,q-1} - \delta_{q,q+1}$$

$$\sigma_q \cdot e^{i\alpha_q} = 1 - \frac{t_{q-1,q} \cdot t_{q,q-1}}{r_{q-1,q} \cdot r_{q,q-1}}; \quad r_{q,q-1} = \sqrt{R_{q,q-1}} \cdot e^{i\delta_{q,q-1}} \text{ etc.}$$

and

$$t_{q,q-1} = \sqrt{T_{q,q-1}} \cdot e^{i\beta_{q,q-1}} \quad \text{and} \quad \boldsymbol{R}_q = \sqrt{R_{q,q-1} \cdot R_{q,q+1}}$$

and from this follows

$$r_{q,q-1} \cdot r_{q,q+1} \cdot e^{-ix_q} = \boldsymbol{R}_q \cdot e^{-iy_q}, \qquad (q = 1, 2, 3).$$

As in § 4 II + III + IV are considered as a single system (and identical with II in fig. 4) and (2, 1—3) is employed (Index 2 being changed to Index 4):

$$r_{04} = \frac{r_{01}\,(1 - r_{10} \cdot r_{14} \cdot \sigma_1 \cdot e^{-i(x_1 - \alpha_1)})}{1 - r_{10} \cdot r_{14} \cdot e^{-ix_1}} \quad ; \quad t_{04} = \frac{t_{01} \cdot t_{14} \cdot e^{-i\frac{x_1}{2}}}{1 - r_{10} \cdot r_{14} \cdot e^{-ix_1}}$$

and in these formulae the following substitutions are made, derived from (4, 2—3):

$$r_{14} = \frac{r_{12}((1-\boldsymbol{R}_3\cdot e^{-iy_3})-\sigma_2\boldsymbol{R}_2\cdot e^{-iy_2+i\alpha_2}\cdot(1-\sigma_3\boldsymbol{R}_3\cdot e^{-iy_3+i\alpha_3}))}{(1-\boldsymbol{R}_3\cdot e^{-iy_3})-\boldsymbol{R}_2\cdot e^{-iy_2}(1-\sigma_3\boldsymbol{R}_3\cdot e^{-iy_3+i\alpha_3})}$$

and

$$t_{14} = \frac{t_{12}\cdot t_{23}\cdot t_{34}\cdot e^{-i\left(\frac{x_2}{2}+\frac{x_3}{2}\right)}}{(1-\boldsymbol{R}_3\cdot e^{-iy_3})-\boldsymbol{R}_2\cdot e^{-iy_2}(1-\sigma_3\boldsymbol{R}_3\cdot e^{-iy_3+i\alpha_3})}$$

and we arrive at

$$\left.\begin{aligned} {}^4 = \frac{\sqrt{R_{01}}\cdot e^{i\delta_{01}}((1-\boldsymbol{R}_3\cdot e^{-iy_3})(1-\sigma_1\boldsymbol{R}_1\cdot e^{-i(y_1-\alpha_1)}) \\ -\boldsymbol{R}_2\cdot e^{-iy_2}(1-\sigma_3\boldsymbol{R}_3\cdot e^{-i(y_3-\alpha_3)})(1-\sigma_1\cdot\sigma_2\cdot\boldsymbol{R}_1\cdot e^{-i(y_1-\alpha_1-\alpha_2)}))}{(1-\boldsymbol{R}_3\cdot e^{-iy_3})(1-\boldsymbol{R}_1\cdot e^{-iy_1}) \\ -\boldsymbol{R}_2\cdot e^{-iy_2}(1-\sigma_3\boldsymbol{R}_3\cdot e^{-i(y_3-\alpha_3)})(1-\sigma_2\boldsymbol{R}_1\cdot e^{-i(y_1-\alpha_2)})} \end{aligned}\right\} \quad (5, 1)$$

and

$$\left.\begin{aligned} {}^1 = \frac{\sqrt{T_{01}\cdot T_{12}\cdot T_{23}\cdot T_{34}}\cdot e^{-i\left(\frac{x_1}{2}+\frac{x_2}{2}+\frac{x_3}{2}\right)+i(\beta_{01}+\beta_{12}+\beta_{23}+\beta_{34})}}{(1-\boldsymbol{R}_3\cdot e^{-iy_3})(1-\boldsymbol{R}_1\cdot e^{-iy_1})} \cdot \\ -\boldsymbol{R}_2\cdot e^{-iy_2}(1-\sigma_3\boldsymbol{R}_3\cdot e^{-i(y_3-\alpha_3)})(1-\sigma_2\boldsymbol{R}_1\cdot e^{-i(y_1-\alpha_2)}) \end{aligned}\right\} \quad (5, 2)$$

We now consider the properties in transmission in the case where the filter is constructed symmetrically, i. e. when $\boldsymbol{R}_1 = \boldsymbol{R}_3 = \boldsymbol{R}$

$$y_1 = y_3, \quad \sigma_2 = \sigma_3 \quad \text{and} \quad n_1 = n_3.$$

In this case we obtain

$$I(\lambda) = \frac{\boldsymbol{T}_1\cdot\boldsymbol{T}_2^2\cdot\boldsymbol{T}_4}{\left|(1-\boldsymbol{R}\cdot e^{-iy_1})^2-\boldsymbol{R}_2\cdot e^{-iy_2}(1-\sigma_2\boldsymbol{R}\cdot e^{-i(y_1-\alpha_2)})^2\right|^2} \quad (5, 3)$$

$\boldsymbol{T}_1 = T_{01}\cdot\dfrac{n_1\cdot\cos\chi_1}{n_0\cdot\cos\varphi}$; $\boldsymbol{T}_2 = \boldsymbol{T}_3 = T_{12} = T_{23}$ and $\boldsymbol{T}_4 = T_{34}\cdot\dfrac{n_4\cdot\cos\chi_4}{n_1\cdot\cos\chi_1}$

are the energies transmitted through Systems I, II, III, and IV, when each of the systems are considered separately.

The denominator P in (5, 3) can be expressed by

$$\left.\begin{aligned} P = {} & 1 + \boldsymbol{R}^4 + 4\boldsymbol{R}^2 + \boldsymbol{R}_2^2 + 4(\sigma_2\boldsymbol{R}\boldsymbol{R}_2)^2 + \boldsymbol{R}_2^2\cdot(\sigma_2\boldsymbol{R})^4 + 4\boldsymbol{R}\cdot\boldsymbol{R}_2\cdot\cos(y_1 - y_2) \\ & + 4\sigma_2\cdot\boldsymbol{R}^3\cdot\boldsymbol{R}_2\cdot\cos(y_1 - y_2 + \alpha_2) - 4\boldsymbol{R}(\boldsymbol{R}^2+1)\cos y_1 \\ & - 4\sigma_2\boldsymbol{R}\cdot\boldsymbol{R}_2^2((\sigma\boldsymbol{R})^2+1)\cdot\cos(y_1 - \alpha_2) - 2\cdot\boldsymbol{R}_2\cdot\cos y_2 \\ & - 2\boldsymbol{R}_2\sigma_2^2\cdot\boldsymbol{R}^4\cdot\cos(y_2 - 2\alpha_2) - 8\sigma_2\boldsymbol{R}_2\cdot\boldsymbol{R}^2\cdot\cos(y_2 - \alpha_2) \\ & - 2\boldsymbol{R}_2\cdot\boldsymbol{R}^2\cos(2y_1 - y_2) + 2\cdot\boldsymbol{R}^2\cos 2y_1 + 2(\boldsymbol{R}_2\sigma_2\boldsymbol{R})^2\cos(2y_1 - 2\alpha_2) \\ & + 4\sigma_2\boldsymbol{R}_2\boldsymbol{R}\cdot\cos(y_1 + y_2 - \alpha_2) + 4\boldsymbol{R}_2\cdot\boldsymbol{R}\cdot(\sigma_2\boldsymbol{R})^2\cdot\cos(y_1 + y_2 - 2\alpha_2) \\ & - 2\boldsymbol{R}_2\cdot(\sigma_2\boldsymbol{R})^2\cos(2y_1 + y_2 - 2\alpha_2). \end{aligned}\right\} (5,$$

We now make the approximation $\alpha_2 = 0$ and consider the case $y_1 = y_2\,(= y_3) = y$ in detail. It is easy to show from (5, 4) that P in this case can be expressed by a polynomial in $\sin^2\frac{y}{2}$:

$$P = \boldsymbol{A} + \boldsymbol{B}\sin^2\frac{y}{2} + \boldsymbol{C}\sin^4\frac{y}{2} + \boldsymbol{D}\sin^6\frac{y}{2} \qquad (5, 5)$$

$$\boldsymbol{A} = ((1 - \boldsymbol{R})^2 - \boldsymbol{R}_2(1 - \sigma_2\boldsymbol{R})^2)^2 \qquad (5, 6)$$

$$\boldsymbol{C} = 16\boldsymbol{R}(2\boldsymbol{R}_2(\sigma_2\boldsymbol{R})^2 - \boldsymbol{R}(6\sigma_2^2\boldsymbol{R}_2 - (\sigma_2\boldsymbol{R}_2)^2 - 1) + 2\sigma_2\boldsymbol{R}_2) \qquad (5, 7)$$

$$\boldsymbol{D} = 64\boldsymbol{R}_2(\sigma_2\boldsymbol{R})^2 \qquad (5, 8)$$

and

$$\boldsymbol{B} = \boldsymbol{M} - \boldsymbol{A} - \boldsymbol{C} - \boldsymbol{D} \text{ with } \boldsymbol{M} = ((1 + \boldsymbol{R})^2 + \boldsymbol{R}_2(1 + \sigma_2\boldsymbol{R})^2)^2. \qquad (5, 9)$$

The coefficient $\boldsymbol{A}$ is determined directly from (5, 3) when $y = 360^\circ\cdot(m - 1)$, and $\boldsymbol{M} = \boldsymbol{A} + \boldsymbol{B} + \boldsymbol{C} + \boldsymbol{D}$ is determined when $y_1 = y_2 = 180^\circ\cdot(2m - 1)$ is substituted in the denominator and simultaneously we get

$$I_{\max} = \frac{(\boldsymbol{T}_1\cdot\boldsymbol{T}_2)^2}{\boldsymbol{A}} \text{ (when } \boldsymbol{T}_1 = \boldsymbol{T}_4 \text{ as is often the case)} \qquad (5, 10)$$

and

$$F = \frac{I_{\max}}{I_{\min}} = \frac{\boldsymbol{M}}{\boldsymbol{A}}. \qquad (5, 11)$$

The values of y at which maximum or minimum of $I(\lambda)$ occur are determined by $\frac{dP}{dy} = 0$,

i. e. $$\sin\frac{y}{2}\cdot\cos\frac{y}{2}\left(\boldsymbol{B} + 2\,\boldsymbol{C}\sin^2\frac{y}{2} + 3\,\boldsymbol{D}\sin^4\frac{y}{2}\right) = 0\,.$$

Only one peak is present (for a given order m) at $y = 360^\circ\cdot(m-1)$ if there is no value of y which satisfies the equation

$$\boldsymbol{D}\cdot\sin^4\frac{y}{2} + 2\,\boldsymbol{C}\cdot\sin^2\frac{y}{2} + \boldsymbol{B} = 0 \text{ or } \sin^2\left(\frac{y}{2}\right) = -\frac{\boldsymbol{C}}{3\,\boldsymbol{D}} \pm \frac{\sqrt{\boldsymbol{C}^2 - 3\,\boldsymbol{BD}}}{3\,\boldsymbol{D}}. \qquad (5, 12)$$

A further investigation shows that the coefficients $\boldsymbol{B}$ and $\boldsymbol{D}$ are always positive numbers, from which it follows that if $\boldsymbol{C} \geqslant 0$, only a single peak results; if, however, $\boldsymbol{C} < 0$; $\boldsymbol{C}^2 - 3\,\boldsymbol{B}\cdot\boldsymbol{D} > 0$, and three peaks result (for a given order m).

We now introduce $\boldsymbol{R} = \boldsymbol{H}$ corresponding to $\boldsymbol{C} = 0$, i. e. determined by

$$\boldsymbol{H}^2 - \boldsymbol{H}\left(3 - \frac{\boldsymbol{R}_2}{2} - \frac{1}{2\cdot\sigma_2^2\cdot\boldsymbol{R}_2}\right) + \frac{1}{\sigma_2} = 0, \qquad (5, 13)$$

and the final result is then the following:

if $\boldsymbol{R} \leqslant \boldsymbol{H}$, only one peak is present at $y = 360^\circ\cdot(m-1)$;

if $\boldsymbol{R} > \boldsymbol{H}$, three peaks result, the one at $y = 360^\circ\cdot(m-1)$

and the others at $y = \pm v + 360^\circ\cdot(m-1)$ determined by

$$\sin^2\frac{v}{2} = -\frac{\boldsymbol{C}}{3\,\boldsymbol{D}} + \frac{\sqrt{\boldsymbol{C}^2 - 3\,\boldsymbol{BD}}}{3\,\boldsymbol{D}}, \qquad (5, 14)$$

and the two minima between the 3 peaks at $y = \pm u + 360^\circ\cdot(m-1)$ are determined by

$$\sin^2\frac{y}{2} = -\frac{\boldsymbol{C}}{3\,\boldsymbol{D}} - \frac{\sqrt{\boldsymbol{C}^2 - 3\,\boldsymbol{BD}}}{3\,\boldsymbol{D}}. \qquad (5, 15)$$

Calculation of W_2, W_{10} and W_{1000}.

The k'th intensity band width W_k is determined in the usual way (from (5, 5)) by means of the equations

$$\left.\begin{aligned} (k-1)\ \boldsymbol{A} &= \boldsymbol{B}\cdot\sin^2\frac{\gamma_k}{2}+\boldsymbol{C}\sin^4\frac{\gamma_k}{2}+\boldsymbol{D}\sin^6\frac{\gamma_k}{2};\\ \gamma_k &= y-360\,(m-1)\ \text{and}\ W_k=\frac{\gamma_k\cdot\lambda_m}{180\cdot f}. \end{aligned}\right\}\quad(5,16)$$

In the case of $\boldsymbol{R}=\boldsymbol{H}$ we have $\boldsymbol{C}=0$, and $\boldsymbol{B}$ has a small positive value, and W_{10} and still better W_{1000} can be determined approximately by

$$\sin\frac{\gamma_k}{2}=\sqrt[6]{\frac{(k-1)\,\boldsymbol{A}}{\boldsymbol{D}}}\qquad(5,16\,a)$$

and

$$W_k=\frac{\gamma_k}{180}\cdot\frac{\lambda_m}{f}\quad(k=10\text{ and }1000\text{ respectively}).$$

In the case of W_2, $\boldsymbol{B}\sin^2\frac{\gamma_k}{2}$ has to be taken into account ($f\cong m$ for filters with silver layers).

Table 18 contains the results of calculations made in the special case of a symmetrical filter with four silver layers placed in a dielectric with $n=1.36$. The calculations are carried out by means of Tables 6—13 and are analogous to the calculations of Table 17. When the thickness t'' of the central silver layers has been chosen, $\boldsymbol{R}=\sqrt{R'\cdot R''}=\boldsymbol{H}$ is calculated from (5, 13) so that only one peak results. Next R', t' $\boldsymbol{T}_1$ and $I_{\max}$, F, W_2, W_{10} and W_{1000} (2nd order) are calculated. For comparison $I_{\max}$ $F=\frac{I_{\max}}{I_{\min}}$; W_2 and W_{10} for filters of the Fabry-Perot type ML_4M and for filters of the type $M'L_4M''L_4M'$ (Table 17) have been added. In Table 18, t for the Fabry-Perot filters has been chosen in such a way that $I_{\max}$ is about the same as for filters of the type $M'L_4M''L_4M''L_4M'$ treated in this section. The contrast factor F is about 10 times higher for this type of compound interference filters than for the type treated in § 4, and F for the latter type is again 10 times higher than the contrast factor F of a Fabry-

	ML_4M				$M'L_4M''L_4M'$				$M'L_4M''L_4M'L_4M'$				
λ $\nu - i\varkappa$	t	R	I_{max} I_{max}/I_{min}	W_2 W_{10} $(=3\cdot W_2)$	t' t''	R' R''	I_{max} I_{max}/I_{min}	W_2 W_{10} $(=W_2\cdot\sqrt{3})$	t' t''	R' R''	I_{max} I_{max}/I_{min}	W_2 W_{10} $(\simeq 1.5\cdot W_2)$	W_{1000}
4000	550	.7469	0.1475	186 Å	449 Å	.6684	0.152	260 Å	344 Å	.5493	0.157	251 Å	1018 Å
0.18—i 1.95			$0.48\cdot 10^2$	558	600	.7709	$0.58\cdot 10^3$	450	600	.7709	$0.79\cdot 10^4$	395	
4000	450	.6690	0.285	258	334	.5342	0.297	357	256	.3996	0.273	348	1681
0.18—i 1.95			$0.25\cdot 10^2$	774	500	.7155	$0.16\cdot 10^3$	618	500	.7155	$0.13\cdot 10^4$	542	
4500	400	.7351	0.388	221	297	.5914	0.406	317	235	.4649	0.360	312	1184
0.14—i 2.42			$0.43\cdot 10^2$	663	500	.8150	$0.42\cdot 10^3$	549	500	.8150	$0.59\cdot 10^4$	477	
5000	400	.8022	0.347	176	286	.6575	0.404	282	229	.5414	0.358	277	1022
0.14—i 2.89			$0.83\cdot 10^2$	528	500	.8649	$1.0\cdot 10^3$	489	500	.8649	$2.29\cdot 10^4$	424	
5500	375	.8257	0.345	168	280	.7126	0.379	252	226	.6082	0.337	248	861
0.15—i 3.36			$1.10\cdot 10^2$	504	500	.8951	$2.3\cdot 10^3$	436	500	.8951	$7.71\cdot 10^4$	380	
6000	350	.8466	0.368	159	269	.7508	0.386	231	218	.6567	.345	229	815
0.15—i 3.82			$1.45\cdot 10^2$	477	500	.9188	$4.8\cdot 10^3$	400	500	.9188	$22.3\cdot 10^4$	348	
6560	350	.8802	0.3975	133	249	.7702	0.463	222	204	.6831	0.414	218	757
0.13—i 4.27			$2.46\cdot 10^2$	399	500	.9398	$7.7\cdot 10^3$	385	500	.9398	$51.2\cdot 10^4$	332	
6560	300	.8375	0.502	185	194	.6583	0.585	339	156	.5473	0.532	337	1183
0.13—i 4.27			$1.28\cdot 10^2$	555	400	.9084	$1.4\cdot 10^3$	587	400	.9084	$4.37\cdot 10^4$	503	
7100	300	.8582	0.475	173	217	.7416	0.516	268	178	.6478	0.466	265	915
0.14—i 4.68			$1.72\cdot 10^2$	519	450	.9363	$5.0\cdot 10^3$	464	450	.9363	$27.3\cdot 10^4$	400	
7680	300	.8756	0.450	162	212	.7615	0.507	265	174	.6731	0.458	263	900
0.15—i 5.11			$2.27\cdot 10^2$	486	450	.9438	$7.3\cdot 10^3$	458	450	.9438	$47.2\cdot 10^4$	395	

Perot filter with the same value of $I_{\max}$, and W_{10} is less for the two compound types than for the Fabry-Perot type. Furthermore these two types of interference filters make it possible (by variation of t' and t'') to vary the band width and at the same time to keep F constant. In many applications a broad band width, combined with a small intensity outside the band, is desirable.

In the formulae (5, 5—16) from which Table 18 has been calculated, the approximation $\alpha_2 = 0$ is done. Actually α_2 is not zero, but has a small negative value. However, this small value of α_2 is large enough to change the line shape considerably in the very neighbourhood of the peak (as was the case in § 4) but the "wings" of the line are almost unaltered, and W_2 and furthermore W_{10} and W_{1000} calculated from (5, 16) will be nearly the same as obtained by an exact numerical calculation.

The exact numerical calculations carried out for this type of compound interference filter are quite analogous to those carried out in § 4. The equation (5, 3) can be written in the following way:

$$I(\lambda) = \frac{(\boldsymbol{T}_1 \cdot \boldsymbol{T}_2)^2}{\varrho_1^4 \left| 1 - \boldsymbol{R}_2 \cdot \left(\frac{\varrho_2}{\varrho_1}\right)^2 \cdot e^{-i(y_2 - 2\varepsilon_2 + 2\varepsilon_1)} \right|^2}, \qquad (5, 17)$$

With

$$\varrho_1 \cdot e^{i\varepsilon_1} = 1 - \boldsymbol{R} \cdot e^{-iy_1} \qquad (5, 17a)$$

and

$$\varrho_2 \cdot e^{i\varepsilon_2} = 1 - \sigma_2 \boldsymbol{R}_2 \cdot e^{-iy_1 + i\alpha_2} \qquad (5, 17\,b)$$

to be calculated in the first step, and the next step is to calculate

$$\varrho_3 \cdot e^{i\varepsilon_3} = 1 - \boldsymbol{R}_2 \cdot \left(\frac{\varrho_2}{\varrho_1}\right)^2 \cdot e^{-i(y_2 - 2\varepsilon_2 + 2\varepsilon_1)}, \qquad (5, 17\,c)$$

and finally

$$I(\lambda) = \left(\frac{\boldsymbol{T}_1 \cdot \boldsymbol{T}_2}{\varrho_1^2 \cdot \varrho_3}\right)^2. \qquad (5, 17\,d)$$

In the calculations y_2 is only exactly equal to y_1 at $\lambda = \lambda_m$, but chosen according to

$$y_2 - 360\,(m-1) = (y_1 - 360\,(m-1)) \cdot \frac{360\,m - \delta_{10} - \delta_{12}}{360\,m - 2\,\delta_{21}}, \qquad (5, 18)$$

and the wavelength scale is determined by (3, 27 a) as previously.

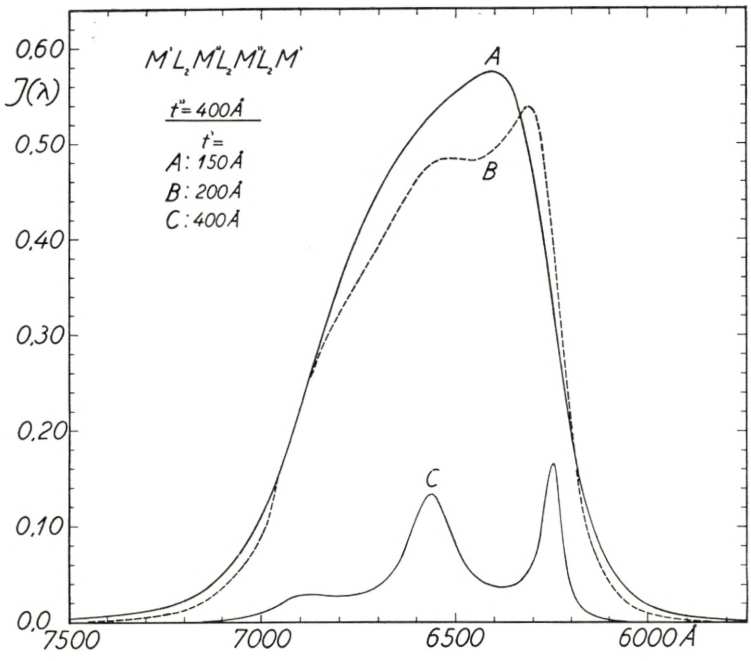

Fig. 34.
$I(\lambda)$ for filters of the type $M'L_2M''L_2M''L_2M'$ the thickness of M'' is 400 Å in all cases. The thickness of M' is A: 150 Å, B: 200 Å and C: 400 Å. The thicknesses of the L_2 layers are chosen such that λ_{max} for $M'L_2M''$ and for $M''L_2M''$ is 6560 Å.

In fig. 34 (analogous to fig. 20) the thickness of the two central silver layers is $t'' = 400$ Å in all the graphs ($\sigma_2 = 1.0542$; $\alpha_2 = -0°.466$). The thickness t' of the two outer silver layers is as follows:

A: $t' = 150$ almost corresponding to $\boldsymbol{R} = \boldsymbol{H}$ determined by (5, 13) (only one peak present).

B: $t' = 200$ Å now $\boldsymbol{R} > \boldsymbol{H}$ (and $\boldsymbol{C} < 0$). Two neighbouring peaks result (the third peak which according to the approximate theory should have a position symmetrical to the second peak, has nearly disappeared in fig. 34).

C: $t' = 400$ Å. The four silver layers are all of equal thickness. Three peaks result. The positions of the peaks (along the abscissa) correspond closely to the values calculated from (5, 14); the line shapes for the two outer peaks are, however, very different from those calculated approximately from (5, 5—9). It is evident from

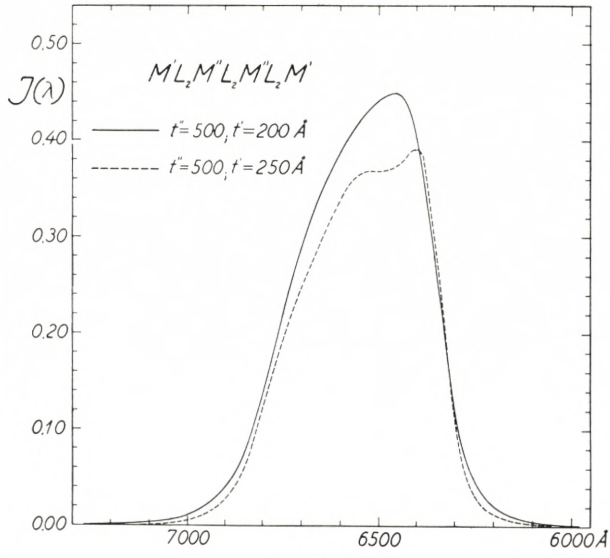

Fig. 35.
$I(\lambda)$ for two filters of the type $M'L_2M''L_2M''L_2M' \cdot t'' = 500$ Å for both filters. Unbroken line: $t' = 200$ Å. Broken line: $t' = 250$ Å d_1 and d_2 are determined such that λ_{max} for the filters $M'L_2M''$ and $M''L_2M''$ is 6560 Å.

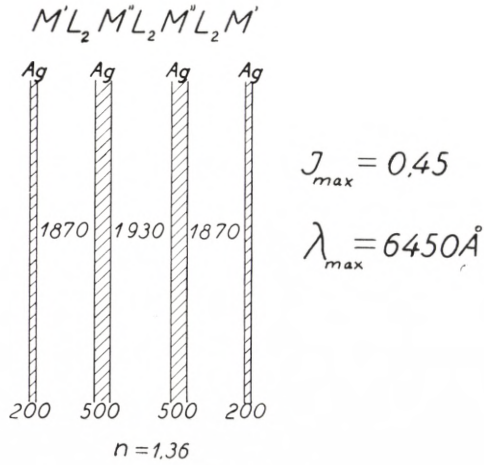

Fig. 36.
(All measures in Å).
The relative measure for the thin layers in the compound filter, $I(\lambda)$ of which is shown in fig. 35 (unbroken line).

fig. 34 and from other numerical calculations not given here, *that* I_{max} *reaches its highest value if* $\boldsymbol{R}$ *very closely corresponds to* $\boldsymbol{R} = \boldsymbol{H}$ *determined by* (5, 13) ($\boldsymbol{R}_2$ *regarded as constant*). At $\boldsymbol{R} > \boldsymbol{H}$ (curve B) and for $\boldsymbol{R} < \boldsymbol{H}$ I_{max} decreases, and at $\boldsymbol{R} = 0$ we have $M''L_2M''$ (i. e. the Fabry-Perot filter fig. 11 Curve C) with $I_{max} = 0.30$. (The same data are used as in fig. 20).

In fig. 35 again a filter of the type $M'L_2M''L_2M''L_2M'$ is considered, but here the thickness of the two central silver layers is 500 Å for both curves. The unbroken curve is $I(\lambda)$ when the thickness of the two outer silver layers is $t' = 200$ Å, this corresponds closely to $\boldsymbol{R} = \boldsymbol{H}$ determined by (5, 13); i. e. only one peak results. The broken curve is $I(\lambda)$ when $t' = 250$ Å; $\boldsymbol{R} > \boldsymbol{H}$ and an unsymmetrical line shape with two peaks results. Also here I_{max} reaches its highest value near $\boldsymbol{R} = \boldsymbol{H}$; i. e. for $\boldsymbol{R} > \boldsymbol{H}$ and $\boldsymbol{R} < \boldsymbol{H}$ I_{max} will decrease. For $\boldsymbol{R} = 0$ the filter is reduced to the Fabry-Perot filter $M''L_2M''$ (fig. 11 Curve D) with $I_{max} = 0.12$. Both in fig. 34 and fig. 35 $v - i\varkappa = 0.13$—i. 4.27 is regarded as constant and the wavelength scale is given by

$$\lambda = \frac{6560}{1 + \frac{y}{360}}.$$

In fig. 37 $I(\lambda)$ (unbroken line) corresponding to a compound filter of the second order $M'L_4M''L_4M''L_4M'$ is shown. We get

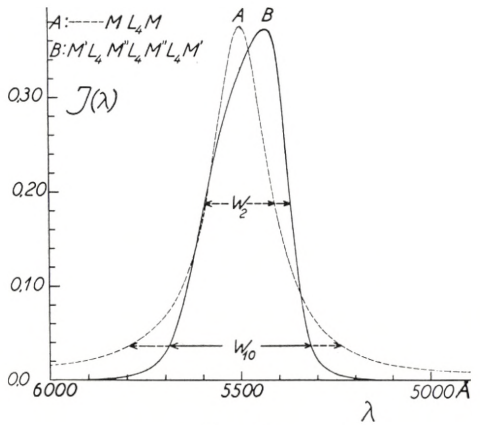

Fig. 37.
Unbroken line: $I(\lambda)$ for the filter $M'L_4M''L_4M''L_4M'$ the data of which are shown in fig. 38. Broken line: $I(\lambda)$ for a filter ML_4M with $t = 360$ Å. (The filter is shown in fig. 10).

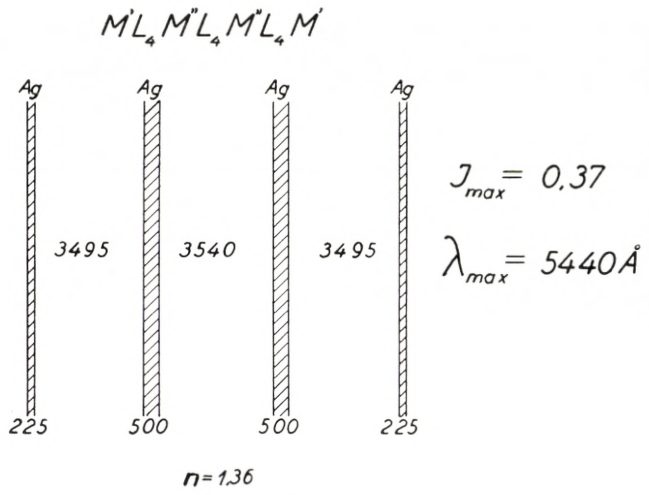

Fig. 38.
The filter $I(\lambda)$ of which is shown in fig. 37 (unbroken line). The relative dimensions are true to scale.

from fig. 37 $W_2 = 225$ Å and $W_{10} = 370$ Å in good agreement with the values calculated from the approximate theory with $\alpha_2 = 0$. (Table 18). Also here $I_{max} = 0.37$ is much higher than I_{max} of the Fabry-Perot filter $M''L_4M''$, which is equal to 0.14. t' has been chosen in such a manner that $\boldsymbol{R} = \boldsymbol{H}$ (determined by (5, 13)), and the thicknesses of the dielectric layers have been chosen in such a way that the Fabry-Perot filters $M'L_4M''$ and $M''L_4M''$ both have a peak at 5500 Å. For comparison $I(\lambda)$ (broken line) for a Fabry-Perot filter ML_4M with the same I_{max} as for the compound filter, has been added. (The Fabry-Perot filter is the same as that shown in fig. 10). It should be noticed that W_{10} for the compound filter is considerably less than W_{10} for the Fabry-Perot filter and that $W_{10} \simeq 1.5 \cdot W_2$ for the compound filter.

In fig. 39 again $I(\lambda)$ corresponding to the filter in fig. 38 is shown (unbroken line) $\alpha_2 = -0.575°$. The broken line is

$$I(\lambda) = \frac{0.337}{1 + 18.54 \sin^2\left(\frac{y}{2}\right) + 77062 \cdot \sin^6\left(\frac{y}{2}\right)}$$

calculated from (5, 5—9) with $\alpha_2 = 0$. Just as in fig. 25 the deviation between the two curves is rather great in the neigh-

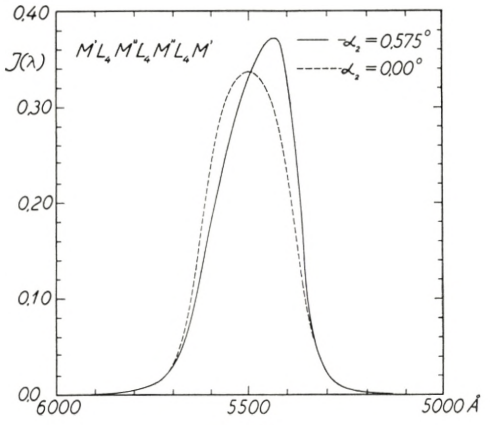

Fig. 39.
Unbroken line: $I(\lambda)$ for the filter in fig. 38 $\alpha_2 = -0.575°$.
Broken line: $I(\lambda)$ calculated from (5, 5—9) with $\alpha_2 = 0$.

bourhood of the peak. However, the deviations in W_2 and in W_{10} are small. As in case of fig. 34—35 the small negative value of α_2 gives rise to a shift in λ_{max} towards violet (in comparison with λ_{max} for the filters $M'L_4M''$ and $M''L_4M''$) and to an unsymmetrical line shape. Finally it should be noted that I_{max} is raised by about 10 per cent. similarly to the filters of the type in § 4.

The thin silver layers at the outside of a filter (such as that in fig. 38) will more easily deteriorate through chemical action than the central thicker silver layers. However, the two outer silver layers can be replaced by dielectric layers as shown in fig. 40. The line shape will be almost the same as that shown in fig. 37 (unbroken line), but I_{max} will be raised from 0.37 to 0.58 as no absorption takes place in the dielectric layers. (H in fig. 40 means a $\frac{\lambda}{4}$-layer of ZnS with $n = 2.36$).

When the four silver layers are of the same thickness, three peaks result, with intensities lower than I_{max} for the filter $M''L_2M''$ (fig. 34, C). If the thicknesses of the inner silver layers are smaller than that of the outer layers, the separation of the three peaks increases and as α_2 increases the difference in intensities of the three peaks will continue to increase. In fig. 41 (unbroken line) $I(\lambda)$ is indicated, calculated for a filter shown in fig. 42 a. The

$$HL\,HL_2M''L_4M''L_2HL\,H$$

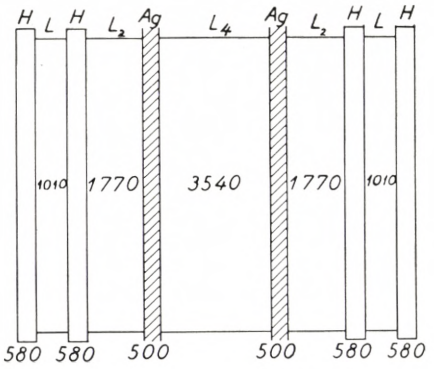

Fig. 40.
Filter of the compound type treated in this section with each of the external silver layers replaced by three dielectric layers.

$L = \frac{\lambda}{4}$-layer with $n_L = 1.36$

$H = \frac{\lambda}{4}$-layer with $n_H = 2.36$

thickness of the outer silver layers is equal to 400 Å and of the central silver layers equal to 150 Å. $\nu - i\varkappa = 0.13$—i. 4.27 has been regarded as constant, and for this reason the calculation is only approximate for a filter of the 1st order.

If the central silver layers are replaced by two thin ZnS layers,

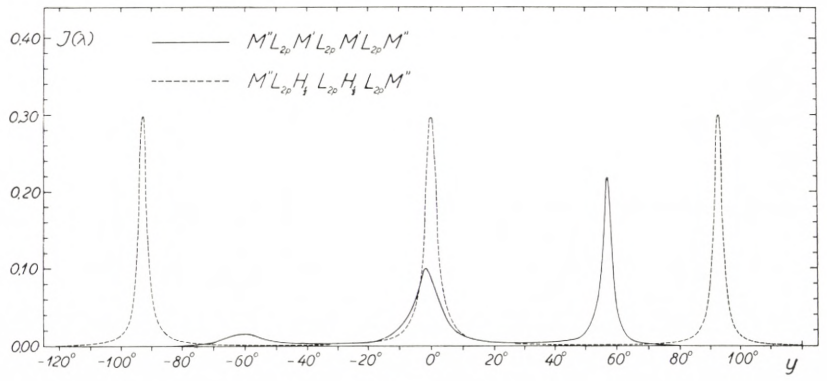

Fig. 41.
Continuous curve: $I(\lambda)$ for the filter $M''L_2M'L_2M'L_2M''$ constructed as shown in fig. 42 a. Broken line curve: $I(\lambda)$ for the filter $M''L_2H_{\frac{1}{2}}L_2H_{\frac{1}{2}}L_2M''$ constructed as shown in fig. 42 b.

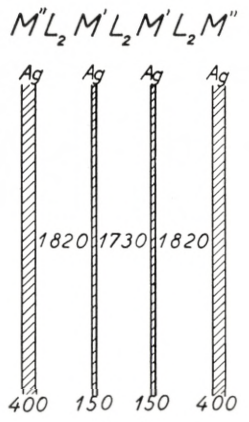

Fig. 42 a.

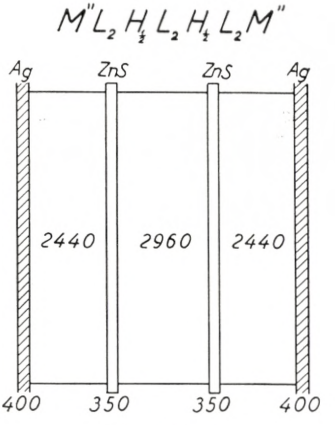

Fig. 42 b.

Fig. 42 a. The filter the $I(\lambda)$ of which is shown in fig. 41 (unbroken line).
Fig. 42 b. The filter $I(\lambda)$ of which is shown in fig. 41 (broken line).
The low index layers L_2 of the filters are determined in such a manner that the filters $M''L_2M'$, $M'L_2M'$, $M''L_2H_{\frac{1}{2}}$, and $H_{\frac{1}{2}}L_2H_{\frac{1}{2}}$ all have peak transmission at $\lambda = 6560$ Å.

then $a_2 = 0$ and in this case $I(\lambda)$ can be calculated by means of (5, 5—9). $I(\lambda)$ has been calculated (analogously to page 60) corresponding to a thickness of the ZnS layers equal to $\frac{\lambda}{8\,n_H}$ at $\lambda = 6560$ Å, i. e. $x = 90°$ (fig. 42 b). If $\nu - i\varkappa = 0.13$—i. 4.27 and x are regarded as independent of the wavelength, we obtain (from (4, 17) and (5, 5—9))

$$I(\lambda) = \frac{0.001817}{0.006146 + 15.979 \sin^2\frac{y}{2} - 60.959 \sin^4\frac{y}{2} + 58.140 \cdot \sin^6\frac{y}{2}}$$

$I(y)$ is shown in fig. 41 (broken line curve).

Fig. 43 shows the positions of the peaks for a higher order filter $M''L_{2p}H_{\frac{1}{2}}L_{2p}H_{\frac{1}{2}}L_{2p}M''$ as compared with the positions

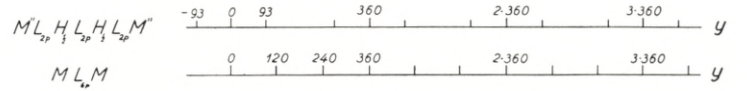

Fig. 43.
The position of the peaks on the y scale for a higher order filter $M''L_{2p}H_{\frac{1}{2}}L_{2p}H_{\frac{1}{2}}L_{2p}M''$ as compared with the position of the peaks for a Fabry-Perot filter $M''L_{6p}M''$.

of the peaks for a Fabry-Perot filter $M''L_{6p}M''$. (The values of I_{max} are the same for the two filters).

The Filter $M'L_4M''L_4M''L_4M'$ Used as Phase Plate.

In fig. 44 the phase change at transmission is shown for a filter $M'L_4M''L_4M''L_4M'$ (like that in fig. 38). The phase difference between P_2 (light passing through the phase plate) and P_1 (light passing outside the phase plate) is, according to (5, 2),

$$\left.\begin{aligned}\xi(\lambda) = &\left(2\beta_1 + 2\beta_2 - \frac{360}{\lambda}\cdot n\,(2\,d_1 + d_2) - \varepsilon_3(\lambda)\right)\\ &+ \frac{360}{\lambda}(2\,t' + 2\,t'' + 2\,d_1 + d_2).\end{aligned}\right\} \qquad (5,\ 18)$$

β_1 is the phase change at transmission for the outer silver layers and β_2 the phase change for the central silver layers.

d_1 is the thickness of the two outer dielectric layers and d_2 for the central dielectric layer and the approximations $\beta_{01} = \beta_{34} = \beta_1$ and $2\beta_1 + 2\beta_2 = \beta_0 - k\cdot\lambda$ are made.

$\varepsilon_3(\lambda)$ (the phase change from multiple reflections in the layers) is calculated from (5, 17 c).

Calculation of $R(\lambda)$.

The intensity distribution $R(\lambda)$ in reflection from a filter of this compound type can be calculated directly from (5, 1); this equation can (in the case of symmetry) be written as follows:

$$R_{04}(\lambda) = \frac{R_{01}\varrho_4^2\left|1 - \boldsymbol{R}_2\cdot\frac{\varrho_2}{\varrho_1}\cdot\frac{\varrho_5}{\varrho_4}\cdot e^{i(\varepsilon_2-\varepsilon_1)+i(\varepsilon_5-\varepsilon_4)-iy_2}\right|^2}{(\varrho_1\varrho_3)^2},$$

where $\varrho_1\cdot e^{i\varepsilon_1} = 1 - \boldsymbol{R}\cdot e^{-iy_1}$; $\varrho_2\cdot e^{i\varepsilon_2} = 1 - \sigma_2\cdot\boldsymbol{R}\cdot e^{-i(y_1-\alpha_2)}$ $\left(\boldsymbol{R} = \sqrt{R'\cdot\boldsymbol{R}_2}\right)$ and $\varrho_3\cdot e^{i\varepsilon_3} = 1 - \boldsymbol{R}_2\cdot\left(\frac{\varrho_2}{\varrho_1}\right)^2\cdot e^{2i(\varepsilon_2-\varepsilon_1)-iy_2}$ have previously been calculated. If further $\varrho_4\cdot e^{i\varepsilon_4} = 1 - \sigma_1\boldsymbol{R}\cdot e^{-i(y_1-\alpha_1)}$ and $\varrho_5\cdot e^{i\varepsilon_5} = 1 - \sigma_1\cdot\sigma_2\cdot\boldsymbol{R}\cdot e^{-i(y_1-\alpha_1-\alpha_2)}$ are calculated by means of Rybner's tables [4], we finally obtain

$$R(\lambda) = R'\cdot\left(\frac{\varrho_4\cdot\varrho_6}{\varrho_1\cdot\varrho_3}\right)^2 \quad (\varrho_6 \text{ denote the bracket in the numerator}).$$

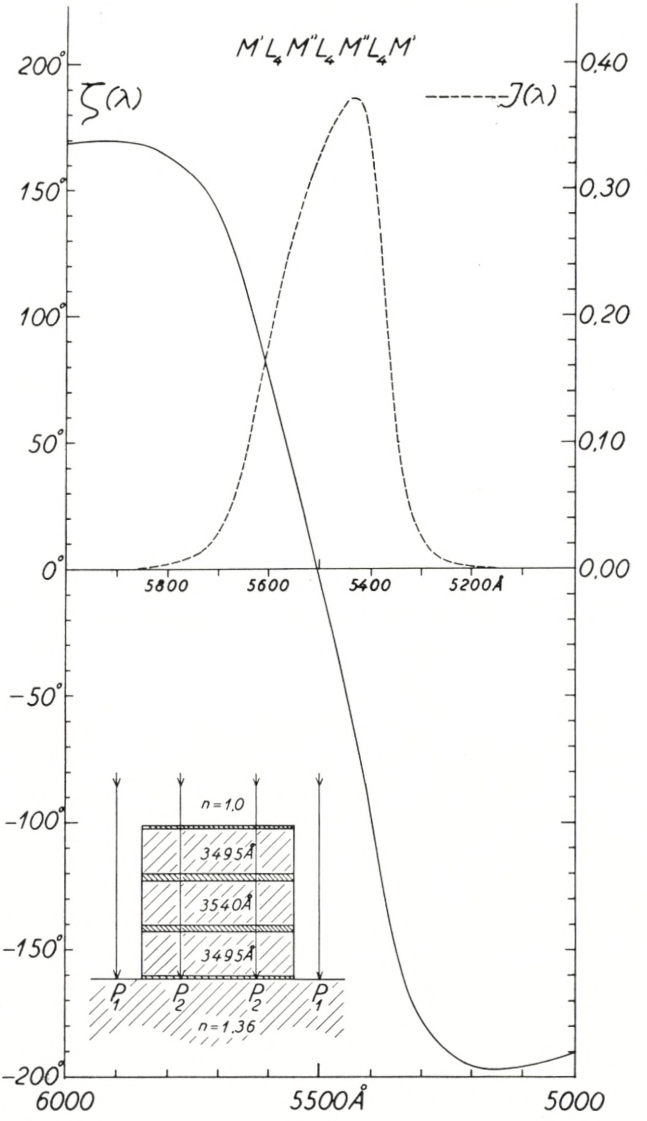

Fig. 44.

Unbroken line: Phase change at transmission through a filter of the type $M'L_4M''L_4M''L_4M'$. (Phase difference between P_2 and P_1). Broken line: $I(\lambda)$ for the same filter. The phase plate is shown below in the left corner of fig. 44.

This calculation has been done in case of three filters. (The $I(\lambda)'^s$ for these filters are shown in fig. 34 Curve A, fig. 35 unbroken line and fig. 37 unbroken line corresponding to $R(\lambda)$ in

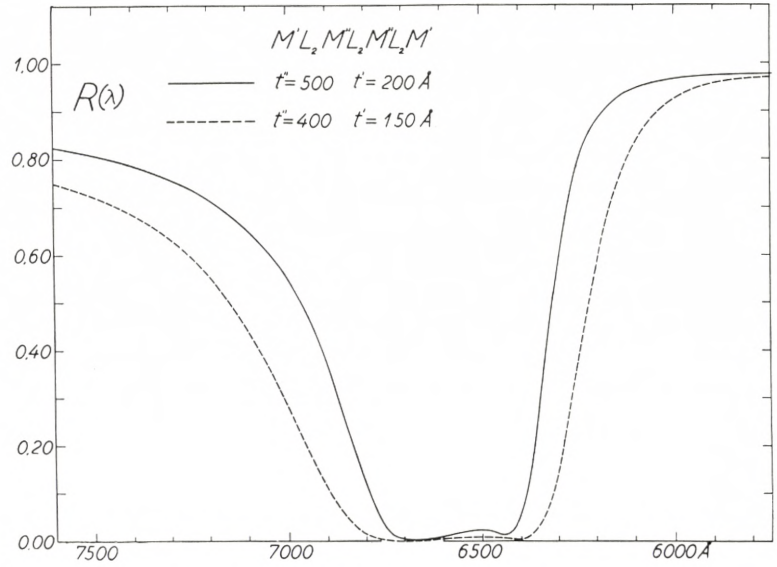

Fig. 45.
Unbroken line: $R(\lambda)$ for the filter shown in fig. 36 and the $I(\lambda)$ for the same filter is shown in fig. 35. (Unbroken line). $\alpha_1 = -2°.084$; $\alpha_2 = -0°.230$. Broken line: $R(\lambda)$ of a filter of the same type but with thinner silver layers. The corresponding $I(\lambda)$ curve is given in fig. 34 (Curve A) $\alpha_1 = -2°.971$; $\alpha_2 = -0°.466$.

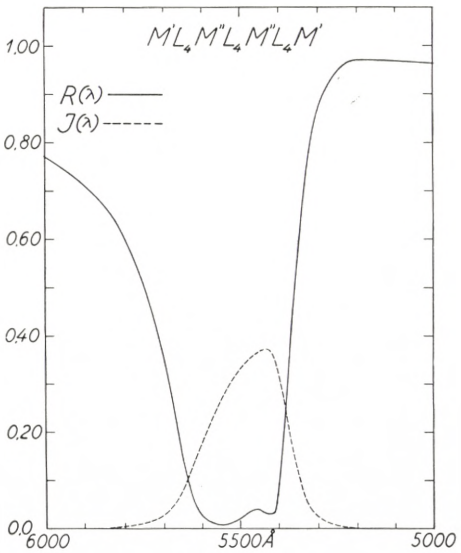

Fig. 46.
Unbroken line: $R(\lambda)$ for the compound filter constructed as shown in fig. 38. Broken line: $I(\lambda)$ for the same filter. $\alpha_1 = -3°.386$; $\alpha_2 = -0°.575$.

fig. 45 broken and unbroken line, and to fig. 46 unbroken line, respectively).

A general mathematical analysis has not been carried out and would be rather complicated because the value of α_1 here is essential for the shape of the $R(\lambda)$ curve.

The three curves of $R(\lambda)$ (fig. 45—46) have much the same trend (two minima). It should be noticed that the broad minimum towards longer wavelength is near zero intensity especially in the case of fig. 45.

In the previous section only the case $y_2 = y_1$ has been considered in detail. If $y_2 = m \cdot y_1$ ($m = 2, 3, 4 \ldots\ldots$), the condition which expresses that only one peak must occur (at a definite order) is more complicated. However, the condition which expresses that $I_{\max}$ should have its highest value for a definite value of R_2 is the same as in the case of $y_2 = y_1$, and in reality the only difference in the the case of $y_2 = m \cdot y_1$ is that W_2 becomes smaller than in case of $y_2 = y_1$ and satellite bands occur corresponding to the higher orders for the filter $M'' L_{2m} M''$.

§ 6. Improvements of the Interference Filters $ML_{2m}M$, $M'L_{2m}M''L_{2m}M'$ and $M'L_{2m}M''L_{2p}M''L_{2m}M'$ by Means of $\frac{\lambda}{4}$-layers with Alternately Low (L) and High (H) Index of Refraction.

The simplest improvement is to replace the L_{2m} layer with three dielectric layers $L' H_{2m-2} L'$.

From (2, 17 a) we get at normal incidence

$$\frac{1 - r_{20}}{1 + r_{20}} = \frac{n_L}{n_H} \frac{(1 - \sqrt{R_{10}} \cdot e^{-i(x_1 - \delta_{10})})}{(1 + \sqrt{R_{10}} \cdot e^{-i(x_1 - \delta_{10})})}. \qquad (6, 1)$$

The maximum value of R_{20} occurs when $x_1 = \delta_{10}$, and in this case R_{20} is determined by

$$\frac{1 - \sqrt{R_{20}}}{1 + \sqrt{R_{20}}} = \frac{n_L}{n_H} \cdot \left(\frac{1 - \sqrt{R_{10}}}{1 + \sqrt{R_{10}}} \right) = a, \quad \text{i. e.} \quad R_{20} = \left(\frac{1 - a}{1 + a} \right)^2. \qquad (6, 2)$$

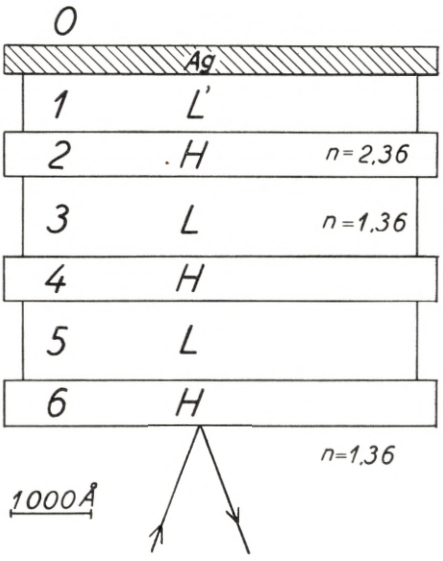

Fig. 47.
The reflective system I or II of fig. 6.

The next improvements of the filter $ML_{2m}M$ (or more correctly $ML'L_{2m-2}L'M'$) would be $ML'HL_{2m-4}HL'M$ and $ML'HLH_{2m-6}LHL'M$, etc.

Again by (2, 17 a) we get

$$\frac{1-r_{30}}{1+r_{30}} = \frac{n_H}{n_L}\left(\frac{1+\sqrt{R_{20}}}{1-\sqrt{R_{20}}}\right) = \left(\frac{n_H}{n_L}\right)^2\left(\frac{1+\sqrt{R_{10}}}{1-\sqrt{R_{10}}}\right)$$

and in general

$$\frac{1-\sqrt{R_{q,0}}}{1+\sqrt{R_{q,0}}} = \left(\frac{n_L}{n_H}\right)^{q-1}\cdot\left(\frac{1-\sqrt{R_{10}}}{1+\sqrt{R_{10}}}\right) \qquad (6, 3)$$

and

$$\delta_{q,0} = -(q-2)\cdot 180^\circ. \qquad (6, 4)$$

In this way the reflectivity from each of the systems I and II of a filter like that in fig. 6 can easily be calculated. The calculation of transmission T and of $\sigma\cdot e^{i\alpha}$ is carried out by means of the following general theorem:

If two filters A and B (fig. 48) only differ in such a way that

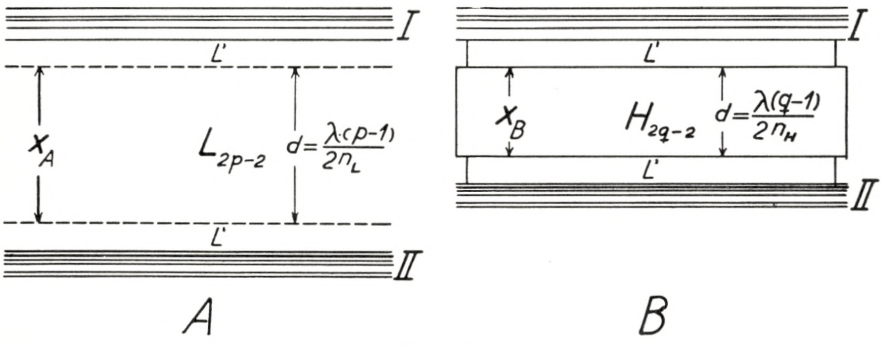

Fig. 48.

the layer L_{2p-2} *at A is replaced by the layer* H_{2q-2} *at B*, where L and H are exactly $\frac{\lambda}{4}$-layers for a wavelength λ_1 (corresponding to $x_A = 360° \cdot (p-1)$ and $x_B = 360° \cdot (q-1)$), then $I(\lambda_1)$, $R(\lambda_1)$, $\zeta(\lambda_1)$, etc., are identical for the two filters (follows direct from the recurrence formulae (2,7—8)), and we get $\frac{T_A}{1-R_A} = \frac{T_B}{1-R_B}$ (which is a special case of (2,18b)) and $\frac{1-\sigma_A \cdot R_A \cdot e^{i\alpha_A}}{1-R_A} \simeq \frac{1-\sigma_B \cdot R_B \cdot e^{i\alpha_B}}{1-R_B}$. From these equations R_B, T_B, σ_B and α_B can easily be calculated for the wavelength λ_1 with good accuracy when $t > 350$ Å.

When we add more quarter wavelength layers to the silver layer, (fig. 47) R_{0q} increases according to (6, 3). This means that the absorption factor A_{0q} as well as σ_q and α_q will decrease.

To calculate $I(\lambda)$ for filters of the type § 3 when I and II of fig. 6 consist of several layers, we must first calculate $y(\lambda)$ by means of (2, 7) and (3, 6a), and next y is substituted in (3, 5b).

In fig. 49 $y(\lambda)$ is calculated for different numbers of dielectric layers but with the same thickness $t = 350$ Å of the silver layers. $\lambda_1 = 6560$ Å $n_L = 1.38$ (MgF_2) and $n_H = 2.36$ (ZnS). From fig. 49 it is obvious that besides the main peak at 6560 Å neighbouring peaks occur. E. g. the filter $ML'HLHL\ H_2\ LHLHL'M$ has peaks at 5130 Å, 4740 Å, and 4340 Å (where $y = 360° \cdot p$) (Curve C). For comparison a Fabry-Perot filter $ML'L_8L'M$ has been added (Curve D, broken line). This filter has neighbouring peaks at 5480 Å, 4700 Å, and 4120 Å (read off from fig. 49). Not only the

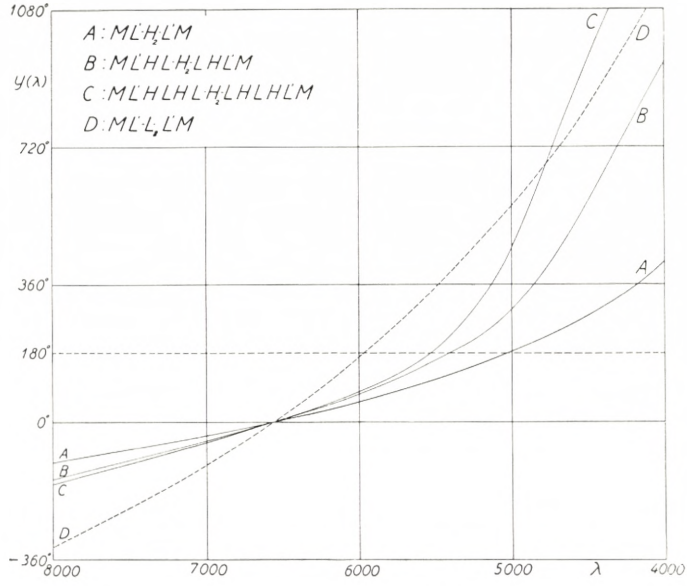

Fig. 49.
$y(\lambda)$ calculated for filters of different kinds A—D. $n_L = 1.38$, $n_H = 2.36$ and $t = 350$ Å for the M layers.

main peak at 6560 Å, but also the neighbouring peaks will according to (2,18 b) have the same $I_{\max} = \left(\frac{T}{1-R}\right)^2$ for the two filters C and D. In Table 19 some characteristic properties of the filters A—D have been added.

TABLE 19.

	q	R_{0q}	f	W_2	$\lambda_{\min}$	$I_{\min}$	$\lambda_{2\,(\max)}$
A	2	0.9243	1.61	102.1 Å	5030 Å	$4.65 \cdot 10^{-3}$	4180 Å
B	4	0.9734	2.11	26.6	5410	$1.05 \cdot 10^{-3}$	4860
C	6	0.9908	2.33	8.2	5530	$0.49 \cdot 10^{-3}$	5130
D		0.8740	5.00	56.3	5970	$2.91 \cdot 10^{-3}$	5480

$\lambda_1 = 6560$ Å and $I_{\max} = 0.398$ in all the filters A—D (fig. 49)

$$f = -\left(\frac{dy}{d\lambda}\right)_{\lambda=\lambda_1} \cdot \frac{\lambda_1}{360} \quad \text{and} \quad I_{\min} = \left(\frac{T_1}{1-R_1}\right)^2 \cdot \left(\frac{1-R_{\min}}{1+R_{\min}}\right)^2.$$

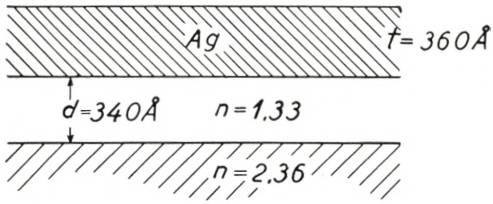

Fig. 50.

Filters of this silver multiple dielectric layer type have been described and produced by TURNER [20] and DUFOUR [21].

Calculation of $I(\lambda)$ for such a filter at oblique incidence can be carried out in an analogous way for the s and p component treated separately. (First R_{0q}, δ_{0q} from (2, 7—11) and (1, 12—13), next $y(\lambda)$ from (3, 6 a), and finally $I(\lambda)$ from (3, 5 b) are to be calculated).

The simplest filter of this type is $ML'H_{2m-2}L'M$. This filter is of interest for special purposes because the violet shift of λ_1 at oblique incidence is smaller than in the filter $ML_{2m}M$. As mentioned above, the highest value of R_{02} occurs when L' has a thickness of $\frac{\delta_{10}}{180} \cdot \frac{\lambda_1}{4\, n_L}$, i. e. $x_1 = \delta_{10} \simeq 141°$. If x_1 is considerably less than this value ($x_1 \simeq 60°$), a calculation shows that the splitting up into two components λ_s and λ_p is small up to an angle of incidence of 60°. If $n_H = 2.36$, n_L should be below 1.34 to get the best result. (Fig. 50).

§ 7. Multiple Dielectric Layer Interference Filters.

Each of the systems I and II (in the case of filters of § 3 or I—IV in the case of filters of § 4—5) consist in this case of 3—11 quarter wavelength layers of dielectrics with alternately low (n_L) and high (n_H) index of refraction in this case beginning with a a high index layer on the filter blank.

If I and II (fig. 6) each consist of q quarter wavelength layers $D_q = HLHLHLH \ldots\ldots$, the reflectivity R_q of the system D_q is at the peak λ_1 (where the layers are exactly $\frac{\lambda}{4}$-layers) determined by (6, 3) to be

$$R_q(\lambda_1) = \left(\frac{1 - \left(\frac{n_L}{n_H}\right)^q \cdot \frac{n_G}{n_H}}{1 + \left(\frac{n_L}{n_H}\right)^q \cdot \frac{n_G}{n_H}} \right)^2 \qquad (7, 1)$$

n_G is the index of refraction of the filter blank (glass plate $n_G = 1.518$).

To calculate $I(\lambda)$ for filters with reflective systems of this type R_q, δ_q must be calculated by means of (2, 7) as a function of $x = 180° \cdot \frac{\lambda_1}{\lambda}$ (at normal incidence). SCHRÖDER [22] has from (2, 7) developed a general mathematical expression for $1 - R_q(x)$ and made calculations for $r = 0.25$ and $r = 0.40$ ($r = \frac{n_H - n_L}{n_H + n_L}$ at $\varphi = 0$). ABELÈS [7] has expressed $R_q(x)$, $\delta_q(x)$ in terms of TCHEBYCHEFF's polynomials, and by means of an *NBSMTP* table $R_9(x)$ has been calculated. Further investigations concerning $R_q(x)$, $\delta_q(x)$ have been made by DUFOUR [23], DUFOUR and HERPIN [24], and VAŠÍČEK [25].

Some of these calculations have been repeated here, carried out direct from the recurrence formula (2,7) by means of RYBNER's tables [4] .All these calculations show that within a span of $2v$ in x $180 - v < x < 180 + v$ the difference $R_q(x) - R_q(180)$ will be sufficiently small to make use of D_q as a reflective coating for interference filters within the region $\lambda_0 < \lambda < \lambda_2$. λ_1 corresponds to $x = 180°$; λ_0 to $x = 180° + v$ and λ_2 to $x = 180° - v$, $x = \frac{\lambda_1}{\lambda} \cdot 180°$ and $R_q(-x) = R_q(x)$.

This wavelength region $\lambda_0 < \lambda < \lambda_2$ is almost independent of q when $q > 5$; outside this region $R_q(x)$ decreases rapidly; according to VAŠÍČEK [25] the more the greater q is.

The value of v is a function of r only. When $n_L = 1.38$ (MgF_2) and $n_H = 2.36$ (ZnS) (as in Table 20), we have $r = 0.262$ and $v \simeq 30°$. When $\lambda_1 = 5500$ Å, this corresponds to $\lambda_0 = 4715$ Å and $\lambda_2 = 6600$ Å, and for $\lambda_1 = 6560$ Å we get $\lambda_0 = 5620$ Å and $\lambda_2 = 7870$ Å. If $r = 0.4$, we get $v \simeq 50°$, at $\lambda_1 = 6560$ Å this corresponds to $\lambda_0 = 5130$ Å and $\lambda_2 = 9080$ Å. ($r = 0.4$ corresponds closely to MgF_2 and Sb_2S_3 which according to SCHRÖDER

[22] can be employed in the red-infrared region). So with this type of filters the wavelength region covered by the filter is more restricted than by filters with silver layers.

TABLE 20.

q	R_q $x = 180°$	R_q $x = 180° \pm 30°$	$f = \frac{1}{2} \cdot \left(\frac{dy}{dx}\right)_{x=180°}$	W_2 $\lambda_1 = 6560$ Å
1	0.2056	0.1946	1.40	
2	0.4089	0.3671	1.74	
3	0.5962	0.5162	2.00	
4	0.7399	0.6298	2.15	294 Å
5	0.8386	0.7134	2.25	164
6	0.9022	0.7747	2.32	92.7
7	0.9416	0.8199	2.37	53.0
8	0.9654	0.8664	2.39	30.8
9	0.9796	0.8902	2.40	17.0
10	0.9881	0.9086	2.40	10.4
11	0.9930	0.9231	2.41	6.1
12	0.9959	0.9342	—	3.6
13	0.9976	0.9436	—	2.1
14	0.9986	0.9513	—	1.2
15	0.9992	0.9577	—	0.7

In Table 20

$$f = -\left(\frac{dy}{d\lambda}\right)_{\lambda=\lambda_1} \cdot \frac{\lambda_1}{360} = \frac{1}{2} \cdot \left(\frac{dy}{dx}\right)_{x=180} \simeq \frac{y(180) - y(176)}{8}$$

and

$$W_2 = \frac{(1 - R_q) \cdot \lambda_1}{f \cdot \pi \cdot \sqrt{R_q}}$$

for filters of the type $D_q L_2 D_q$ (q uneven) or $D_q H_2 D_q$ (q even). The final f value is a function of r only and decreases when r increases. In fig. 51 $y(\lambda)$ is shown for filters of a different kind of the type in § 3. Curve A corresponds to $D_3 L_2 D_3$ which is very closely equal to $y(\lambda)$ for $ML_4 M$. Curve B corresponds to $D_7 L_2 D_7$ (or very closely to $D_6 H_2 D_6$). Curve C refers to $y(\lambda)$ for $ML_6 M$ and Curve E to $D_7 L_4 D_7$ (f for this filter is 3.37). All the filters have peak transmission at $\lambda_1 = 6560$ Å.

Reflective coatings D_q for FABRY-PEROT interferometers and filters of the type $D_q L_2 D_q$ with $q = 7, 9, 11$ have in recent years

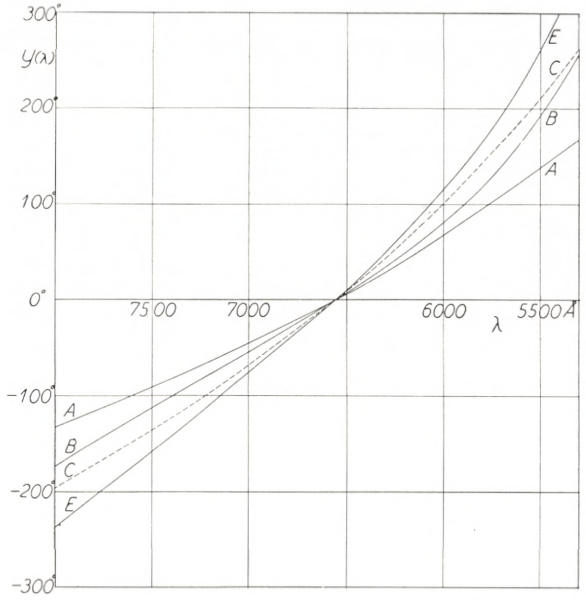

Fig. 51.
$y(\lambda)$ for filters of different kinds. A: $D_3\,L_2\,D_3$ ($D_3 = HLH$) or $ML_4\,M$. B: $D_7\,L_2\,D_7$ ($D_7 = HLHLHLH$). C: $ML_6\,M$ and E: $D_7\,L_4\,D_7$. $n_L = 1.38$, $n_H = 2.36$ (and $t = 350$ Å for the M-layers).

been made in many laboratories [26—30], most of them with cryolite and ZnS as low and high index materials. Because of absorption in the ZnS layers such coatings can only be employed for $\lambda > 4000$ Å. From measurements of I_{max} and W_2 at $D_7\,L_2\,D_7$ filters RING and WILCOCK [30] have calculated the absorption in a D_7 system of layers to be 0.017 at 4100 Å and 0.008 at 4500 Å. POLSTER [29] has produced filters $D_7\,L_2\,D_2$ with I_{max} as high as 0.80 at $\lambda_1 = 5500$ Å, which corresponds to a still smaller absorption in a D_7 system of layers. Because of crystalline structure in the spacer layer L_2 and absorption in the D_q layers it has not been possible so far to obtain a value of W_2 lower than 10—15 Å [30].

At an oblique angle of incidence φ we have $x_H = \frac{\lambda_0}{\lambda} \cdot 180° \cdot \cos\chi_H$ and $x_L = \frac{\lambda_0}{\lambda} \cdot 180° \cdot \cos\chi_L$ (if $x_H = x_L = \frac{\lambda_0}{\lambda} \cdot 180°$ at $\varphi = 0$). To obtain $I(\lambda)$, $R_q(\lambda)$ and $\delta_q(\lambda)$ must be calculated separately for the s and p component by means of the recurrence formula (2, 7) combined with (2, 10—11). To find (λ_s, λ_p) corresponding to λ_0

at $\varphi = 0$ for a filter $D_q\, L_2\, D_q$ it is sufficient to determine x_L in such a way that $y = 2\,(x_L - \delta_q\,(x_L))$ is equal to $360 \cdot p$, $(p = 0, 1, 2, 3 \ldots)$. Such a calculation of $y(x_L)$ in the neighbourhood of the peak can be carried out by means of RYBNER's tables [4] or by means of a graphical method (to be described in a following paper).

In Table 21 (λ_s, λ_p) have been calculated for two filters $D_6\, H_2\, D_6$ and $D_7\, L_2\, D_7$ with $\lambda_0 = 6560$ Å. It should be noticed, however, that if the dispersion of MgF_2 and ZnS is neglected, $\frac{\lambda_s}{\lambda_0}$, $\frac{\lambda_p}{\lambda_0}$ are independent of λ_0.

TABLE 21. ($\lambda = 6560$ Å)

	φ	15°	30°		45°		60°		75°	
		s & p	s	p	s	p	s	p	s	p
$D_6H_2D_6$	λ_{max}/λ_0	0.9897	0.9613	0.9605	0.9215	0.9176	0.8805	0.8702	0.8497	0.8318
	λ_{max}	6493	6306	6301	6045	6019	5776	5709	5574	5456
$D_7L_2D_7$	λ_{max}/λ_0	0.9866	0.9482	0.9491	0.8616	0.8958	0.8286	0.8399	0.7771	0.7968
	λ_{max}	6472	6220	6226	5849	5876	5436	5510	5098	5227
	r	0.2620	0.2840	0.2398	0.3103	0.2124	0.3428	0.1774	0.3720	0.1448

In Table 22 W_2 has been calculated for $\varphi = 75°$ in the case of the filter $D_7\, L_2\, D_7$

$$f_s = -\left(\frac{dy}{d\lambda}\right)_{\lambda=\lambda_s} \cdot \frac{\lambda_s}{360} = \left(\frac{dy}{dx_L}\right)_{\lambda=\lambda_s} \cdot \frac{1}{2} \cdot \frac{\lambda_0}{\lambda_s} \cdot \cos \chi_L$$

(and analogously for the p component).

TABLE 22.

	s	p
λ_{max}	5098 Å	5227 Å
f	1.90	3.35
R_q	0.9887	0.6618
W_2	9.7 Å	208 Å

$\varphi = 75°$ $D_7L_2D_7$ filter.

Calculations at oblique incidence up to $\varphi = 30°$ have also been done by DUFOUR and HERPIN [24].

In Tables 20—22 $n_H d_H = n_L d_L = \frac{\lambda_0}{4}$ to obtain optimum conditions at $\varphi = 0$. However, to obtain optimum conditions at a definite angle of incidence φ and at a definite wavelength λ_1 we must require that

$$x_H = x_L = 180° \text{ or } n_H d_H = \frac{\lambda_1}{4 \cdot \cos \chi_H} \text{ and } n_L d_L = \frac{\lambda_1}{4 \cos \chi_L} \quad (7, 2)$$

and in this case we have $\lambda_1 = \lambda_s = \lambda_p$ (no split-up into two components), only $W_2^{(s)}$ will be different from $W_2^{(p)}$ because r_s and r_p are different (Tables 21—22). It should further be noted that if (7, 2) is satisfied at e. g. $\varphi = 45°$, $\lambda_s - \lambda_p$ in the whole region $0 < \varphi < 45°$ will be very small.

Finally it should be mentioned that for special purposes it would perhaps be valuable to construct all-dielectric filters also of the types described in § 4 and § 5. If the absorption in a D_7 system is 0.01 and in a D_9 system 0.02 [28] $I_{\max}$ for the filter $D_5 L_2 D_9 L_2 D_5$ would be 0.75, for the filter $D_3 L_2 D_7 L_4 D_7 L_2 D_3$ 0.90, and for the filter $D_3 L_2 D_9 L_2 D_9 L_2 D_3$ 0.60 ($I_{\max}$ for the filter $D_9 L_2 D_9$ would be 0.11). Filters of a similar type have been suggested by TURNER [31].

Summary.

A general theory of interference filters has been developed concerning filters with two three and four systems of reflective layers.

In § 1 and § 2 the general equations for a system of thin layers have been developed, which are to be used at the calculation of all the optical properties of the system such as R, T, δ, β, etc. (reflectivity, transmission, phase change at reflection and transmission, etc.) when the indices of refraction (n, $\nu - i\varkappa$) and the thicknesses (d, t) of all the layers in the system are known. These general equations in § 2 have been developed from FRESNEL's equations at a boundary treated in § 1. In § 3 a

general theory has been developed for interference filters with two systems of reflective layers I and II. This theory has been used for a numerical calculation of $I(\lambda)$, $R(\lambda)$ for the FABRY-PEROT filter $ML_{2m}M$ ($M = Ag$ layer, $L = \frac{\lambda}{4}$-layer of dielectric), and furthermore the phase change at transmission through the filter $\zeta(\lambda)$ has been calculated. (The filter used as phase plate). Next, $I(\lambda)_s$ and $I(\lambda)_p$ of the filter ML_2M have been calculated at the oblique incidence φ. ($\varphi = 45°, 60°, 75°$). In § 4 a general theory of interference filters with three systems of reflective layers I, II, III has been developed. The condition to get only one peak (at a definite order) is

$$\boldsymbol{R} \leqslant 1 - \sqrt{1 - \frac{1}{\sigma_2}};\ \boldsymbol{R} = \sqrt{R' \cdot R''}\ \left(\sigma_2 \simeq \frac{1 - A''}{R''} \quad \text{and} \quad R''\right.$$

refer to the centre layer II and R' to the outer layers II and III), and this condition corresponds closely to the condition of obtaining the highest value of $I_{\max}$ at a definite value of R''. This theory has been applied to numerical calculations of $I(\lambda)$ (and in a few cases also $R(\lambda)$) in the case of filters with three silver layers $M'L_{2m}M''L_{2m}M'$. Also $\zeta(\lambda)$ has been calculated.

In § 5 quite an analogous theory has been developed for filters with four systems of reflective layers I—IV. Here the equation for obtaining optimum conditions is $\boldsymbol{R} \leqslant \boldsymbol{H}$, where $\boldsymbol{H}$ is determined by

$$\boldsymbol{H}^2 - \boldsymbol{H}\left(3 - \frac{\boldsymbol{R}_2}{2} - \frac{1}{2 \cdot \sigma_2^2 \cdot \boldsymbol{R}_2}\right) + \frac{1}{\sigma_2} = 0 \quad (\boldsymbol{R}_2 = R'');$$

$\boldsymbol{R}_2$, σ_2 refer to II, III and R' to I, IV ($\boldsymbol{R} = \sqrt{R' \cdot R''}$). Here again $I(\lambda)$, $\zeta(\lambda)$ and $R(\lambda)$ have been calculated for filters with four silver layers $M'L_{2m}M''L_{2m}M''L_{2m}M'$.

In § 6 is treated the improvement of filters with silver layers by means of quarter wavelength layers of dielectrics (L and H layers of fluoride and ZnS). The properties of filters such as $ML'H_2L'M$ and $ML'HLH_2LHL'M$ have been calculated.

In § 7 the application of multiple dielectric layer systems $D_q = HLHLHLHL \ldots .$ (q layers) instead of silver layers as

reflective systems I—IV has been treated. The limited wavelength region $\lambda_2 - \lambda_0$ for high reflectivity has been determined for $r = 0.26$ and $r = 0.40$. Furthermore, the properties of the filters $D_6 H_2 D_6$ and $D_7 L_2 D_2$ have been calculated at oblique incidence ($\varphi = 15°$, $30°$, $45°$, $60°$ and $75°$) as well. Filters of the types $D_5 L_2 D_9 L_2 D_5$ and $D_3 L_2 D_7 L_4 D_7 L_2 D_3$ have also been mentioned.

Acknowledgement.

These investigations have been made at the Physics Department of the Royal Veterinary and Agricultural College, Copenhagen. I wish to thank the director of the Physics Department, Professor Ebbe Rasmussen, for the great interest he has taken in this work.

Physics Department,
Royal Veterinary and Agricultural College, Copenhagen.

References.

1. Max Born: Optik (1933). (Berlin, Verlag von Julius Springer)
2. Herbert Mayer: Physik Dünner Schichten (1950). (Wissenschaftliche Verlagsgesellschaft, M. B. H. Stuttgart)
3. H. Geiger & Karl Schell: Handbuch der Physik, Vol. 20, 242
4. Jørgen Rybner and K. Steenberg Sørensen: Table for Use in the Addition of Complex Numbers. (Jul. Gjellerups forlag, København 1948)
5. F. Abelès: Ann. de Phys. **3**, 516 (1948)
6. Kozŏ Ishiguro and Toshio Katŏ: J. Phy. Soc. of Japan, **8**, 77 (1953)
7. F. Abelès: Theses (Paris, 1950)
8. W. Geffchen: Ann. d. Phys. **40**, 385 (1941) and D. R. P. No. 716154 (1942)
9. L. G. Schulz: J. Opt. Soc. Am. **41**, 1047 (1951)
10. H. Kuhn: J. Phys. et le Radium, **11**, 422 (1950) or H. Kuhn and B. A. Wilson: Proc. Phys. Soc. B, **63**, 745 (1950)
11. L. N. Hadley and D. M. Dennison: J. Opt. Soc. Am. **37**, 451 1947) — ibid. **38**, 483, (1948)
12. M. Locquin: Contraste de Phase et Contraste par Interference, p. 115 (Editions de la "Revue d'Optique Théorique et Instrumentale", Paris 1952)
13. Ch. Dufour: ibid. p. 109
14. A. F. Turner: J. Opt. Soc. Am. **36**, 711 (A) (1946)
15. P. Leurgans and A. F. Turner: ibid. **37**, 983 (A) (1947)
16. A. E. Gee and H. D. Polster: ibid. **39**, 1044 (1949)
17. B. H. Billings: ibid. **40**, 471 (1950)

17a. H. D. Polster: ibid. **39**, 1038 (1949)

18. Ch. Dufour: J. Phys. et le Radium **11**, 413 (1950)
19. W. Geffcken: Zs. f. angew. Phys., VI, 249 (1954)
20. A. F. Turner: J. Phys. et le Radium **11**, 444 (1950)
21. Ch. Dufour: Thèses (Paris 1950) and Revue d'Optique **31**, 1 (1952)
22. H. Schröder: Zs. f. angew. Phys. III, 53 (1951)
23. Ch. Dufour: Revue d'Optique **31**, 1 (1952) and ibid. **32**, 321 (1953)
24. Ch. Dufour and A. Herpin: Optica Acta **1**, 1 (1954)

25. A. Vašíček: Czechosl. J. Phys. **3**, 206 (1953)
26. M. Bannung: J. Opt. Soc. Am. **37**, 792 (1947)
27. Ch. Dufour: Le Vide, No. 16—17, 480 (1948) or Thèses (Paris 1950)
28. A. H. Jarret and von Klüber: Nature **169**, 790 (1952) and A. H. Jarret: ibid. 170, 455 (1952)
29. H. D. Polster: J. Opt. Soc. Am. **42**, 21 (1952)
30. J. Ring and W. L. Wilcock: Nature **171**, 648 (1953) — ibid. **173**, 994 (1954)
31. A. F. Turner: J. Opt. Soc. Am. **42**, 878 (1952)

Indleveret til selskabet den 1. oktober 1954
Færdig fra trykkeriet den 10. juni 1955.